Understanding hazards of nanoplastics using Daphnia magna

Kelpsiene, Egle

2023

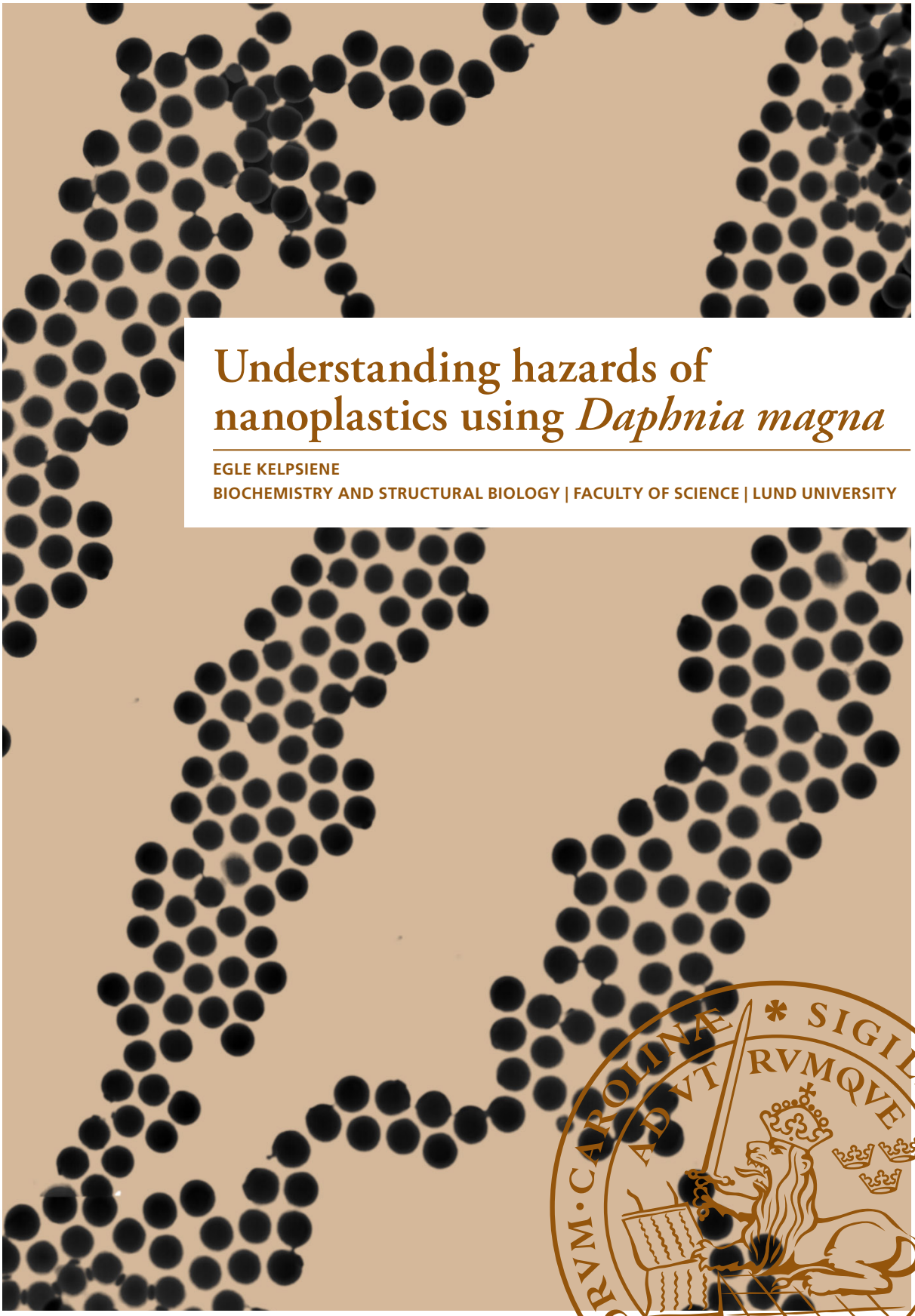

Understanding hazards of nanoplastics using *Daphnia magna*

EGLE KELPSIENE
BIOCHEMISTRY AND STRUCTURAL BIOLOGY | FACULTY OF SCIENCE | LUND UNIVERSITY

Printed by Media-Tryck, Lund 2023 NORDIC SWAN ECOLABEL 3041 0903

Faculty of Science
Department of Chemistry
Biochemistry and Structural Biology

ISBN 978-91-7422-970-7

Understanding hazards of nanoplastics using *Daphnia magna*

Egle Kelpsiene

DOCTORAL DISSERTATION

Thesis for the degree of Doctor of Philosophy (PhD) at the
Faculty of Science at Lund University, Sweden.
To be publicly defended on the 19th of October at 9:00 a.m. in lecture hall A, at
Kemicentrum at the Department of Chemistry.

Faculty opponent: Dr. Isabel Lopes

Thesis advisors: Dr. Tommy Cedervall, Dr. Martin Lundqvist, Dr. Mikael T. Ekvall

Organization LUND UNIVERSITY Biochemistry and Structural Biology Box 124 SE-221 00 Lund Sweden	**Document name** Doctoral Dissertation
	Date of issue 2023-10-19
Author(s) Egle Kelpsiene	Sponsoring organization

Title and subtitle Understanding hazards of nanoplastics using *Daphnia magna*

Abstract

This thesis presents the results of studies focused on effects caused by nano-sized particles using freshwater filter feeder *Daphnia magna*. I showed that both positively and negatively surface charged PS NPs induced significant mortality in *D. magna* after a life-time (103 days) of exposure at low concentrations. Previously, it was shown that negatively surface charged PS NPs are acutely not toxic toward *D. magna*.

Secondly, I analyzed metabolic responses in *D. magna* after 37 days of exposure to low concentrations of PS NPs. The observed results revealed that levels of free amino acids were affected at PS NPs concentrations as low as 3.2 µg/L, which is lower than various NPs concentrations quantified in nature.

Nanomaterials, including PS NPs, adsorb biomolecules on their surfaces and form corona. Therefore, I identified proteins that bind to differently surface charged PS NPs. The results showed that the profiles of bound proteins are different depending on the particle size and charge, which can partly explain differences in acute toxicity.

PLA is recognized as an alternative to synthetic plastics, therefore recently has received a lot of attention. I evaluated the effects of PLA breakdown nanoplastics and PLA NPs on *D. magna* after acute exposure. The observed results showed that neither PLA NPs nor PLA nanoplastics induced adverse effects on *D. magna*. Contrarily, PLA plastic cup nanoplastics significantly extended the survival of *D. magna* compared to a control group.

Key words *Daphnia magna*, nanoplastics, polystyrene, polylactic acid nanoparticles

Classification system and/or index terms (if any)

Supplementary bibliographical information		**Language** English
ISSN:		**ISBN:** 978-91-7422-970-7 (print) 978-91-7422-971-4 (pdf)
Recipient's notes	**Number of pages:** 75	Price
	Security classification	

Signature Date 2023-09-01

Understanding hazards of nanoplastics using *Daphnia magna*

Egle Kelpsiene

LUND
UNIVERSITY

Author photo

Coverphoto by Egle Kelpsiene

Faculty of Science
Department of Chemistry

ISBN 978-91-7422-970-7 (print)
ISSN 978-91-7422-971-4 (pdf)

Printed in Sweden by Media-Tryck, Lund University
Lund 2023

Media-Tryck is a Nordic Swan Ecolabel certified provider of printed material. Read more about our environmental work at www.mediatryck.lu.se
MADE IN SWEDEN

"If you understand your painting beforehand,
you might as well not paint it."

— Salvador Dalí

Table of Contents

Popular Science Summary

Global plastic production has increased rapidly from 2 million tons in 1950 to ~390 million tons in 2021. It is predicted that global production might reach up to ~450 million tons in 2025. Such a rapid increase in production generates a huge amount of waste. Therefore, plastic pollution became a global problem. Mismanaged plastic waste can affect processes in the natural environment, as well as alter people's livelihood and social well-being.

Large plastic pieces (> 5 mm) are a serious threat to mammals, fish, reptiles, and sea birds. It is estimated that over 1 million aquatic animals are killed each year due to ingestion and/or entanglement of macroplastics. Over time macroplastics are subjected to several biological, physical, and chemical degradation processes. Therefore, gradually, large plastic pieces break down into smaller micro- (< 5 mm and >1 μm) and, eventually, nano- (< 1 μm or <100 nm) plastics. Nanoplastics, as the name implies, are tiny plastic particles. For the comparison, we should imagine sizes of, for example, yeasts (3-10 μm), bacteria (1-10 μm), or viruses (0.05-0.1 μm). Nanoplastics would be somewhere between the size of viruses and DNA, between 10^{-6} m and 10^{-9} m.

For example, single-use plastics break down and produce nanoplastics. Therefore, Europe Union countries banned the one-time use plastic items, such as plastic cutlery, stirrers, and straws. Even though nanoplastics are tiny, they cause a lot of concerns. They do not fully decompose, they are not harmless, they can penetrate living organisms via the skin and the respiratory system, can accumulate in digestive tract, and travel along the food chain. Several toxicity studies showed that nanoplastics have negative effects on bacterial diversity, algal cells, behavior, and the immune system of various aquatic organisms.

The concentration of nanoplastics has been quantified to be < 600 μg/L. This raises several questions – how are organisms affected at low concentrations of nanoplastics? What are the effects of nanoplastics in nature in the long run? I aimed to answer these questions in this thesis. I showed that polystyrene nanoparticles with carboxylic surface charge previously shown to be acutely non-toxic, appeared to be toxic after long-term exposure. Additionally, I showed that levels of free amino acids were affected at polystyrene nanoparticles concentrations as low as 3.2 μg/L after 37 days of exposure.

Once nanoparticles are in the environment or other type of media, they are in contact with various biomolecules, such as proteins, lipids, metabolites, etc. These molecules create some sort of coating, called corona. Nanoparticles-coated corona could be pictured as something like bumblebees covered in

pollen. In this thesis, I showed that different proteins bind to the polystyrene nanoparticles depending on their surface charge.

Due to plastic production, their generated waste, and caused adverse effects, people are trying to find better alternatives. For the last several years, bioplastics have attracted a lot of attention as a potential environmentally friendly alternative to conventional plastics. Yet, there are several unanswered questions regarding bioplastics. One of which is – what are the effects caused by bioplastics on aquatic organisms? I showed that there is a positive effect of bioplastics in crustaceans. Worth mentioning, I performed a short-term experiment, therefore it is difficult to speculate if the same tendencies would be observed after a long-term exposure scenario.

Abstract

The work presented in this thesis focuses on effects caused by nano-sized particles, covering both engineered polystyrene nanoparticles (PS NPs), polylactic acid (PLA) NPs, and breakdown PLA nanoplastics, using freshwater filter feeder *Daphnia magna*. The thesis is divided into the following main sections – background, methods, followed by results and discussion, closing remarks, and future perspectives.

Numerous studies are showing that positively surface charged PS NPs induce acute toxicity in various organisms, whereas PS NPs with a negative surface charge appear not to be acutely toxic [1], however, in those studies, long-term effects of charged PS NPs were not investigated. Therefore, I evaluated the toxicity of both positively and negatively surface charged PS NPs after a life-time (103 days) exposure to *D. magna* at low concentrations (**Paper I**). I was able to show that, contrary to the acute toxicity test results [1], regardless of the surface charge, PS NPs significantly increased mortality in *D. magna*.

Secondly, as **Paper I** showed that survival was significantly affected in *D. magna* after life-time exposure to low concentrations of PS NPs, I wanted to assess the effects of these PS NPs at a molecular level. Therefore, metabolic responses in *D. magna* were determined after 37 days of exposure to low concentrations of PS NPs by using ^{1}H nuclear magnetic resonance (NMR) analysis (**Paper II**). The observed results revealed that levels of free amino acids were affected at PS NPs concentrations as low as 3.2 μg/L, which is lower than various NPs concentrations quantified in nature.

Moreover, knowing that (1) NPs can adsorb various molecules to their surfaces, and (2) *D. magna* can excrete biomolecules as a response to the presence of toxicants, I set up experiments to identify proteins that bind to differently surface charged PS NPs (**Paper III**). The results showed that the profiles of bound proteins are different depending on the particle size and charge, which can partly explain differences in acute toxicity.

Finally, bioplastics are often recognized as more environmentally friendly alternatives to synthetic plastics, therefore I assessed the possible effects on *D. magna* after short-term exposure to PLA NPs and PLA breakdown nanoplastics (**Paper IV**). The observed results show that neither PLA NPs nor PLA nanoplastics induced adverse effects on *D. magna*. Contrarily, there was a trend of extended survival of *D. magna* after exposure to all PLA nanoplastics, however, only PLA plastic cup nanoplastics showed a significant difference compared to a control group.

Acknowledgments

"Science is not an individual sport and there are many ways how teamwork can make science work better". These past years were full of kind people, new experiences, as well as continuous cycle of trying, learning, and growing. A lot of people one way or another contributed along the PhD journey. Therefore, thanks to each one of you for being supportive and kind throughout these years.

First and foremost, I want to give my warmest wishes to my supervisor **Tommy**. Thank you for always being available with advice whenever needed, nice long talks or random chit-chat, your cheerful attitude, introducing me to a very small part of protein science, encouragement, and a good practice example of how fun can be to do science. *"The sky is the limit"* and yet you are right! I appreciate all your help and support during these years!

I was lucky to have two co-supervisors, **Martin** and **Mikael**, who happened to have expertise in different fields. Thank you both for teaching me new techniques, all your tips and tricks, always being cheerful, kind and helpful to me, and fruitful and interesting discussions!

Lars-Anders, you were the first person I met here at Lund University. Thank you for opening your lab doors, your trust in me, all your advice during the SITES AquaNET project and at the beginning of my PhD, your nice words after my presentations, and most importantly for always being so kind! I will never forget your advice that *"Only dead fish goes with a flow"*! Take care!

During these years in Sweden, I met two incredible friends – **Micaela** and **Franca**. Thank you both for your friendship, after-work activities, long coffee and lunch breaks, sharing happiness, frustrations, and ideas about work and life. Thanks for all the good times together (and many more to count!) and cheers to our friendship! *Muchas gracias por todos mis queridas chicas!*

I had an opportunity to be a part of **CeeNano** group, which was full of good discussions, laughter, and a good atmosphere! Big thanks to present and former CeeNano group members: **Erik G.**, thank you for being such a nice colleague and friend, all your help in the lab, and nice discussions. **Tania**, thank you for all your help, the long discussions about life and work, and joining me in yoga classes. **Nicholas**, thank you for all the interesting discussions about science and life. **Shanti**, **Jing**, **Isabella**, **Melinda**, **Lennart**, **Lauge**, **Erik B.**, **Oscar**, **Hugo**, and **Cesare**, for always being helpful, cheerful, and kind.

Dev, thank you for being such a good friend and colleague and always being kind to answer all my hundred work-related questions! Wish you the best of luck in your career!

Maryam and **Magnus**, you have already heard a lot of people saying that the department would collapse if you were not around. I could not agree more! Thank you both for being kind, cheerful, and always helpful!

Sara, and all present and former members of Sara's group: **Kalyani**, **Tinna**, **Rebecca**, **Eimantas**, **Mattias**, **Lei**, **Thom**, **Max**, **Emil**, **Andreas**, **Veronica**, **Tanja**, **Celia**, and others that I might have forgotten to mention, for all your help and lovely discussions.

Katja, for your cheerful attitude and all your help related to mass spec.

Anders, for all the fruitful discussions and all your help related to metabolomics.

Big thanks to present and former CMPS staff for creating a great environment at the department. Also, to present and former CMPS PhD students: **Helin**, **Carmen**, **Lovisa**, **Ipsita**, **Mads**, **Niels**, **Balder**, **Olof**, **Samuel**, **CJ**, **Camille**, and **Simon**, and others that I might have forgotten to mention, for your positive attitude! Best of luck with your journey toward a Dr. degree!

Humberto, **Judith**, **Swati**, and **Naveen,** for your friendship, board games (many more board games to play though!), hiking and camping tours, and other after-work activities!

All collaborators within **Mistra Environmental Nanosafety Program**, for fruitful meetings and discussions!

Mariana and **Irene**, thank you for your warm reception when I visited your lab in Barcelona. Thank you for all the new experiences and lessons learned!

Many thanks to my **parents**, my **brother**, and **his family**, for all your support during all those years while living abroad! *Jei ne jūs, nebūčiau pasiekus tiek, kiek pasiekiau! Didelis ačiū už viską!*

Last, but not least, the greatest thanks to my beloved husband **Vinardas**! You are the one I cannot thank enough!! Thanks for everything and, of course, for proofreading my thesis and giving such good advice! I love you!

Best wishes,

Egle

List of publications

This doctoral thesis is based on the following publications and a manuscript:

Paper I

Long-term exposure to nanoplastics reduces life-time in *Daphnia magna*

Egle Kelpsiene*, Oscar Torstensson, Mikael T. Ekvall, Lars-Anders Hansson, and Tommy Cedervall. *Scientific Reports*, **10**, 5979, 2020

Paper II

Metabolomics-based analysis in *Daphnia magna* after exposure to low environmental concentrations of polystyrene nanoparticles

Egle Kelpsiene, Tommy Cedervall*, and Anders Malmendal. *Environmental Science: Nano*, 2023

Paper III

Protein binding on acutely toxic and non-toxic polystyrene nanoparticles during filtration by *Daphnia magna*

Egle Kelpsiene, Irene Brandts, Katja Bernfur, Mikael T. Ekvall, Mariana Teles, and Tommy Cedervall*. *Environmental Science: Nano*, **9**, 2500-2509, 2022

Paper IV

Prolonged survival time of *Daphnia magna* exposed to polylactic acid breakdown nanoplastics

Egle Kelpsiene, Melinda Rydberg, Mikael T. Ekvall, Martin Lundqvist, and Tommy Cedervall*. *PLoS ONE*, **18**(9), e0290748, 2023.

Author's contribution to the papers

Paper I

Long-term exposure to nanoplastics reduces life-time in *Daphnia magna*

I, together with co-authors, planned the experiments. I have performed the experiment, characterization of PS NPs, and analyzed the survival and reproduction data. I wrote the first draft of the manuscript, as well as revised it according to the co-authors' and reviewers' comments.

Paper II

Metabolomics-based analysis in *Daphnia magna* after exposure to low environmental concentrations of polystyrene nanoparticles

I, together with co-authors, planned the experiments. I performed the experiment and characterization of PS NPs. Sample preparation and NMR spectroscopy were performed by Dr. Anders Bay Nord at the Swedish NMR Centre, University of Gothenburg. Dr. Anders Malmendal analyzed NMR data and did the statistical analysis. Zeta potential measurements were performed together with Dr. Martin Lundqvist. I wrote the first draft of the manuscript, as well as revised it according to the co-authors' and reviewers' comments.

Paper III

Protein binding on acutely toxic and non-toxic polystyrene nanoparticles during filtration by *Daphnia magna*

I, together with co-authors, planned the experiments. The initial experiments were performed by Dr. Irene Brandts. I repeated and performed new experiments. I characterized PS NPs. MS and MS/MS analysis were performed by Dr. Katja Bernfur. I have analyzed the raw data provided by Dr. Katja Bernfur. Dr. Martin Lundqvist performed zeta potential and FTIR measurements. I, together with co-authors, wrote the manuscript and revised it according to the reviewers' comments.

Paper IV

Prolonged survival time of *Daphnia magna* exposed to polylactic acid breakdown nanoplastics

I, together with co-authors, planned the experiments. The initial experiments were performed by a Master's student Melinda Rydberg. I repeated and performed new experiments. I characterized PLA NPs and PLA nanoplastics.

TEM images were taken by Dr. Ola Gustafsson at the Department of Biology, Lund University. I analyzed the data, wrote the manuscript partly based on Melinda Rydberg's Master's thesis, and revised it according to the co-authors' and reviewers' comments.

List of publications not included in thesis

I. Controlled protein mediated aggregation of polystyrene nanoplastics does not reduce toxicity towards *Daphnia magna*

Rebecca Frankel, Mikael T. Ekvall, **Egle Kelpsiene**, Lars-Anders Hansson, and Tommy Cedervall*. *Environmental Science: Nano*. **7**, 1518-1524, 2020.

II. Transfer of cobalt nanoparticles in a simplified food web: from algae to zooplankton to fish

Nanxuan Mei, Jonas Hedberg, Mikael T. Ekvall, **Egle Kelpsiene**, Lars-Anders Hansson, Tommy Cedervall, Eva Blomberg, and Inger Odnevall*. *Applied Nano*, **2**, 184-205, 2021.

III. Review of ecotoxicological studies of widely used polystyrene nanoparticles

Egle Kelpsiene*, Mikael T. Ekvall, Martin Lundqvist, Oscar Torstensson, Jing Hua, and Tommy Cedervall. *Environmental science. Processes & impacts*, **24**, 8-16, 2021.

IV. Size fractionation of high-density polyethylene breakdown nanoplastics reveals different toxic response in *Daphnia magna*

Mikael T. Ekvall, Isabella Gimskog, Jing Hua, **Egle Kelpsiene**, Martin Lundqvist, and Tommy Cedervall*. *Scientific Reports*, **12**, 3109, 2022.

V. Label-free detection of polystyrene nanoparticles in *Daphnia magna* and assessment of barrier integrity using an in vitro intestinal model

Jasreen Kaur, **Egle Kelpsiene**, Govind Gupta, Illia Dobryden, Tommy Cedervall, and Bengt Fadeel*. *Nanoscale Advances*, **5**, 3453-3462, 2023.

VI. The effect of natural biomolecules on yttrium oxide nanoparticles from a *Daphnia magna* survival rate perspective

Egle Kelpsiene, Tingru Chang, Aliaksandr Khort, Katja Bernfur, Inger Odnevall, Tommy Cedervall, and Jing Hua*. *Nanotoxicology*, 1-15, 2023.

Abbreviations

DLS	Dynamic light scattering
FTIR	Fourier-transform infrared spectroscopy
HDPE	High density polyethylene
LDPE	Low density polyethylene
MNP	Micro(nano)particle
MP	Microparticle
MS	Mass spectrometry
MS/MS	Tandem mass spectrometry
MW	Molecular weight
NMR	Nuclear magnetic resonance
NOM	Natural organic matter
NP	Nanoparticle
NTA	Nanoparticle tracking analysis
PAE	Phthalate
PDI	Polydispersity index
PE	Polyethylene
PET	Polyethylene terephthalate
PLA	Polylactic acid
PP	Polypropylene
PS	Polystyrene
PVC	Polyvinyl chloride
ROS	Reactive oxygen species
SDS-PAGE	Sodium dodecyl sulfate polyacrylamide gel electrophoresis
TEM	Transmission electron microscopy
UV	Ultraviolet

Background

Plastic pollution in the aquatic environment

Plastics were invented at the beginning of the twentieth century and from the 1950s onwards their production started to increase dramatically. Global plastic production has grown from 2 million tons in 1950 to approximately 390 million tons in 2021 [2]. Plastic gained a lot of attention not only because of its low production cost, but also due to its practical characteristics, such as lightweight, toughness, flexibility, and waterproof material. Different types of plastics are commonly used in packaging, the construction industry, vehicles, electronics, agriculture, and health care [3]. The most common ones in Europe are polypropylene (PP) and polyethylene (PE), the latter is available in high- (HDPE), medium-, low- (LDPE), and linear low-density resins, followed by polyvinyl chloride (PVC), polyethylene terephthalate (PET), and polystyrene (PS) [2]. PE, PP, PS, and polyphthalamide (a subgroup in the polyamide/nylon family) are among the most abundant polymer types detected in the aquatic environment [4].

The worldwide annual emission of plastic pollution to rivers, lakes, and oceans has been estimated to reach 53 million metric tons per year by 2030 [5]. It is quite alarming considering that of all the plastic produced, only 9-10% is recycled, 10-11% has been incinerated, and nearly 30% is still in use due to its long lifetime. The remaining 50% has been disposed in landfills [6]. In Europe, the annual plastic production has fluctuated for the last couple of years and increased from 53.9 million tons in 2020 to 57.2 million tons in 2021 [2]. Almost 5.5 million tonnes of plastic was recycled in 2021, representing an increase of about 20% compared to 2018 [2].

Large plastic pieces, macroplastics (diameter ≥ 5 mm), raise both esthetical and environmental issues. Large plastic pieces, the ones that are visible by the naked eye, are mainly released from disposable products that are produced in large quantities [7]. For example, plastic bottles, lids, and bags are among the most common objects found on European beaches [8]. Larger aquatic organisms are often exposed to plastic debris either via entanglement, which also includes

abandoned fishing nets, or ingestion, which can be intentional, accidental, or indirect (i.e., via ingesting organisms that have ingested the plastic). This has effects on movements, feeding, and reproduction, as well as might trigger skin damage. All mentioned adverse effects eventually might lead to death [9]. Macroplastics have become a serious threat to mammals, fish, reptiles, and seabirds [10,11] and is estimated to kill over 1 million aquatic animals each year [12].

Macroplastics are exposed to several physical, biological, and chemical degradation processes and, therefore, break down into smaller, micro- (< 5 mm and >1 μm) and eventually to nano- (< 1 μm or < 100 nm) plastics, which are often called secondary products [13]. These processes mainly occur due to various environmental conditions, such as photodegradation by ultraviolet (UV) radiation [14], wave action and sand friction [14], oxidative degradation [15], or biodegradation by microorganisms [16] (Figure 1). The produced broken down plastics, in the nano-size range, have different physicochemical properties in comparison with the bulk material, which will determine their environmental fate and risk [17]. Besides the degradation into smaller plastic pieces from macro pieces, micro(nano)particles (MNPs) can be intentionally engineered (primary products) with determined size and shape. The engineered MNPs may also eventually be released into the environment [18]. Primary MNPs can enter the water bodies through domestic waste, industrial activities, and personal care products [19]. Because most leaks of MNPs occur during the use of plastic-containing cosmetic and personal care products, several European Union (EU) countries have banned the use of MNPs in such products [20]. Further, in 2019, the EU established a law to ban the most common single-use plastic items, such as plastic cutlery, stirrers, and straws. EU member states aim to reduce packaging waste per capita by 15% by 2040. Restaurants that provide takeaways will be responsible to serve 40% of their meals in reusable or refillable packaging by 2040 compared with consumption in 2018 [21].

Micro(nano)plastics are ubiquitous and can reach the most distant areas of the world [22]. Micro(nano)plastics are present in nature in various forms, such as fragments, pellets, fibres, films, granules, and expanded polystyrene foam [23]. The distribution of micro(nano)plastics depends on the environmental conditions, polymer density, and biofouling level [24,25]. For example, while PE, PS, and PP tend to float due to their low density (~1 g/cm^3), PET and PVC are more likely to sink (>1 g/cm^3). Due to many various factors, the distribution and fate of micro(nano)plastics are difficult to monitor and quantify [26]. However, most micro(nano)plastics released to land will finally end up in the marine environment [27-29]. Rivers are the main pathways for plastic to enter seas [30]. For example, ten rivers in the world (eight in Asia and two in Africa) are

the source of 90% of the plastic that reaches the sea every year [29]. Lebreton *et al.* [27,31] estimated that between 1.15 and 2.41 million tonnes of plastic waste enter the sea every year.

The presence and chemical composition of nanoplastics in seawater samples have been identified in the North Atlantic Subtropical Gyre [32], as well as quantified in the surface water samples from lakes and streams in Siberian Arctic tundra (mean 51 μg/L), a forest landscape in southern Sweden (mean 563 μg/L) [22], and snow samples in the remote high-altitude Alps, Austria (mean 46.5 μg/L) [33]. It is worth mentioning that PS was not found either in southern Sweden or in high-altitude Alps, Austria. However, the highest concentrations were quantified for PE, followed by PP, PVC, and PET in Sweden [22], whereas, mainly PP and PET were identified in the high-altitude Alps, Austria [33]. PS, as well as PE, PP, and PVC, were found in Siberian Arctic tundra [22] and the surface waters of Italian Subalpine [34]. However, the presence of PS breakdown products, such as styrene oligomers were reported in different water bodies [35,36].

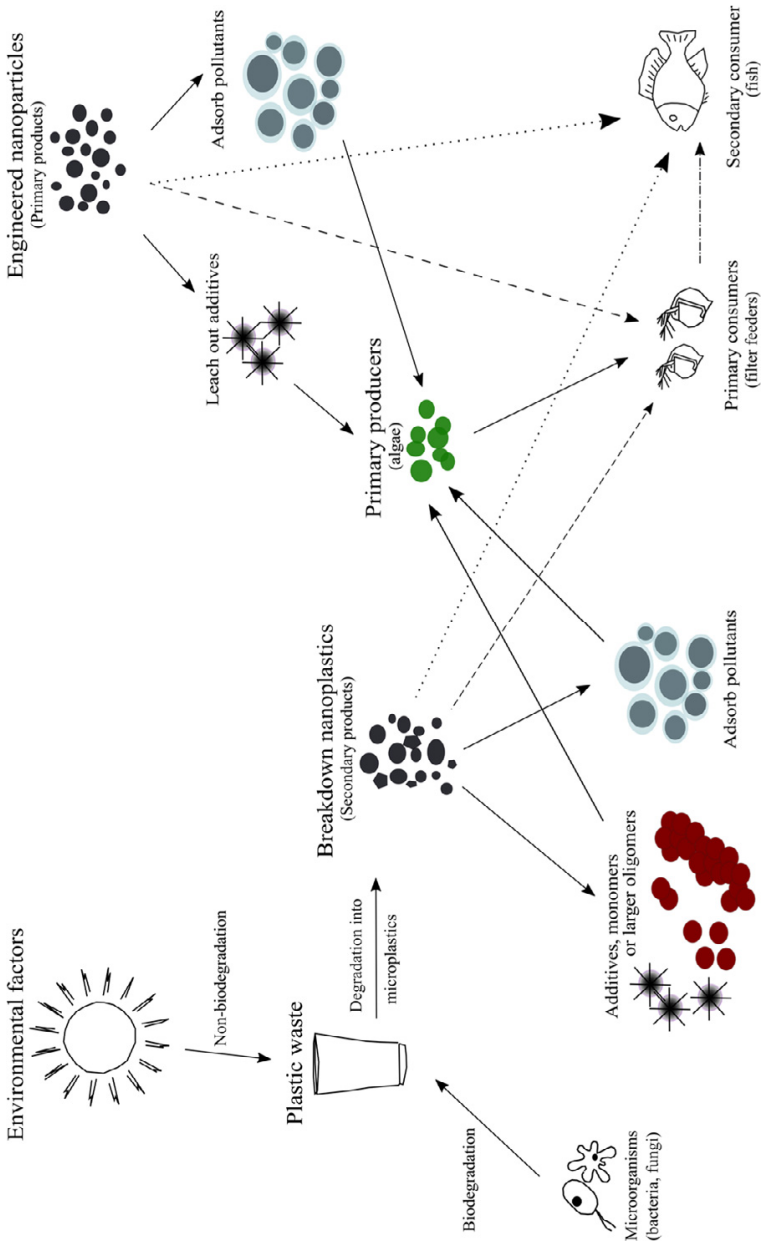

Figure 1. Flow diagram of the fate of plastic particles in the natural environment. Plastic nano-sized particles can enter the aquatic food web either as a breakdown nanoplastics or as engineered nanoparticles. NPs can be passively taken up by fish with ingested water (dotted line arrows), migrate through the aquatic food web (solid black line arrows) or be taken up directly (dashed line arrows) by primary consumers (filter feeders) and transferred (dash-dotted line arrow) to the secondary and top consumers (fish). Reprinted with permission and modified from Kelpsiene *et al*., 2021 [37].

The term *"nanoparticle"* is often defined as an intentionally produced particle, which has at least one dimension between 1 nm and 100 nm and is homogenous in shape and size [38,39]. PS NPs are often used as model particles for nanoplastics in toxicological studies due to their uniform size and composition. The term *"nanoplastics"* refers to particles that were unintentionally produced during the degradation process of the larger plastic objects [40]. NPs and nanoplastics share similar properties, however, it is thought that breakdown products in the environment are often diverse in size and shape, which can affect their stability and biological impact. The breakdown process also changes the surface chemical composition compared to the bulk material [40,41]. Due to small sizes, relatively low concentrations, and interaction with various substances in nature, it is difficult to separate and identify nanoplastics [40].

In the present thesis, the term *"nanoplastic"* will be referred to broken down plastic particles, released after the mechanical breakdown process, whereas *"nanoparticle"*, with an abbreviation NP(s), will be used for engineered polystyrene nanoparticles.

Degradation of plastics

Plastic objects degrade into micro- and eventually nanoplastics (Figure 2) after being subjected to environmental factors, such as light, heat, moisture, physical, and biological activities[26]. Degradation refers to any physicochemical bulk material changes, which includes surface embrittlement and cracking, as well as changes at the molecular level such as the formation of new molecules due to bond cleavage or oxidation of long polymer chains [42].

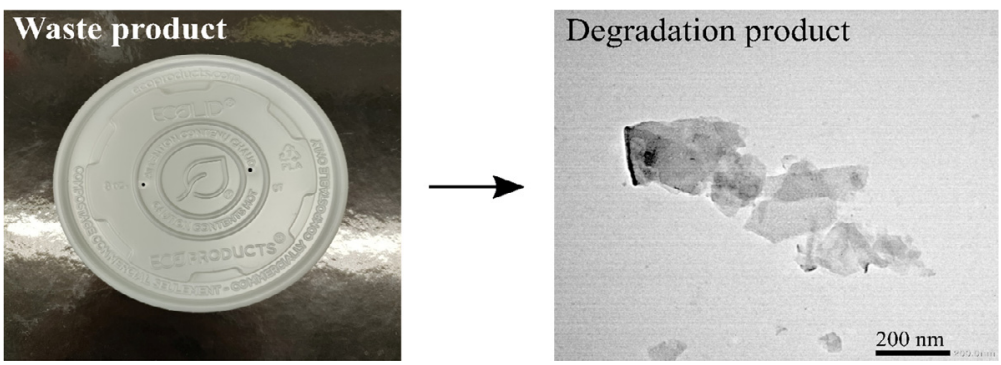

Figure 2. TEM image of PLA plastic soup lid breakdown nanoplastics (on the right) after a mechanical breakdown by using food immersion blender (**Paper IV**).

Degradation of plastics is primarily triggered by UV radiation and visible light in the natural environment. Besides physicochemical modifications, plastics exposed to sunlight experience visual changes [43]. Virgin plastic pellets are often white or colorless, whereas field-collected weathered plastic pellets include yellowish, orange, brownish, and darker colors [44,45]. The color change might be related to chemical modifications and the adsorption of contaminants from the environment [43]. Plastics are further fragmented when it is additionally subjected to mechanical forces, such as wave action or abrasion with sand, followed by biological degradation [46].

Thermal degradation of plastics refers to degradation of the polymer at elevated temperatures that does not require the involvement of oxygen [47]. For example, LDPE and PS thermally degrade at 425 ˚C [48] and 850 ˚C [49], respectively. Hydrolysis degrades polymers, which have a hydroxyl group in it, for example, PET or PLA [42,50,51]. Whereas polymers with carbon-carbon backbones, such as PS, PP, PE, or PVC, are extremely resistant to degradation [52].

Biological degradation, involving living microorganisms, can be aerobic, anaerobic, occurring in sediments and landfills, and partly aerobic and anaerobic, which takes place in composts and soil [53]. Most identified bacteria that degrades plastic belong to the phyla Proteobacteria, Firmicutes, and Actinobacteria [54]. For example, bacterial isolates, such as *Bacillus* sp., *Citrobacter* sp., *Pseudomonas* sp., *Rhodococcus* sp., *Stenotrophomonas* sp., or others are able to degrade various polymers, such as PP, PE, PS, PET, LDPE, or PLA [54-58].

Mechanisms of nanoparticles toxicity

The uptake, fate, and toxicological effects of NPs depend on their physical and chemical properties, such as size, surface charge, shape, and stability [59,60]. All of these in some way affect how NPs interact with living systems and up till now, there is no clear indication which of these parameters are the key factors affecting the toxicity.

The smaller the particle the greater the surface-to-volume ratio, which determines their high reaction capacity and catalytic activity [59]. The number of particles increases due to the breakdown process. This leads to a greater total surface area of nanoplastics to adsorb larger amount of pollutants and their ability to enter the cells [18]. Therefore, nanoplastics become an even larger risk to the environment compared to microplastics. Size-dependent toxicity has

been shown for *Daphnia magna* after exposure to 55-330 nm PS NPs in 24 h toxicity test. The results showed that smaller (50 nm) induced acute toxicity while larger (120-330 nm) PS NPs did not [1]. Size-dependent adverse effects have also been shown for other organisms, for example, the unicellular dinoflagellate *Karenia mikimotoi* [61], nematode *Caenorhabditis elegans* [62], earthworm *Eisenia fetida* [63], and zebrafish *Danio rerio* larvae [64] after exposure to PS NPs.

Surface charge determines NPs ability to interact with biological systems [65,66]. Positively charged NPs are known to interact more with cell membrane than neutral or negatively charged particles [67]. Positively surface charged (PS-NH_2) PS NPs have been shown to induce greater toxicity towards various aquatic organisms, such as *D. magna* [1,68], green algae *Pseudokirchneriella subcapitata*, *Scendesmus* sp., *Chlorella* sp. [69,70] or zebrafish *D. rerio* [71], compared to negatively charged (PS-COOH) PS NPs.

NPs are often synthesized in various shapes, for example, spheres, sheets, tubes, rods, etc. Spherical NPs are more susceptible to be taken up by cells compared to nanotubes and nanofibers [72,73]. Furthermore, the formation of aggregates is an important process as aggregates of NPs are thought to sediment faster. Particle aggregates potentially might reduce toxicity compared to dispersed NPs, which are more mobile and available to be taken up by organisms and thus more toxic [74].

Effects of nanoparticles to aquatic organisms

PS NPs are often used as model particles for nanoplastics, which allows to have controlled exposure scenarios and experimental reproducibility. Numerous published papers are showing that such particles interact and have adverse effects on various living organisms from different ecological niches. It has been shown that 80 nm PS NPs decrease the bacterial diversity in aquatic systems [75] and 50 nm to 70 nm PS NPs damage algae cells' photosynthesis [76,77]. Various sizes (26 nm to 100 nm) of PS NPs have been shown to accumulate in the gut [78], affect the feeding behaviour [79], reduce reproduction [76,79], and survival [1,78,80] in *Daphnia* sp. Additionally, 50 nm PS NPs have been shown to travel through a food web, starting with algae, and have an effect on metabolism, behavior [1,81], as well as trigger immune and antioxidant responses [82], and provoke DNA damage [83] in a top predator, fish.

It is worth mentioning that most of the studies focus on effects after short-term exposure and use high concentrations (ranging from 10 mg/L to 1100 mg/L) of PS NPs. Considering published papers that focus on the effects on *Daphnia* sp. caused by PS NPs (excluding fluorescent PS NPs or tests caused by combined effects), most of them performed acute toxicity tests (≤96 h; 12 studies out of 21 studies, Table 1, Figure 3). Nine studies out of 21 studies performed no longer than 21 days exposure, and only two papers (that are presented in this thesis, **Papers I** and **II**), focused on longer than 21 days toxicity.

However, there is a need to evaluate the toxicity of more realistic particles, such as breakdown nanoplastics, which are more diverse in shape and size. To date, there are only a few studies available showing the effects of breakdown nanoplastics on *Daphnia* sp. For example, HDPE breakdown nanoplastics (~110 nm) showed that a purified nanoplastics fraction does not induce significant mortality in *D. magna* after a life-time exposure, but small molecules released from HDPE breakdown nanoplastics do [84]. I showed that PLA breakdown nanoplastics did not have adverse effects on *D. magna*, contrarily nanoplastics from a PLA plastic cup extended survival rate in *D. magna*, showing a significant difference compared to a control group (**Paper IV**).

Table 1. Summary information on published papers that focus on the exposure of PS NPs to *Daphnia* species. 'Conc.' stands for concentration and 'sign' stands for significant. For clarification, papers mentioned in this table were reviewed until the 27th of July, 2023.

Exposure period	PS NPs		Lowest conc. (mg/L; unless stated differently) showed sign. results	Ref.
	Size (nm)	Concentration (mg/L; unless stated differently)		
24 h	100	0.1–1000	1	[85]
	50	25–150	75	[1]
	20–100	0.5–20	EC_{50}=2.45±0.12	[86]
48 h	26, 100	0.0001–100	EC_{50}=13.0±1.4	[87]
	50–100, 110, 300	1–100	LC_{50}=5.24	[88]
	50	1.4 and 2.7	1.4	[80]
	130–150	0.3–4.8 mmol	EC_{50}=1.28 mmol	[89]
	20–100	0.5–100	0.5	[90]
48 h and 96 h	75	10-400 and 0.1, 1	LC_{50}=80.02 and 0.1*	[91]
48 h and 21 days		10-400 and 0.1-2	LC50=76.69 and 0.1*	[92]
96 h		1	1	[93]
21 days	75	0.1-2	0.5	[94]
		0.1-2	0.1	[95]
		1	1	[96]
		0.1-2 and 0.0001	0.0001	[97]
		0.1-2	0.5	[98]
		0.01-2	0.1	[99]
		0.001	0.001	[100]
	70	0.22–150	0.22	[76]
37 days	53, 62	0.0032-0.32	0.0032	[101] (**Paper II**)
103 days	26, 53, 62	0.0032–7.6	0.32	[78] (**Paper I**)

*Two different experiments performed in studies, therefore there are two lowest concentrations that showed significant differences.

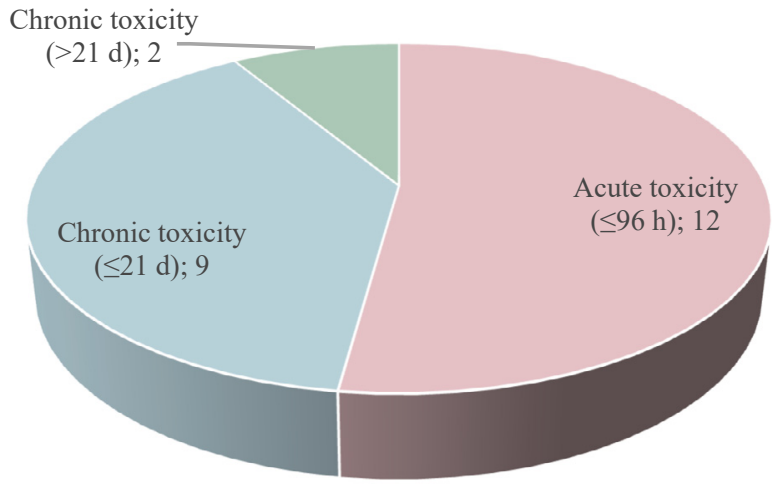

Figure 3. A pie chart represents data corresponding to the data shown in Table 1. Most of the published studies focus on the effects of PS NPs after acute (up to 96 h) exposure or 21 days exposure, 12 and 9 publications, respectively, to *Daphnia* species. To date, there are only two published studies (**Papers I** and **II**), that focused on longer than 21 days exposure scenarios (103 days and 37 days, respectively).

Plastic additives – an underestimated concern

Plastic polymers are known to have more than 400 intentionally added compounds [102], many of which are regulated under European and North American legislation to limit their negative effects. There are various types of additives used in plastics, for example, plasticizers, antioxidants, antimicrobials, UV stabilizers, and many more, which are added during polymerization and processing to improve the physical and chemical properties of the material [103,104]. Such additives are found not only in standard plastics but may also be detected in bioplastics or biodegradable polymers [105]. Most of these compounds are weakly bonded to the polymer and can therefore easily leach out from the material and move through the environmental matrices [103,106].

Phthalates (PAEs), bisphenols, and polychlorinated biphenyls are well-known additives and have been proven to have adverse effects on living organisms and shown to interfere with normal hormonal processes [107]. Therefore, since

2011, Europe banned various PAEs compounds in plasticized materials related to children's toys [108]. Additives are shown to be more toxic to biota compared to 'pure' plastics. As mentioned previously, small molecules released from HDPE breakdown nanoplastics exhibited greater toxicity towards *D. magna* compared to purified nanoplastics fractions [84]. Furthermore, *D. magna* exposed to flexible PVC MPs containing the plasticizer diisononylphthalate induced morphological changes and reduced number of offspring. Whereas, the exposure to rigid PVC MPs lacking plasticizer did not induce toxic effects in *Daphnia* [109].

These are important findings suggesting that even though some plastic debris might be difficult to ingest by organisms, long-term effects can derive from additives leaching into the environment. Therefore, there is a need to further explore the effects caused by additives, as well as their interaction with biota.

Corona formation on the surfaces of nanoparticles and its biological impact

Once NPs enter the environment or biological fluids, they adsorb proteins and other biomolecules that will form a layer called corona, which can be either environmental (eco-) or biological (bio-) corona, depending on the environment the particles are in [110,111]. Initially, NPs interact with a different mixture of biomolecules in the environment and form eco-corona outside an organism. The eco-corona is mainly composed of metal ions, inorganic anions, and organic chemicals [112]. However, once NPs are internalized by an organism and enter biological fluids, the eco-corona develops into a bio-corona or protein corona. The latter corona consists of proteins, lipids, polysaccharides, and metabolites [113-116]. Corona layer formed on the surfaces of NPs is an important factor as the cell identifies and interacts with the entire complex of NP-corona rather than with the "naked" entity of an NP [117]. The corona layer influences the identity, stability, migration, cellular uptake, toxicity, and circulation time of NPs [118-120].

Proteins remain fundamental in studies focusing on coronas, due to their important role in receptor engagement and signalling, as well as relatively simple identification. Proteins, adsorbed to surfaces on NPs, provide a biological identity to nanomaterials [121]. The formation of protein corona is dynamic and mainly depends on the features of NPs such as size [122], charge [123],

and colloidal stability [124], as well as temperature [125], pH, UV exposure [126], incubation time [119], and types and concentrations of proteins [127].

Proteins have different affinities towards NPs, which determines the proteins that would be adsorbed to the surface of the NP. Proteins with a higher affinity form "hard" corona, and are more tightly bound to the surface, whereas proteins with lower binding affinity form "soft" corona, and such proteins can be removed after several washes with isotonic buffered solution [128-130]. Due to the Vroman effect, even though the most abundant proteins bind first, they will be replaced over time with proteins with higher affinity but lower concentration [131].

The protein corona serves as a coating, which reduces the direct damage induced by NPs by limiting the interaction between NPs and the cell membrane [132,133]. Although bare NPs exist only for a short period in the blood system, they can affect the vitality of endothelial cells, trigger thrombocyte activation, and induce hemolysis [119]. Bare NPs are both taken up more by human cells and adhere to the cell membrane compared to those with the presence of pre-formed corona [134].

Natural organic matter (NOM) is a complex matrix of organic materials, which is abundantly present in the environment, and can interact with NPs that come into contact with it [135]. NOM can derive from degradation products of organic matter, such as humic acid, fulvic acid, etc., or fractions released from organisms, such as proteins, carbohydrates, etc. [136]. Similarly, to protein corona, NOM can also adsorb to the surface of NPs and thereby affect their stability, mobility, and toxicity [135,137,138]. NPs interaction with NOM has previously been shown to influence the environmental fate of metallic NPs [139,140]. The reduced toxicity towards *Ceriodaphnia cf. Daphnia* and *D. pulex* has been observed after exposure to copper and zinc NPs in the presence of NOM [141,142]. The biomolecules, which derived from *Daphnia* as excretion products, have been shown to reduce the toxicity towards *D. magna* after exposure to PS NPs, tungsten carbide–cobalt NPs, and yttrium oxide NPs [85,143,144].

Bioplastics – promising alternatives (?)

In recent years, bioplastics have attracted considerable attention as an environmentally friendly alternative to synthetic plastics. Currently, bioplastics, including biobased and biodegradable plastics, still represent less than 1% of plastics produced annually. However, global bioplastics production

is set to increase from approximately 2.23 million tonnes in 2022 to approximately 6.3 million tonnes in 2027 [145]. The Swedish association of grocery retailers aim that all plastic packaging should be produced of either renewable or recycled raw materials by 2030 [146].

The term *"bioplastics"* is often used to describe two main groups of plastics: (1) bio-based plastics, which at least partly are made from biological matter, and (2) biodegradable plastics, which have been produced in a way that could be broken down by microorganisms at specific conditions [147]. For plastic to be considered biodegradable, they need to fully undergo a biodegradation process [148].

For example, PLA plastics are considered bio-based and biodegradable polymers and have recently received a lot of attention. PLA is one of the most widely used biodegradable polyesters, which is synthesized via chemical polymerization of lactic acid. Lactic acid is produced during the fermentation of glucose, which can be obtained from various sources of sugar [149]. Worth mentioning that PLA degrades under specific conditions, which include an oxygen environment, high temperature (58-80 ˚C), high humidity (>60% moisture), and the presence of microorganisms [150]. The degradation of a PLA brush (a structure in which one end of a polymer chain is fixed to a solid surface in a solvent [151]) with a thickness of ~10 nm takes between 25 to 450 hours at 37 ˚C from pH 8 to pH 7 [152]. Whereas there was no obvious degradation of PLA brushes when acidic buffers (pH 6 and pH 3) were used [152].

Biodegradable plastics offer promising alternatives in terms of end-of-life management of plastics, yet the decomposition of biodegradable plastics will be incomplete in the natural environment, as the degradation of such plastics occurs under certain conditions. Therefore, it will result in the generation of MNPs [153]. Liu and co-authors showed that more secondary nanoplastics were released from biodegradable PLA plastics compared to PS plastics after 60 days of degradation [154]. The knowledge about PLA MNPs is still limited, however studies are showing that PLA MPs (between ~50 μm and ~65 μm) have negative effects on European flat oyster *Ostrea edulis* [155], blue mussels *Mytilus edulis* [156], and zebrafish larvae and adults [157,158].

Conventional plastics more often are replaced with bioplastics especially in food packaging ware to reduce plastic pollution. It is an almost impossible task to create or find a material that would have full functionality and entirely biodegrade in each environment. Furthermore, the degradation rate of biodegradable plastics is not higher than 10 % within one year in freshwater or seawater [159], suggesting that biodegradable plastics can remain for a long time in water systems. The information about the effects caused by bioplastics is

still limited. Therefore, there is a need to focus more and get a better understanding of the effects caused by bioplastics on various aquatic organisms in future studies.

Research objectives

The broader scope of this thesis was to get a better understanding of the effects caused by both NPs and nanoplastics using keystone species *D. magna,* commonly found in most freshwater ecosystems. Papers included in this thesis have specific and at the same time overlapping objectives.

Acute (24-48 h) exposure scenarios usually use high concentrations of toxicants and do not provide a full picture regarding NPs toxicity, especially when it comes to low concentrations. Therefore, I performed long-term experiments in **Papers I** and **II** using low concentrations of PS NPs. Secondly, in **Papers II** and **III**, I focused on possible mechanisms behind toxicity of PS NPs. Finally, I aimed to evaluate the effects caused by biodegradable nanoplastics compared to synthetic PS NPs (**Papers I** and **IV**).

Specifically, in **Paper I**, I assessed the effects of PS NPs with sizes ranging between 26 nm to 62 nm in *D. magna* after a life-time (103 days) exposure at low concentrations. In **Paper II**, metabolomic responses in *D. magna* were analyzed after long-term (37 days) exposure to differently surface charged but similar sizes (53 nm and 62 nm) PS NPs at low concentrations. In **Paper III**, I analyzed proteins that bind to differently surface charged and sized (53 nm to 200 nm) PS NPs after passing through the digestive system of *D. magna*. **Paper IV** focused on the effects of PLA NPs (250 nm) and PLA breakdown nanoplastics (~170 nm) released from various items in *D. magna*.

Materials and Methods

Model organism

Daphnia sp. are small crustacean zooplankton (adults range from < 1 mm to 5 mm in size, Figure 4), which belong to the Cladocera superorder. *Daphnia* sp. play an important role in ecosystems as they transfer energy from the bottom of the food chain to species at higher levels [160]. The genus *Daphnia* includes more than 100 known species of freshwater organisms commonly found in ponds and lakes. *Daphnia* sp. are often used in ecotoxicological studies due to their importance in the food webs, short generation time, and unique life cycle [161]. *Daphnia* sp. are filter feeders, where the food is taken up with the help of a filtering apparatus, which produce a water current. *Daphnia* sp. can feed through either active filtration or passive uptake. *Daphnia* sp. actively feed on particles from around 1 µm up to 50 µm [162], however, it has been shown that individuals can ingest particles lower than 100 nm in size [162,163] or even up to 300 µm [164]. The gut of daphnids consists of three parts: the esophagus, the midgut, and the hindgut, with a pH ranging from 5.5-6.0 at the anterior section up to 7.2 in the posterior section [165]. The color of the gut depends on the diet. The gut of *Daphnia* sp. feeding on green algae, for example, *Scenedesmus* sp., is green or yellow [160].

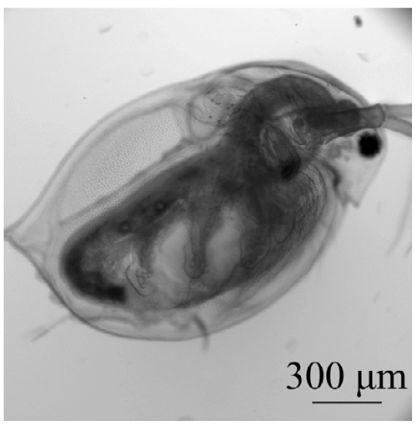

Figure 4. *Daphnia magna* adult (photo by Egle Kelpsiene).

Daphnia sp. mainly reproduce asexually through parthenogenesis. The female produces a first clutch of eggs after around 5-10 days in the brood chamber. The embryos hatch in the brood chamber after one day and are released from the brood chamber after about three days. Offspring are clones of the mother, except that the brood chamber is not already developed [160]. *Daphnia* sp. may survive up to 60 days

under laboratory conditions and produce a clutch of eggs every 3-4 days until death [160]. However, in **Paper I**, daphnids survived up to 103 days under laboratory conditions.

D. magna was used as a model organism to study the effects caused by PS NPs (**Papers I-III**), PLA NPs, and PLA breakdown nanoplastics (**Paper IV**). The *D. magna* culture used in all studies presented in this thesis originates from Lake Bysjön, southern Sweden (55°40′31.3″N 13°32′41.9″E) and has been kept in the laboratory for several hundred generations.

Plastics and their preparation

Differently surfaced charged (aminated and carboxylic) PS NPs with sizes ranging between 26 nm to 200 nm were purchased from Bangs Laboratories Inc. (www.bangslabs.com) and used as model particles for nanoplastics in **Papers I-III**. Before the experiments, PS NPs were diluted to 10 mg/mL and dialyzed in Standard RC Tubing, Dialysis Membrane (MWCO: 3.5 kD) for either 24 h (**Paper I**) or 72 h (**Papers II-III**) at 4 ˚C in 10 L of MilliQ water to separate the NPs from additives creating a stock solution suitable for testing the effects caused by NPs.

PLA NPs (250 nm) were purchased from CD Bioparticles (www.cd-bioparticles.com) and used in **Paper IV**. PLA NPs were diluted to 10 mg/L and dialysis was performed in the same manner as for PS NPs in **Papers II-III**.

To evaluate the effects of various PLA items available in supermarkets were chosen as the model plastic in **Paper IV**. The PLA plastic was broken down using the protocol previously published for PS and HDPE [41,84]. Briefly, two grams of unpigmented plastics were cut into small pieces (ca. 1×1 cm) into a glass beaker and rinsed with tap water. The beaker was filled with 200 mL tap water and a Bosch ErgoMixx 600 W hand-held food blender was turned on at maximum speed for 2 minutes. A 50 mL syringe was used to remove 100 mL of the water and filtered through a 0.8 µm cellulose acetate syringe filter (Whatman, GE) into a glass bottle storage container. The breakdown process was repeated to prepare 500 mL.

Techniques for nanoparticles characterization

It is important to characterize NPs to ensure the reproducibility of toxicological studies, as well as it is crucial to understand how the physical and chemical properties of NPs influence the observed effects [166]. Several techniques were used to characterize the sizes and stability of NPs and nanoplastics used in **Papers** presented in this thesis. Techniques will be briefly overviewed in the following sections.

Dynamic light scattering (DLS) is used to determine the NPs sizes, ranging between 1 nm and 1000 nm, in colloidal suspension and based on the principle of Brownian motion [167]. DLS provides the size distribution of the particles assuming they are spherical. Even though non-spherical particles can be measured, the contribution of rotational diffusion of non-spherical particles is not considered and might give false results in terms of size. DLS is used to measure the hydrodynamic size of particles of dispersed colloidal samples, to study the stability of formulations, and to detect the presence of aggregation and agglomeration [168]. The accuracy of the results might be reduced due to aggregation or agglomeration of the particles [169], as well as measurements can depend on pH, temperature [170], or viscosity of the solvent [171]. Samples should be prepared in solvents, such as water, ethanol, or diluents, for example, 10% methanol in water, otherwise, it can interfere with background noise and give false results. It is recommended not to prepare particles in deionized water as the sizes obtained in deionized water are often 2-10 nm larger than the actual sizes. Higher concentrations of NPs can result in artificially smaller sizes, whereas too diluted samples might not be analyzed due to not enough scattered light, therefore it is important to find an optimal concentration of the sample [172]. It is suggested to run serial dilutions on DLS to determine the optimal concentration and observed any size changes. Similarly, artificial sizes can be observed if particles are agglomerated or aggregated, as large agglomerates will scatter more light, giving misleading results as the larger-sized particles will dominate the signal. Samples should be clear and homogenous. It is recommended to avoid fluorescent NPs on DLS as they can interfere with a wavelength of the laser and, thus, particle sizes might be incorrect [172]. Otherwise, control experiments are needed to be performed to assess any possibility of absorption of light by fluorophores.

While using DLS, ***the polydispersity index*** (PDI) is also measured, which describes the degree of non-uniformity of the size distribution of particles. PDI values vary between 0 to 1, where for the perfectly uniform sample, PDI should

be equal to 0. Whereas PDI values greater than 0.7 indicate that the sample has a broad particle size distribution and is not suitable to be measured by DLS [173].

Particle sizes were characterized using DLS on DynaPro Plate Reader II (Wyatt instruments, USA) in **Papers I-IV**.

Nanoparticle tracking analysis (NTA) is a technique that obtains size information by tracking single particles based on their diffusion coefficient in successive optical video images [167]. NTA can detect particles with sizes between 30 nm and 1000 nm and concentrations of 10^7–10^9 particles/mL, therefore dilution of the sample is often required to identify and track particles [167]. The NTA software can detect and track individual NPs based on Brownian motion by relating the movement to the particle size. NTA results often have high error bars, which can be a consequence of different particle counts between measurements, as the software can detect more or slightly fewer particles between several measurements of the same sample [174]. NTA requires at least 0.7 µL of the sample and provides a concentration of particles/mL, however, the concentration reported is not fully accurate. The great advantage of NTA is that it allows to distinguish two or more size populations occurring in the sample.

Concentrations (particles/mL) and sizes of particles were measured by NTA NanoSight LM10 (Amesbury, UK) in **Paper IV**.

Zeta potential measures the surface charge of NPs, which is an important parameter to determine the physical stability of nanosuspensions [175]. A colloid system is considered to be stable when zeta potential values are greater than +30 mV or lower than -30 mV [176]. Low zeta potential values might result in particle aggregation and flocculation due to the van der Waals forces and, therefore, indicate particle physical instability [177]. It is worth noting that depending on the pH of the medium, zeta potential might be more positive or more negative. Additionally, the presence of ions or biomolecules in the medium can interact with NPs and thus influence the dispersion and zeta potential measurements. The concentration of the sample also affects the measurements, as in more concentrated samples, zeta potential values increase, and opposite, they decrease within a dilution factor [172].

Surface charges of NPs were measured using Zetasizer Ultra or Zetasizer Nano ZS (Malvern Instruments, Worcestershire, UK) in **Papers II-IV**.

Fourier-transform infrared spectroscopy (FTIR) is a vibrational spectrometry used to identify and characterize organic, inorganic, and polymeric materials, as well as detecting contamination in a material, finding additives, and identifying oxidation or decomposition. In IR spectroscopy, some of the IR radiation passes through a sample and some of it is adsorbed [178]. The IR spectrum of the sample shows the excitation of vibrational modes of the molecules, which correlates to chemical bonds and functional groups present in the molecule. Materials have their unique composition and differently arranged atoms. Therefore, two compounds will never have the same IR spectrum, allowing to identify and characterize materials. Middle IR region (4000-300 cm^{-1}) is most used and divided into four regions: (1) the single bond region (~2500-4000 cm^{-1}; O-H, N-H, C-H), (2) the triple bond region (~2000-2500 cm^{-1}; C≡C, C≡N), (3) the double bond region (~1500-2000 cm^{-1}; C=C, C=O, C=N), and (4) the fingerprint region (~600-1500 cm^{-1}) [179].

FTIR characterization of the chemical composition of particles used was performed on Spectrum Two (PerkinElmer) in **Papers III** and **IV**.

Transmission electron microscopy (TEM) is based on a beam of electrons that creates an image of the specimen. TEM uses electrons, which after the beam passes through the specimen, which should be relatively thin, either scatter or hit a fluorescence screen at the bottom of the microscope. The complete removal of the suspending liquid is often required for sample preparation for TEM. Drying can often introduce artifacts in terms of non-uniform particle deposition and particle aggregation [180]. Therefore, data generated by TEM should be critically evaluated as particle sizes determined based on TEM images might be inaccurate.

Samples for TEM were left to dry on a pioloform-coated single-slot grid (Ted Pella, Cu, Pelco Slot Grids, USA). TEM images were taken for PLA NPs and PLA soup lid breakdown nanoplastics using JEOL JEM-1400 PLUS TEM operated at 100 kV (JEOL Ltd., Japan) in **Paper IV**.

Exposure scenarios

I performed long-term (103 and 37 days) and acute (4 h and ~10 days) experiments in **Papers** presented in this thesis. In the following sections, I will briefly overview set-ups of toxicity tests performed in different **Papers**.

A long-term (103 days) toxicity test was performed to assess the potential effects on survival and reproduction in *D. magna* at low particle concentrations (**Paper I**). Briefly, daphnids were exposed to positively and negatively surfaces charged PS NPs (26 nm, 62 nm, and 53 nm) at concentrations ranging from 0.32 mg/L to 7.6 mg/L. A concentration of 0.32 mg/L was chosen based on preliminary data from the pilot experiment. In total there were 10 replicates for each treatment, having one individual in each glass jar with 80 mL total volume. Throughout the whole exposure period, every third day, alive *D. magna* individuals were gently transferred to a new medium containing 2.5 mL food (algae), with (treatment group) or without (control group) NPs, as shown in Figure 5. Prior to each transfer of alive *D. magna* individuals to a new medium, water was aerated for 24 h to increase the oxygen level. Algae culture was filtered through 20 μm mesh filter to remove larger algal species, such as cyanobacteria, from the culture. The survival rate of daphnids was checked every day, whereas the reproduction rate was checked every third day during the transfer to new media. The oldest daphnid survived for 103 days.

Kaplan Meier survival curves analysis was performed using statistical computing software GraphPad Prism, www.graphpad.com, and one-way ANOVA was used to test for differences in reproduction output in R version 3.6.1, www.r-project.org.

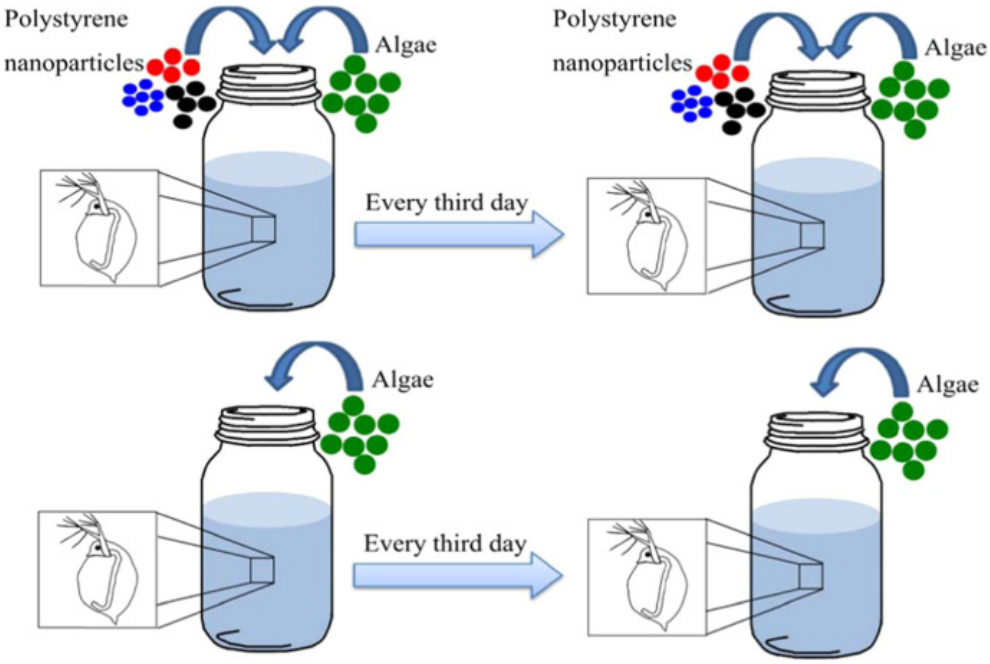

Figure 5. Schematic representation of long-term toxicity test. During the exposure to polystyrene nanoparticles, alive *D. magna* individuals were transferred every third day to fresh medium, containing 2.5 mL of food (algae), with (treatment, upper pictures) or without (control, lower pictures) NPs. Reprinted with permission from Kelpsiene *et al.*, 2020 [78] (**Paper I**).

A long-term (37 days) toxicity test to analyze how the metabolome is affected by PS NPs type, concentration, and daphnid aging after exposure to low concentrations (320 µg/L, 32 µg/L, and 3.2 µg/L) using ^{1}H nuclear magnetic resonance (NMR) metabolomics (**Paper II**). Here, *D. magna* were exposed to positively and negatively surface charged PS NPs (53 nm and 62 nm, respectively). In total, there were 5 replicates for each treatment, with 10 individuals in each glass jar with 80 mL total exposure volume. To fix samples for NMR measurements, the following was performed: Eppendorf tubes containing daphnids were placed in a mixture of dry ice and 99 % acetic acid to quench the metabolism at a similar time of the day to minimize metabolites variation due to the time. The remaining alive *D. magna* individuals were transferred to a fresh medium with (treatment group) or without (control group) PS NPs, containing 5 mL of food (algae), as it is shown in Figure 6. Algae culture was filtered through 20 µm mesh filter before adding to *D. magna*. All offspring were removed once a week during the transfer to a fresh medium. The experiment lasted for 37 days to have at least 6 time points.

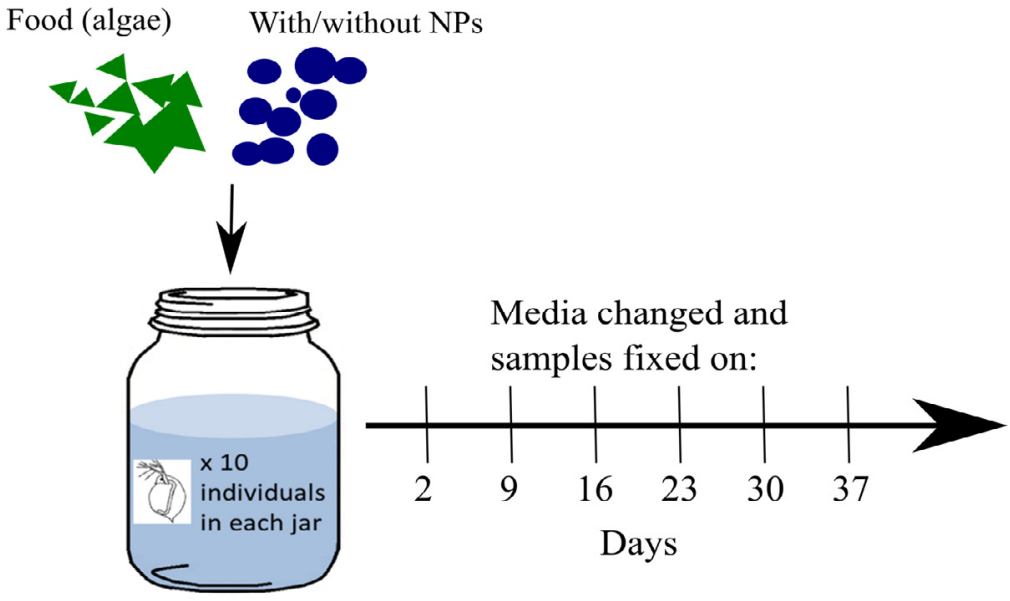

Figure 6. Schematic representation of long-term toxicity test. During the exposure to PS NPs, alive *D. magna* individuals were transferred once a week at similar time of the day to a fresh medium with (treatment) or without (control) PS NPs, containing 5 mL of food (algae). Reprinted with permission from Kelpsiene *et al*., 2023 [101] (**Paper II**).

An acute (4 h) incubation with PS NPs to identify the protein profile bound to positively and negatively surface charged PS NPs (53 nm, 62 nm, and 200 nm) after passing through the digestive tract of *D. magna* (**Paper III**) using mass spectrometry (MS) and tandem mass spectrometry (MS/MS). In this study, *D. magna* was incubated with (treatment group) or without (control group) PS NPs for 4 h. In total there were four replicates for each treatment, with a total of 5 mL of exposure medium. Before the exposure, *D. magna* were left in the clean water for 24 h to allow for gut evacuation as daphnids are grown in the culture where they are fed with algae *ad libitum*. After incubation with or without PS NPs, all daphnids were removed from the 15 mL Falcon tubes, and the NP-proteins complexes were recovered by centrifugation in Eppendorf tubes at 18 000 g for 30 minutes, as it is shown in Figure 7. Proteins then were digestive in solution or in a gel.

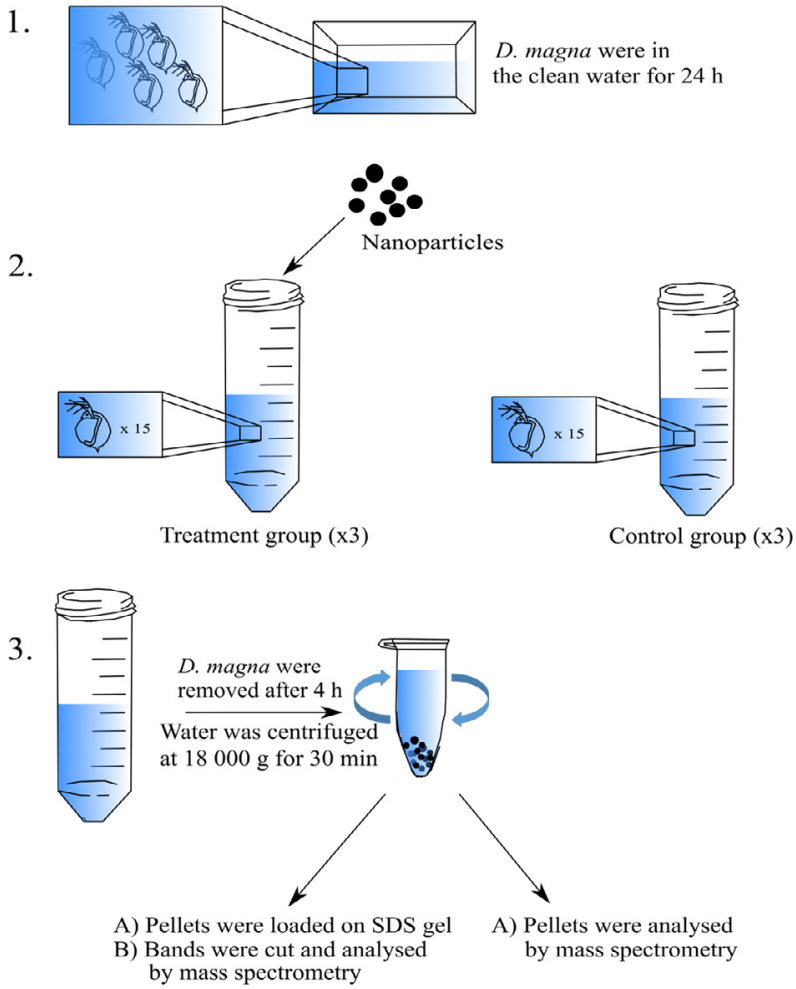

Figure 7. Schematic illustration of the incubation experiment. Reprinted with permission from Kelpsiene *et al.*, 2022 [181] (**Paper III**).

An acute (~10 days) toxicity test to evaluate the effects caused by PLA NPs and PLA breakdown nanoplastics (**Paper IV**). Different PLA products commonly found in supermarkets were broken down to produce nanoplastics. *D. magna* were exposed to various PLA breakdown nanoplastics, as well as dialyzed and non-dialyzed 250 nm PLA NPs.

In the first test, tap water was first filtered through 0.2 µm syringe filter to remove any bacteria that might come with tap water. Then, daphnids were

exposed to nanoplastics produced by the mechanical breakdown process from PLA soup lid, PLA 3D printer filament, and PLA plastic cup. Even though *D. magna* were not fed during the exposure period, there was no significant mortality observed within the first 48 h, therefore it was decided to keep daphnids in the exposure media with (treatment) or without (control) nanoplastics until all the daphnids were immobilized, where the last individual survived for almost 10 days. In total, there were 15 replicates for each treatment with one individual per 50 mL Falcon tube with a total volume of 25 mL.

In the second toxicity test, I evaluated the effects caused by engineered PLA NPs. Here, *D. magna* were subjected to various dilutions factors (1:1, 1:10, or 1:100) of either dialyzed or non-dialyzed PLA NPs. The highest concentration for both dialyzed and non-dialyzed PLA NPs was 10 mg/L. Similarly, as in the first experiment, we kept daphnids in exposure media with (treatment) or without (control) PLA NPs until all the daphnids were immobilized, where the oldest individual survived for almost 6 days. In total, there were 10 replicates for each treatment with one individual per 50 mL Falcon tube with a total volume of 25 mL.

Kaplan Meier survival curves analysis followed by the Log Rank (Mantel-Cox) test and the Gehan-Breslow-Wilcoxon test were performed using statistical computing software GraphPad Prism, www.graphpad.com.

Identification of metabolites and proteins, and determination of total triglyceride concentration

Nuclear magnetic resonance (NMR) spectroscopy and ***mass spectroscopy*** (MS) are two analytical techniques that provide structural information on the analytes. In **Paper II**, ^{1}H NMR spectroscopy was applied to detect metabolites in *D. magna* affected by PS NPs type, concentration, and daphnid aging. Multivariate analysis of variance was performed to determine if there were significant effects due to daphnid aging, the presence, concentration, and type of PS NPs, as well as to identify the lowest PS NPs concentration that induce a significant metabolite response using the Simca-P software (Umetrics, Sweden). Aging and PS NP type effects for individual metabolites were calculated using two-way ANOVA.

Figure 7 shows that two different approaches were used for proteins digestion to further analyze on MS and MS/MS – digestion in solution and digestion in

a gel (**Paper III**). These methods were chosen because even after several attempts it was not possible to visualize any proteins by using sodium dodecyl sulfate polyacrylamide (SDS-PAGE) gel electrophoresis for PS-COOH NPs after being incubated with *D. magna*. SDS-PAGE was used to separate proteins in 4 to 12% premade SDS-PAGE (Bio-Rad) gel, where proteins of different sizes migrate toward the anode due to their negative charge. Smaller molecular weight (MW) proteins will migrate further compared to larger MW proteins. An SDS-PAGE provides only the information regarding the MW of the protein rather than the identity of a protein. MS and MS/MS were used to identify proteins bound to differently surface charged PS NPs after incubation with *D. magna*. Proteins were identified by searching against a database containing all *Daphnia* protein sequences. Proteins with at least two peptides in the sequence were considered for further analysis.

In **Paper III**, to quantify concentration of total triglyceride concentration, three replicates representing each treatment were pooled together and freeze-dried. Analysis was performed according to the manufacturer's instructions (Sigma-Aldrich, USA). Absorbance intensity was recorded at 540 nm using a ProbeDrum spectrophotometer (Probation Labs, Sweden). Data were analyzed using Student's *t*-test using statistical computing software GraphPad Prism, www.graphpad.com.

Results and Discussion

"Nothing is absolute. Everything changes, everything moves, everything revolves, everything flies and goes away."

— Frida Kahlo

The relevance of long-term exposure scenarios

Short or acute (24-48 h) exposure scenarios are often used in standardized toxicological studies to assess the effects of various toxicants on an organism's well-being [37]. Acute toxicity studies generally use high concentrations of toxicants, whereas pollutants are present in low levels in the natural environment [182]. For example, various types of plastics were quantified to vary between 46.5 µg/L [33] and 563 µg/L [22]. Furthermore, according to OECD guidelines, daphnids used in ecotoxicology studies should not be fed during acute toxicity tests [183]. *Daphnia* feed either by actively filtering particles, ranging from 200 nm to 80 µm [162,184] or passively taking up smaller particles [185]. It is known that the filtration rate of daphnids increases if there is a lack of food [186], suggesting that the uptake of NPs would be greater compared to when food is available. Based on OECD guidelines, the reproduction test of daphnids for testing toxicants should last for only 21 days [187]. Adult *Daphnia* females can survive for more than 2 months under laboratory conditions [78,160] (**Paper I**) and may produce a clutch of eggs every 3 to 4 days until its death [160], meaning that reproduction might continue longer than only 21 days.

Previously it has been shown that PS-NH_2 NPs induce greater toxicity to *Daphnia* compared to PS-COOH or plain PS NPs [1,85]. However, both mentioned studies performed 24 h toxicity tests by using high concentrations of NPs. In **Paper I**, I showed that:

(1) the life span, in the life-time exposure scenario, of *D. magna* was shortened almost three times after exposure to PS-NH_2 NPs at a concentration of 0.32

mg/L (Figure 8A). This concentration is almost 5 times lower than the one (1.4 mg/L) used for short-term (48 h) exposure [80]

(2) PS-COOH NPs, which have been shown to not be acutely toxic at a concentration of 50 mg/L [1], significantly affected survival in *D. magna* at concentrations ranging from 0.32 mg/L to 7.6 mg/L in a life-time exposure (Figure 8B-C).

In **Paper I,** I demonstrated the importance of performing more realistic exposure scenarios as they might resemble effects caused by nanoplastics in the natural environment.

Further, I observed that the reproduction rate was not significantly affected either by particle type or concentration used in the study (**Paper I**). However, with an increased concentration, there was a decreasing trend in the number of offspring over lifespan of *D. magna*. This needs to be further investigated to assess if different results could be observed by increasing the number of replicates and knowing that all *Daphnia* individuals indeed are females. The latter was not checked in the study as it can induce additional stress on the daphnids. Furthermore, other sizes and/or types of plastics should be used to assess the reproduction rate in daphnids. Reduction in the number of offspring or delay in the first brood release in *Daphnia* sp. have previously been observed after exposure to PS MNPs [76,188].

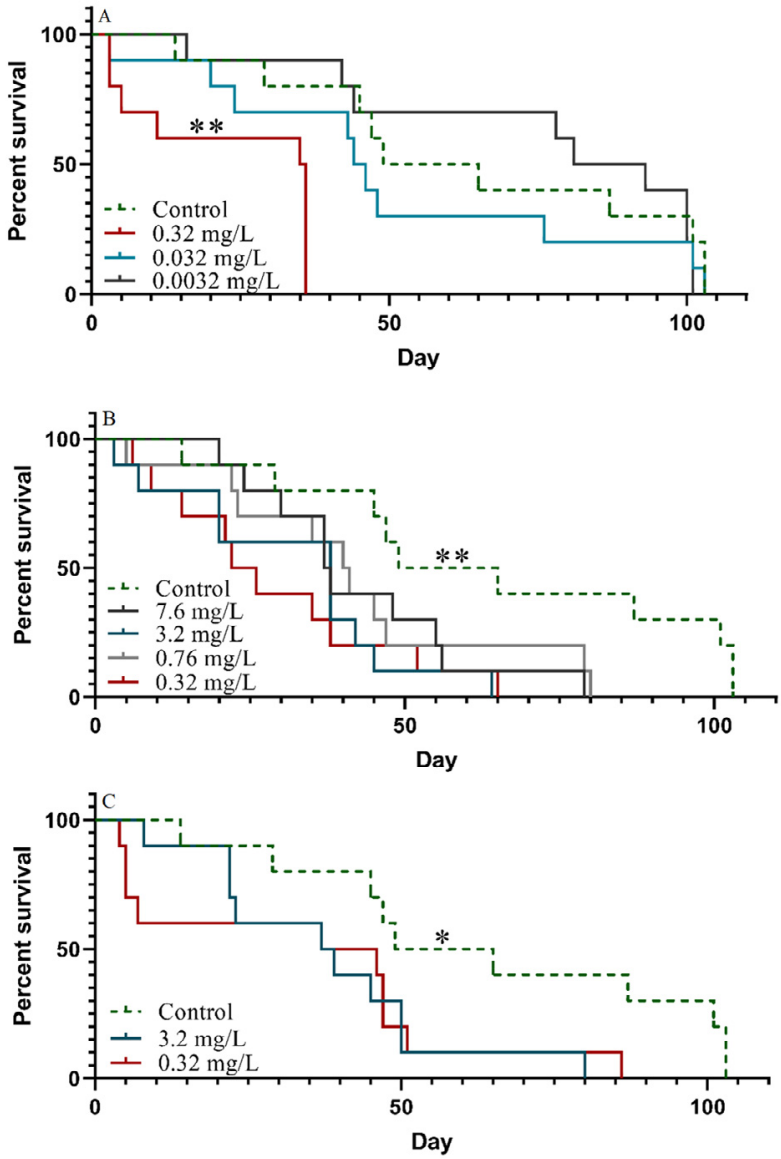

Figure 8. Survival of *D. magna* after exposure to different concentrations of 53 nm PS-NH_2 (A), 62 nm (B) and 26 nm (C) PS-COOH throughout their life-time (103 days). Asterisks indicate significant difference compared to the control group estimated over the whole study period, *p<0.05, **p<0.01. Reprinted with permission from Kelpsiene *et al.*, 2020 [78] (**Paper I**).

Mechanisms behind toxicity of nanoplastics

Toxicity triggered by PS NPs can be looked at from different angles. Size, surface charge, stability of particles, their interaction with organisms' carapace, and biomolecules or small metabolites can induce adverse effects on organisms.

The toxicity caused by PS-NH_2 NPs is often explained by a stronger interaction between a positively charged NP surface and a negatively charged *Daphnia* cell membrane [85]. It has been shown that positively surface charged NPs and PVC MPs induce multiple molting events in *Daphnia* sp. [88,189]. Furthermore, NPs can adhere to the exoskeleton of *Daphnia* sp., which can lead to increased mortality due to the burden on the body by interfering with moving. NPs aggregates have been observed to attach on daphnids exoskeleton, appendages, and antennae [190,191]. In **Papers I** and **II**, I did not observe a significant PS NPs aggregates adhesion on the exoskeleton of *D. magna*. The exposure scenarios in **Papers III** and **IV** were too short to observe any NPs adhesion on surfaces of *Daphnia* sp. However, it would be interesting to investigate if the frequency of molts changes due to exposure to PS NPs.

In **Papers I** and **II**, daphnids were fed with algae during the exposure period. NPs can interact with algae and potentially form aggregates. Due to the formation of aggregates available number of NPs in the size range relevant for direct uptake by organisms reduces, the sedimentation rate increases, and toxicity potentially decreases toward filter feeders. Whereas, dispersed NPs can diffuse, be more mobile, and be available to be taken up by individuals, thus more toxic [74,190]. On the other hand, Frankel and co-authors showed that 50 nm PS-NH_2 NPs aggregates in a size range between 200 nm and 500 nm were acutely (48 h) toxic to *D. magna* as the free, 50 nm, PS-NH_2 NPs [80]. In **Paper I**, I checked the sedimentation of a mixture of NPs and algae, showing that sedimentation did not occur, which to some extent could be explained by a low density of PS (~1 g/cm^3). Therefore, it would be interesting to use different types of plastics, such as PET or PVC, having a slightly greater density (>1 g/cm^3) to see if sedimentation would occur and if it would reduce the toxicity in *Daphnia* sp.

Due to their small size, NPs are often mistaken for food by aquatic organisms [192], which leads to increased accumulation of NPs in the gut. Accumulation of non-nutritious NPs in the gut of exposed individuals can lead to an increased toxicity [85,193]. In **Paper I**, I noted NPs accumulation in some guts of randomly chosen daphnids (Figure 9). Even though accumulation was observed only in

some *Daphnia* individuals, the possibility that accumulation of PS NPs might occur more often in nature cannot be excluded. The accumulation of both fluorescent and non-fluorescent PS NPs has been observed previously in *Daphnia* sp., showing that daphnids can ingest particles of a size up to 10 µm [68,85,194]. The presence of PS NPs in the gastrointestinal tract of *D. magna* has recently been shown using Raman confocal spectroscopy-microscopy and confirmed using TEM [195]. The next step would be to quantify the amount of PS NPs ingested by *Daphnia* sp. within a time.

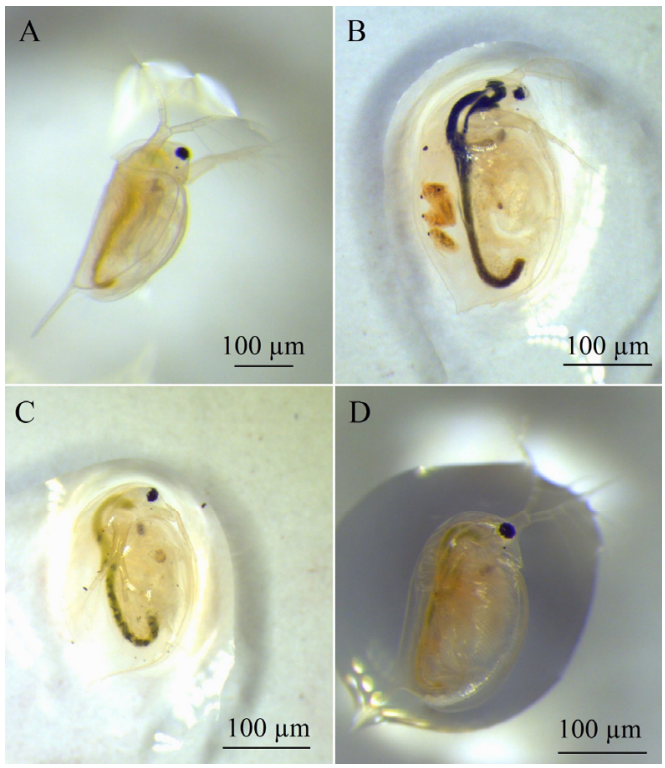

Figure 9. *Daphnia magna* individuals in the control group (A) and after exposure to differently charged and differently sized polystyrene nanoparticles (53 nm PS-NH_2, B; 62 nm PS-COOH, C; 26 nm PS-COOH, D). Localized accumulation and blackish guts were seen in *D. magna* after exposure to 53 nm PS-NH_2 (B) and 62 nm PS-COOH (C). This was not seen in the control group. Pictures were taken for randomly chosen individuals after death. Reprinted with permission from Kelpsiene *et al.*, 2020 [78] (**Paper I**).

Most organisms undergo metabolic changes due to response to various environmental stressors, which can affect the immune response and survival of the organisms [196,197]. An increased stress level could make the daphnid more

sensitive to additional stress factors, for example, predators, shortage of food, environmental factors. Changes in various free amino acids can be perceived as a defense strategy for an organism to help to cope with pathogens or toxicants [198], which require additional energy use and consequently might lead to increased mortality [199]. In **Paper II**, metabolic responses in *D. magna* were analyzed after exposure to low concentrations of PS NPs for 37 days. It was observed that 12 metabolites were significantly affected already at the lowest (3.2 µg/L) concentration and all 15 metabolites showed significant changes due to aging and PS NPs used in the study (Table 2). Changes in metabolites can affect certain functions that the metabolites are responsible for. For example, the increase in glucose levels can be associated with disturbed glucose metabolism due to aging, which has previously been observed for zebrafish [200]. I also observed changes in the concentration of isopropanol, which can be explained by the bacterial conversion of acetone to isopropanol [201]. In **Paper II**, bacterial communities deriving from *D. magna* itself or the original culture were not identified, which would be interesting to study in the future.

Table 2. Metabolites response to daphnid aging ('Aging'), PS NP exposure to all concentrations ('PS NPs'), and the lowest concentration only ('3.2 µg/L of PS NPs') determined using 2-way ANOVA. Reprinted with permission from Kelpsiene *et al*., 2023 [101] (**Paper II**).

Metabolite	Aging	PS NPs	3.2 µg/L of PS NPs	Group
Asparagine	3.6×10^{-32}	3.1×10^{-8}	8.5×10^{-7}	Amino acids
Glutamate	4.2×10^{-26}	4.2×10^{-9}	1.4×10^{-7}	Amino acids
Glutamine	4.8×10^{-18}	0.014	0.13	Amino acids
Isoleucine	3.5×10^{-22}	2.9×10^{-7}	4.1×10^{-5}	Amino acids
Leucine	6.9×10^{-20}	3.2×10^{-6}	2.2×10^{-4}	Amino acids
Lysine	4.1×10^{-17}	3.1×10^{-6}	3.2×10^{-4}	Amino acids
Phenylalanine	5.0×10^{-19}	1.7×10^{-7}	3.5×10^{-5}	Amino acids
Tyrosine	1.5×10^{-9}	6.3×10^{-6}	2.1×10^{-4}	Amino acids
Valine	2.1×10^{-24}	6.2×10^{-8}	4.3×10^{-6}	Amino acids
Methionine sulfoxide	1.7×10^{-35}	1.8×10^{-9}	2.3×10^{-8}	Amino acids
Glucose	2.8×10^{-15}	0.25	0.15	Monosaccharides
Glycogen	7.9×10^{-5}	1.4×10^{-4}	9.2×10^{-6}	Polysaccharides
Unidentified sugar	1.2×10^{-6}	4.8×10^{-5}	1.7×10^{-6}	
Nucleic acid(s)	1.1×10^{-31}	0.097	0.38	
Isopropanol	1.4×10^{-9}	1.7×10^{-28}	8.6×10^{-17}	

Biomolecules, such as proteins, lipids, and small metabolites, can bind to the surfaces of NP and form a corona, which defines the biological identity of the particle [113,114,181,202]. Corona is often perceived as a protective coating and reduced toxicity has been observed for PS NPs and some metallic NPs in *D. magna* [85,143]. On the other hand, 50 nm PS-NH_2 NPs coated with albumin were as toxic to *D. magna* as non-coated the same type PS NPs [80]. In **Paper III**, profiles of protein coronas were identified that bind to surfaces of various PS NPs, with a size ranging from 50 nm to 200 nm. Two different approaches were used in the study, proteins were digestive in a solution or in a gel. First, I showed that different proteins bind to acute toxic 50 nm PS-NH_2 NPs compared to acutely non-toxic 200 nm PS-NH_2 NPs when proteins were separated by SDS-PAGE gel electrophoresis and further analyzed by MS/MS (Figure 10). Proteins that bind to small aminated PS NPs can be divided into two groups. One group is related to the digestive system (e.g., carboxypeptidase B, serine protease, and chymotrypsin elastase family member 2A) and the other group is related to epithelium and intracellular structures and processes (e.g., beta-klotho, actin, tubulin, elongation factors, and histones). The depletion or alteration of proteins that are essential for the

longevity of *Daphnia* sp. can partly explain acute toxicity. For example, alterations in the expression of the *klotho* gene might interfere with the lifespan or fertility in mice [203]. When the rest of the samples were analyzed, I noticed that actin, alpha skeletal muscle was one of the most abundant proteins that bind to all PS NPs, which can partly explain the PS NPs aggregates and its interaction with various parts of the *Daphnia* sp. [190,191]. This protein might be released when an individual is molting, therefore PS NPs interact more with the body surface and increase mortality due to the burden of the body. The next step would be to purify proteins found to bind to surfaces of PS NPs, for example, carboxypeptidase B, coat particles with a purified protein, and assess the toxicity test in daphnids to study if toxicity changes.

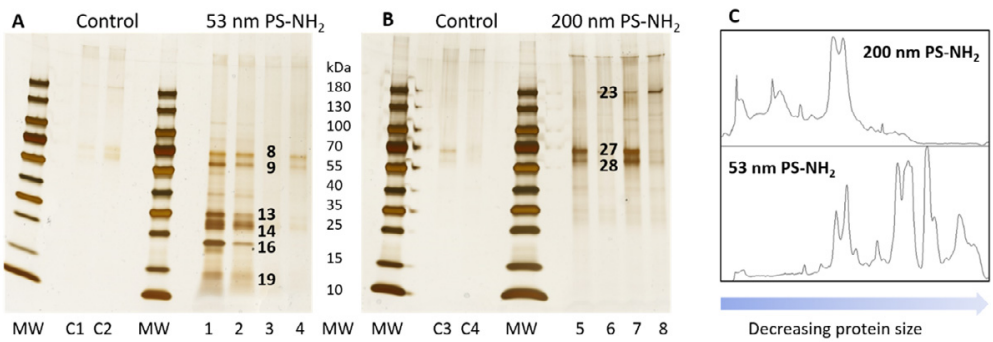

Figure 10. Silver-stained SDS gels after 53 nm (A) and 200 nm (B) PS-NH_2 NPs incubation with *D. magna* in comparison with a control group. The visualization of the size differences in proteins found in both gels (C). Reprinted with permission from Kelpsiene *et al.,* 2022 [181] (**Paper III**).

Further, in **Paper III**, I showed that total triglyceride levels significantly increased already after 4 h exposure to 200 nm PS-COOH NPs compared to other PS NPs used (Figure 11). Similarly to results obtained in this study, higher concentrations of total triglycerides were observed in lipid corona of 200 nm PS-COOH NPs incubated with mouse serum [114]. In **Paper III**, triglyceride levels were observed after a short-term *D. magna* incubation with particles with high concentrations of PS NPs, which raises the question if the same tendencies would be observed by using lower concentrations of PS NPs, other type of NPs, and/or a longer incubation period.

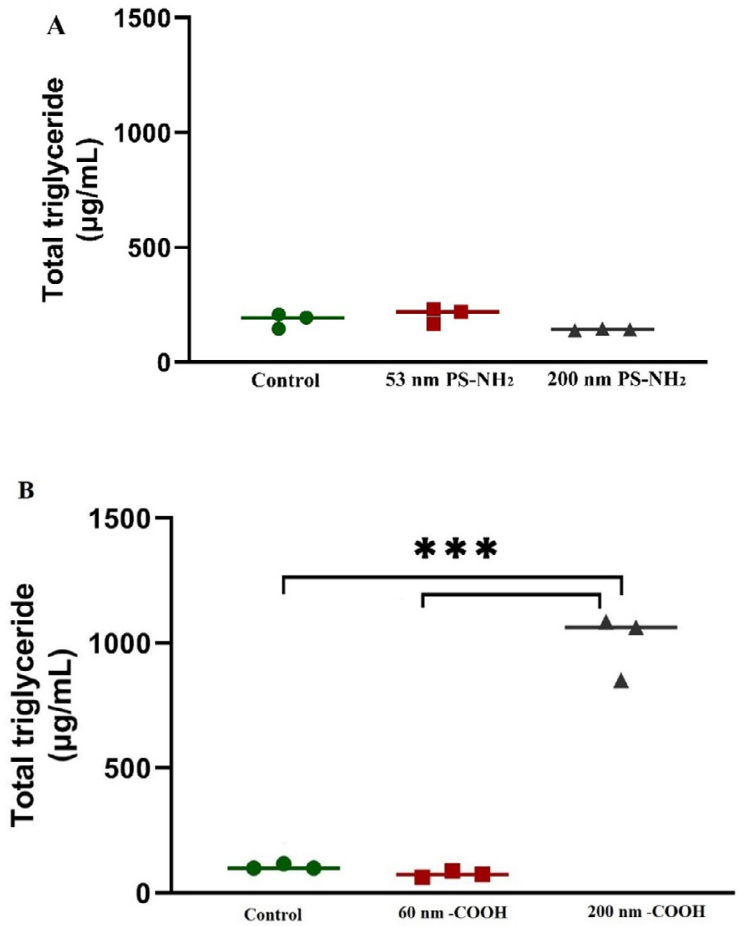

Figure 11. Total triglyceride quantification on PS NPs after incubation with *D. magna* for 4 h. Comparison between PS-NH_2 (A) and PS-COOH (B) NPs lipid corona. Samples were measured in triplicates. Horizontal lines show mean concentration calculated from the three data points (***$p < 0.001$). Reprinted with permission from Kelpsiene *et al*., 2022 [181] (**Paper III**).

Bioplastics *versus* synthetic plastics

There is no doubt that synthetic plastic pollution creates both ecological and social concerns. **Papers I** and **II** clearly showed that PS NPs significantly induced toxicity in *D. magna* after long-term exposure at relatively low

concentrations. Furthermore, I showed that, for example, carboxylated PS NPs previously assumed to be non-toxic after 24 h exposure, appeared to be toxic after a life-time exposure (**Paper I**). Considering that PS in general is one of the most used plastic types, other types of plastics should be considered as alternatives instead of synthetic plastics. Therefore, as mentioned previously, bioplastics have received considerable attention due to their potential environmental advantages.

Biodegradable plastics will never fully degrade in nature without being subjected to certain conditions [150], suggesting that over time these plastics will produce both micro-, and eventually, nanoplastics. In the environment, the breakdown process results in changes in the surface chemical composition of nanoplastics compared to their bulk material [40], which can further affect interactions with biological matter. In **Paper IV,** I mechanically broke down various daily used PLA items, showing that surface chemical composition differs from the bulk material. FTIR spectrum showed that PLA bulk materials have sharp peaks between ~1000 cm^{-1} and ~2000 cm^{-1} due to C-C and/or -CH vibrations at ~1090 cm^{-1}, C-OH side group vibrations at ~1185 cm^{-1}, and C=O stretching at between ~1454 cm^{-1} and ~1751 cm^{-1} [154,204,205], which are less striking due to breakdown procedure. PLA breakdown nanoplastics have broad peaks between ~3500 and ~3000 cm^{-1} region and smaller peaks at ~1700 cm^{-1} due to O–H or C=O stretching of ethers or carbonates [84,154] (Figure 12). Oxidation has previously been observed in the breakdown nanoplastics for PE [84,206]. FTIR spectrum showed that the characteristic peaks of the released nanoplastics were consistent with a bulk material (Figure 12, light orange color columns), indicating that nanoplastics were released from the corresponding PLA items.

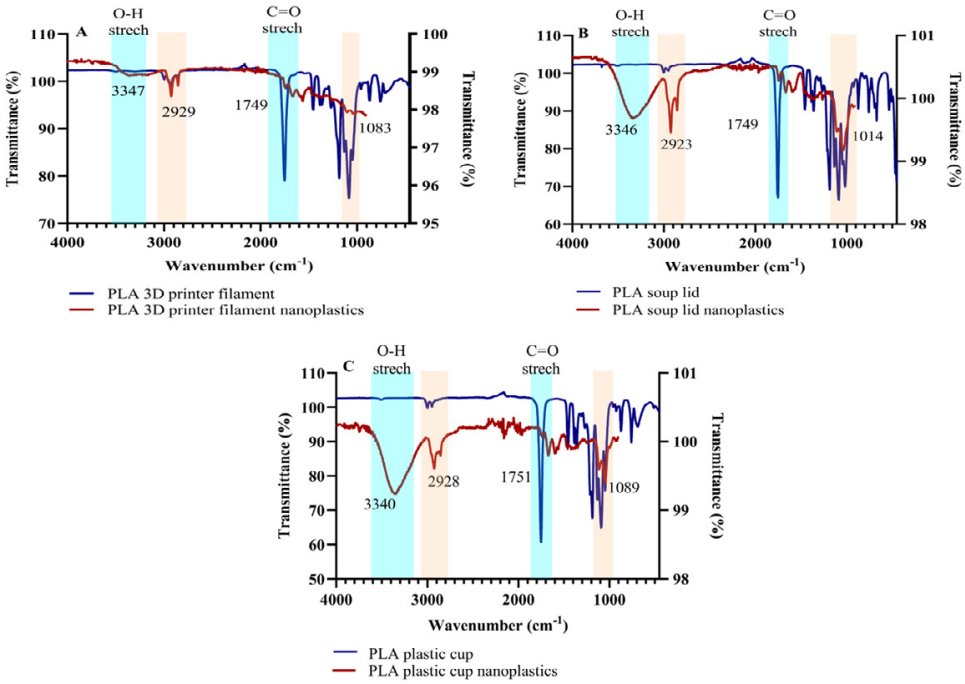

Figure 12. FTIR spectra of different PLA bulk material (blue line, left Y axis) and their breakdown products (red line, right Y axis). Light orange color indicates peaks showing similarities between bulk material and its breakdown products, whereas light blue color indicates oxidation that occurred during the breakdown process in PLA nanoplastics. Reprinted with permission from Kelpsiene *et al.,* 2023 [207] (**Paper IV**).

Interestingly, in **Paper IV**, I observed a positive effect caused by PLA breakdown nanoplastics. Daphnids showed a significantly prolonged survival after exposure to PLA plastic cup nanoplastics compared to a control group. Other PLA breakdown nanoplastics (3D print filament and soup lid) showed a trend for a prolonged survival time in *D. magna* (Figure 13). The observed phenomenon can potentially be explained by bacterial growth on nanoplastics, which could be an additional food source for *D. magna*. However, this needs further investigation. A similar tendency was observed when *D. magna* were exposed to purified fractions of HDPE nanoplastics, where daphnids survived longer compared to the group, containing fractions with smaller sizes of molecules (< ~3 nm) [84].

Further, it has been shown that NPs not only have adverse effects on bacterial community composition [75], but surfaces of NPs can be also used for biofilm formation [208]. Biofilm formation can potentially lead to an increase in the density

of the NP and a decrease in its buoyancy [209], which possibly reduces the toxicity of NPs in filter feeders. The smaller the particle is, the faster it can reach its sinking density [210]. The latter study showed that smaller fragments of low-density plastic polymers sink faster compared to larger ones (5 mm) due to biofouling [210]. Daphnids can accidentally ingest plastic fragments while feeding on the surface of the biofilm, however, it can also serve as an additional source of food and potentially might reduce toxicity as it was shown in **Paper IV**.

Dissolved organic matter (DOC) released from synthetic plastics, such as LDPE, HDPE, PE, and PP, has been shown to stimulate the activity of heterotrophic microbes [211]. Degradation of plastic into smaller pieces [40] can potentially increase the concentration of DOC leaching due to the increase in surface area relative to its volume. In **Paper IV**, I did not measure either if bacteria have started to grow on nanoplastics and form biofilm, sedimentation rate, or concentration of DOC released from PLA nanoplastics. Therefore, it would be interesting to further explore and confirm whether bacteria grow on various types of nanoplastics and act as an additional food source for *Daphnia*.

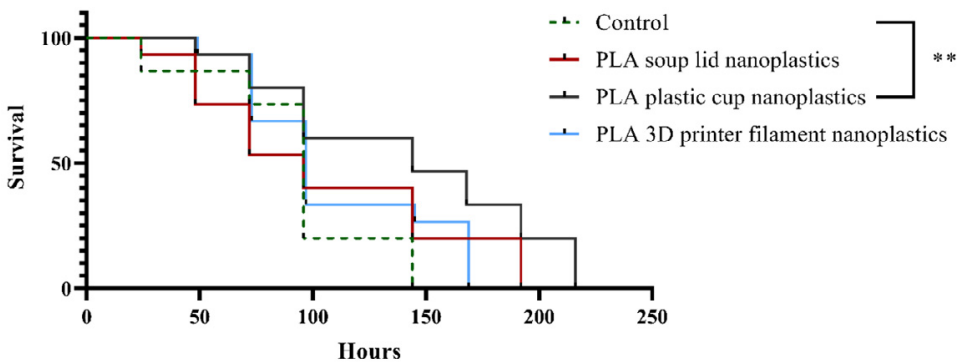

Figure 13. Survival of *Daphnia magna* exposed to different PLA breakdown nanoplastics. The curve of PLA 3D printer filament nanoplastics was nudged on Y axis by 1.00 data units for clearer vision. In total there were 15 replicates for each treatment. Asterisks indicate significant difference between a control group and a treatment estimated over the study period, **p<0.01. Reprinted with permission from Kelpsiene *et al.,* 2023 [207] (**Paper IV**).

Closing remarks and Future perspectives

In this thesis, I have explored various aspects of PS NPs, PLA NPs, and PLA nanoplastics in *D. magna*. In **Paper I**, I stepped forward and performed a life-time experiment. I showed that PS NPs with a negative surface charge previously considered as non-toxic after 24 h [1] exposure, significantly reduced survival rate in *D. magna* after a life-time (103 days) toxicity test at low concentrations of NPs (**Paper I**). This is an important observation, suggesting that short-term toxicity tests, which are often performed by using high concentrations, do not provide a full picture of the potential effects triggered by PS NPs. Besides several ideas for future studies mentioned in a previous chapter, another open question is: what are the effects of PS NPs in a size range of 100 nm to 200 nm after a life-time exposure?

In **Paper II**, I performed experiments even at lower concentrations of PS NPs compared to **Paper I**. The highest (320 µg/L) concentration used in **Paper II** was almost 24 times lower compared to the highest (7600 µg/L) concentration used in **Paper I**. The main finding of **Paper II** was that significant effects in *D. magna* metabolomics were already observed at a concentration of 3.2 µg/L. This is quite alarming considering that this concentration is far below the levels of nanoplastics (46 µg/L – 500 µg/L) [22,33] and is within the concentration range of breakdown styrene oligomers (0.17 µg/L – 4.31 µg/L) [36] quantified in the natural environment. **Paper II** focused only on endometabolites, the metabolites kept by the organism. Therefore, exometabolome, the metabolites that are excreted into the medium, should be explored in future studies.

In **Paper III**, I showed that different proteins bind to acutely toxic 50 nm PS NPs compared to other PS NPs used in the study. To some extent, it confirms that there are different mechanisms behind the toxicity depending on the particle size and/or charge. It is worth mentioning that the profile of proteins was observed after 4 h incubation with PS NPs at high concentrations, which let me think about other questions that should be taken into consideration in future studies: would the profile of proteins be the same if *D. magna* had been incubated for a longer period with lower concentrations of PS NPs? Whether profile of protein corona changes during the time or remain stable? How would

protein corona profile look like if other types of plastic particles and breakdown nanoplastics had been used?

In **Papers I-III**, I used engineered PS NPs as a proxy for nanoplastics. Engineered NPs are uniform in size and shape, which helps to monitor analysis and gives a foundation for future studies. Therefore, the next step would be to use more realistic plastic particles, which are diverse in shape, size, and chemical composition. This approach was touched upon in **Paper IV**. In **Paper IV**, I used PLA NPs and PLA breakdown nanoplastics produced during the breakdown procedure. I showed that PLA breakdown nanoplastics significantly prolonged survival for *D. magna* compared to a control group. This phenomenon has previously been observed when daphnids were exposed to purified HDPE nanoplastics fractions [84]. In both cases, it was hypothesized that the prolonged survival could be due to the bacterial growth on nanoplastics, which could be an additional food source for *D. magna*. This is an interesting observation, which of course needs to be further investigated. How long does it take for bacteria to start growing on nanoplastics? What bacteria groups grow on nanoplastics? Does the diversity of bacteria change over time, plastic, and/or additive type? These and many other open questions would be interesting to investigate in future studies to get more answers regarding nanoplastics effects and interactions with biota.

Based on the results observed in this thesis, it could be speculated that the number of daphnids might be affected due to exposure to nanoplastics in the natural environment. This consequently can trigger the survival of top consumers, which use daphnids as a food source [160]. Furthermore, the accumulation noticed in **Paper I**, allows me to think that effect of nanoplastics can be transferred through the food web in nature and strengthen the results previously obtained under laboratory conditions [1]. In **Paper IV**, daphnids were exposed for a short period, which makes it difficult to extrapolate results, which could be expected to happen in nature. Therefore, more studies should be performed using bioplastics to get a better understanding of such plastics.

Finally, with this thesis, I provide significant new knowledge regarding:

(1) effects caused by PS NPs to *D. magna* after long-term exposure at low concentrations

(2) mechanistic understanding of potential toxicity pathways induced by PS NPs in *D. magna* by analyzing metabolic responses and a profile of protein corona

(3) positive effects observed after exposure to PLA nanoplastics.

References

1 Mattsson, K. *et al.* Brain damage and behavioural disorders in fish induced by plastic nanoparticles delivered through the food chain. *Scientific Reports* **7**, 11452 (2017).

2 Plastics the Facts. An analysis of European plastics production, demand and waste data. *https://plasticseurope.org/wp-content/uploads/2022/10/PE-PLASTICS-THE-FACTS_V7-Tue_19-10-1.pdf* (2022).

3 Andrady, A. L. & Neal, M. A. Applications and societal benefits of plastics. *Philos Trans R Soc Lond B Biol Sci* **364**, 1977-1984 (2009).

4 Erni-Cassola, G., Zadjelovic, V., Gibson, M. I. & Christie-Oleza, J. A. Distribution of plastic polymer types in the marine environment; A meta-analysis. *Journal of Hazardous Materials* **369**, 691-698 (2019).

5 Borrelle, S. B. *et al.* Predicted growth in plastic waste exceeds efforts to mitigate plastic pollution. *Science* **369**, 1515-1518 (2020).

6 Geyer, R., Jambeck, J. R. & Law, K. L. Production, use, and fate of all plastics ever made. *Science advances* **3**, e1700782 (2017).

7 Lechthaler, S., Waldschläger, K., Stauch, G. & Schüttrumpf, H. The way of macroplastic through the environment. *Environments* **7**, 73 (2020).

8 Winton, D. J., Anderson, L. G., Rocliffe, S. & Loiselle, S. Macroplastic pollution in freshwater environments: Focusing public and policy action. *Science of The Total Environment* **704**, 135242 (2020).

9 Thomas, P. J. *et al.* Resolving the effects of environmental micro- and nanoplastics exposure in biota: A knowledge gap analysis. *Science of The Total Environment* **780**, 146534 (2021).

10 Derraik, J. G. The pollution of the marine environment by plastic debris: a review. *Marine pollution bulletin* **44**, 842-852 (2002).

11 Gregory, M. R. Environmental implications of plastic debris in marine settings—entanglement, ingestion, smothering, hangers-on, hitch-hiking and alien invasions. *Philosophical Transactions of the Royal Society B: Biological Sciences* **364**, 2013-2025 (2009).

12 UNESCO facts & figures on marine pollution. *http://www.unesco.org/new/en/natural-sciences/ioc-oceans/focus-areas/rio-20-ocean/blueprint-for-the-future-we-want/marine-pollution/facts-and-figures-on-marine-pollution/* (2017).

13 Stapleton, P. Microplastic and nanoplastic transfer, accumulation, and toxicity in humans. *Current Opinion in Toxicology* **28**, 62-69 (2021).

14 Barnes, D. K. A., Galgani, F., Thompson, R. C. & Barlaz, M. Accumulation and fragmentation of plastic debris in global environments. *Philos Trans R Soc Lond B Biol Sci* **364**, 1985-1998, doi:10.1098/rstb.2008.0205 (2009).

15 Peterson, J. D., Vyazovkin, S. & Wight, C. A. Kinetics of the thermal and thermo-oxidative degradation of polystyrene, polyethylene and poly(propylene). *Macromolecular Chemistry and Physics* **202**, 775-784 (2001).

16 Ru, J., Huo, Y. & Yang, Y. Microbial degradation and valorization of plastic wastes. *Frontiers in Microbiology* **11**, doi:10.3389/fmicb.2020.00442 (2020).

17 Koelmans, A. A., Redondo-Hasselerharm, P. E., Mohamed Nor, N. H. & Kooi, M. Solving the nonalignment of methods and approaches used in microplastic research to consistently characterize risk. *Environmental science & technology* **54**, 12307-12315 (2020).

18 Yee, M. S.-L. *et al.* Impact of microplastics and nanoplastics on human health. *Nanomaterials* **11**, 496 (2021).

19 Napper, I. E. & Thompson, R. C. Release of synthetic microplastic plastic fibres from domestic washing machines: effects of fabric type and washing conditions. *Marine pollution bulletin* **112**, 39-45 (2016).

20 Kentin, E. & Kaarto, H. An EU ban on microplastics in cosmetic products and the right to regulate. *Review of European, Comparative & International Environmental Law* **27**, 254-266 (2018).

21 Commission, E. EU action on single-use plastics. (2021).

22 Materić, D. *et al.* Presence of nanoplastics in rural and remote surface waters. *Environmental Research Letters* **17**, 054036 (2022).

23 Koelmans, A. A. *et al.* Microplastics in freshwaters and drinking water: Critical review and assessment of data quality. *Water research* **155**, 410-422 (2019).

24 Kaiser, D., Kowalski, N. & Waniek, J. J. Effects of biofouling on the sinking behavior of microplastics. *Environmental research letters* **12**, 124003 (2017).

25 Yu, Q. *et al.* Distribution, abundance and risks of microplastics in the environment. *Chemosphere* **249**, 126059 (2020).

26 Andrady, A. L. Microplastics in the marine environment. *Marine Pollution Bulletin* **62**, 1596-1605 (2011).

27 Lebreton, L. C. *et al.* River plastic emissions to the world's oceans. *Nature communications* **8**, 1-10 (2017).

28 Jambeck, J. R. *et al.* Plastic waste inputs from land into the ocean. *Science* **347**, 768-771 (2015).

29 Schmidt, C., Krauth, T. & Wagner, S. Export of plastic debris by rivers into the sea. *Environmental Science & Technology* **51**, 12246-12253 (2017).

30 Wu, P. *et al.* Environmental occurrences, fate, and impacts of microplastics. *Ecotoxicol Environ Saf* **184**, 109612 (2019).

31 Lebreton, L. *et al.* Evidence that the Great Pacific Garbage Patch is rapidly accumulating plastic. *Scientific reports* **8**, 1-15 (2018).

32 Ter Halle, A. *et al.* Nanoplastic in the North Atlantic Subtropical Gyre. *Environmental Science & Technology* **51**, 13689-13697 (2017).

33 Materić, D., Ludewig, E., Brunner, D., Röckmann, T. & Holzinger, R. Nanoplastics transport to the remote, high-altitude Alps. *Environmental Pollution* **288**, 117697 (2021).

34 Sighicelli, M. *et al.* Microplastic pollution in the surface waters of Italian Subalpine Lakes. *Environmental Pollution* **236**, 645-651 (2018).

35 Amamiya, K. *et al.* Evidence of transport of styrene oligomers originated from polystyrene plastic to oceans by runoff. *Science of the Total Environment* **667**, 57-63 (2019).

36 Kwon, B. G. *et al.* Monitoring of styrene oligomers as indicators of polystyrene plastic pollution in the North-West Pacific Ocean. *Chemosphere* **180**, 500-505 (2017).

37 Kelpsiene, E. *et al.* Review of ecotoxicological studies of widely used polystyrene nanoparticles. *Environmental science. Processes & impacts* (2021).

38 Gigault, J. *et al.* Nanoplastics are neither microplastics nor engineered nanoparticles. *Nature Nanotechnology* **16**, 501-507 (2021).

39 Auffan, M. *et al.* Towards a definition of inorganic nanoparticles from an environmental, health and safety perspective. *Nature Nanotechnology* **4**, 634-641 (2009).

40 Gigault, J. *et al.* Current opinion: What is a nanoplastic? *Environmental pollution* **235**, 1030-1034 (2018).

41 Ekvall, M. T. *et al.* Nanoplastics formed during the mechanical breakdown of daily-use polystyrene products. *Nanoscale Advances* **1**, 1055-1061 (2019).

42 Chamas, A. *et al.* Degradation Rates of Plastics in the Environment. *ACS Sustainable Chemistry & Engineering* **8**, 3494-3511 (2020).

43 Masry, M. *et al.* Characteristics, fate, and impact of marine plastic debris exposed to sunlight: A review. *Marine Pollution Bulletin* **171**, 112701 (2021).

44 Frias, J., Sobral, P. & Ferreira, A. M. Organic pollutants in microplastics from two beaches of the Portuguese coast. *Marine pollution bulletin* **60**, 1988-1992 (2010).

45 Izar, G. M. *et al.* Can the colors of beach-stranded plastic pellets in beaches provide additional information for the environmental monitoring? A case study around the Santos Port, Brazil. *International Aquatic Research* **14**, 23 (2022).

46 Andrady, A. L. *et al.* Oxidation and fragmentation of plastics in a changing environment; from UV-radiation to biological degradation. *Science of The Total Environment* **851**, 158022 (2022).

47 Guaita, M., Chiantore, O. & Costa, L. Changes in degree of polymerization in the thermal degradation of polystyrene. *Polymer Degradation and Stability* **12**, 315-332 (1985).

48 Onwudili, J. A., Insura, N. & Williams, P. T. Composition of products from the pyrolysis of polyethylene and polystyrene in a closed batch reactor: Effects of temperature and residence time. *Journal of Analytical and Applied Pyrolysis* **86**, 293-303 (2009).

49 Madorsky, S. L. & Straus, S. Thermal degradation of polymers at high temperatures. *Journal of Research of the National Bureau of Standards. Section A, Physics and Chemistry* **63**, 261 (1959).

50 Sammon, C., Yarwood, J. & Everall, N. An FT–IR study of the effect of hydrolytic degradation on the structure of thin PET films. *Polymer Degradation and Stability* **67**, 149-158 (2000).

51 Elsawy, M. A., Kim, K.-H., Park, J.-W. & Deep, A. Hydrolytic degradation of polylactic acid (PLA) and its composites. *Renewable and Sustainable Energy Reviews* **79**, 1346-1352 (2017).

52 Delplace, V. & Nicolas, J. Degradable vinyl polymers for biomedical applications. *Nature Chemistry* **7**, 771-784 (2015).

53 Shah, A. A., Hasan, F., Hameed, A. & Ahmed, S. Biological degradation of plastics: a comprehensive review. *Biotechnology advances* **26**, 246-265 (2008).

54 Matjašič, T. *et al.* Critical evaluation of biodegradation studies on synthetic plastics through a systematic literature review. *Science of The Total Environment* **752**, 141959 (2021).

55 Auta, H. S., Emenike, C. U., Jayanthi, B. & Fauziah, S. H. Growth kinetics and biodeterioration of polypropylene microplastics by *Bacillus* sp. and *Rhodococcus* sp. isolated from mangrove sediment. *Marine Pollution Bulletin* **127**, 15-21 (2018).

56 Jeon, H. J. & Kim, M. N. Biodegradation of poly (L-lactide)(PLA) exposed to UV irradiation by a mesophilic bacterium. *International Biodeterioration & Biodegradation* **85**, 289-293 (2013).

57 Brandon, A. M. *et al.* Biodegradation of polyethylene and plastic mixtures in mealworms (larvae of *Tenebrio molitor*) and effects on the gut microbiome. *Environmental Science & Technology* **52**, 6526-6533 (2018).

58 Butbunchu, N. & Pathom-Aree, W. Actinobacteria as promising candidate for polylactic acid type bioplastic degradation. *Frontiers in microbiology* **10**, 2834 (2019).

59 Sukhanova, A. *et al.* Dependence of Nanoparticle Toxicity on Their Physical and Chemical Properties. *Nanoscale Res Lett* **13**, 44-44 (2018).

60 Mu, Q. *et al.* Chemical basis of interactions between engineered nanoparticles and biological systems. *Chemical reviews* **114**, 7740-7781 (2014).

61 Zhao, T., Tan, L., Zhu, X., Huang, W. & Wang, J. Size-dependent oxidative stress effect of nano/micro-scaled polystyrene on *Karenia mikimotoi*. *Marine Pollution Bulletin* **154**, 111074 (2020).

62 Liu, H., Tian, L., Wang, S. & Wang, D. Size-dependent transgenerational toxicity induced by nanoplastics in nematode *Caenorhabditis elegans*. *Science of The Total Environment* **790**, 148217 (2021).

63 Xiao, X. *et al.* Visualizing and assessing the size-dependent oral uptake, tissue distribution, and detrimental effect of polystyrene microplastics in *Eisenia fetida*. *Environmental Pollution* **306**, 119436 (2022).

64 Hwang, K.-S. *et al.* Size-dependent effects of polystyrene nanoparticles (PS-NPs) on behaviors and endogenous neurochemicals in zebrafish larvae. *International journal of molecular sciences* **23**, 10682 (2022).

65 Schaeublin, N. M. *et al.* Surface charge of gold nanoparticles mediates mechanism of toxicity. *Nanoscale* **3**, 410-420 (2011).

66 El Badawy, A. M. *et al.* Surface charge-dependent toxicity of silver nanoparticles. *Environmental science & technology* **45**, 283-287 (2011).

67 Yue, Z.-G. *et al.* Surface charge affects cellular uptake and intracellular trafficking of chitosan-based nanoparticles. *Biomacromolecules* **12**, 2440-2446 (2011).

68 Saavedra, J., Stoll, S. & Slaveykova, V. I. Influence of nanoplastic surface charge on eco-corona formation, aggregation and toxicity to freshwater zooplankton. *Environmental pollution* **252**, 715-722 (2019).

69 Nolte, T. M. *et al.* The toxicity of plastic nanoparticles to green algae as influenced by surface modification, medium hardness and cellular adsorption. *Aquatic Toxicology* **183**, 11-20 (2017).

70 Bhattacharya, P., Lin, S., Turner, J. P. & Ke, P. C. Physical adsorption of charged plastic nanoparticles affects algal photosynthesis. *The Journal of Physical Chemistry C* **114**, 16556-16561 (2010).

71 Teng, M. *et al.* Charge-specific adverse effects of polystyrene nanoplastics on zebrafish (*Danio rerio*) development and behavior. *Environment International* **163**, 107154 (2022).

72 Carnovale, C., Bryant, G., Shukla, R. & Bansal, V. Identifying trends in gold nanoparticle toxicity and uptake: size, shape, capping ligand, and biological corona. *ACS omega* **4**, 242-256 (2019).

73 Champion, J. A. & Mitragotri, S. Role of target geometry in phagocytosis. *Proceedings of the National Academy of Sciences* **103**, 4930-4934 (2006).

74 Ramirez, L., Ramseier Gentile, S., Zimmermann, S. & Stoll, S. Behavior of TiO_2 and CeO_2 nanoparticles and polystyrene nanoplastics in bottled mineral, drinking and lake Geneva waters. Impact of water hardness and natural organic matter on nanoparticle surface properties and aggregation. *Water* **11**, 721 (2019).

75 Hao, B. *et al.* Bacterial community are more susceptible to nanoplastics than algae community in aquatic ecosystems dominated by submerged macrophytes. *Water Research* **232**, 119717 (2023).

76 Besseling, E., Wang, B., Lürling, M. & Koelmans, A. A. Nanoplastic affects growth of *S. obliquus* and reproduction of *D. magna*. *Environmental Science & Technology* **48**, 12336-12343 (2014).

77 Li, X. *et al.* Role of heteroaggregation and internalization in the toxicity of differently sized and charged plastic nanoparticles to freshwater microalgae. *Environmental Pollution* **316**, 120517 (2023).

78 Kelpsiene, E., Torstensson, O., Ekvall, M. T., Hansson, L.-A. & Cedervall, T. Long-term exposure to nanoplastics reduces life-time in *Daphnia magna*. *Scientific Reports* **10**, 5979 (2020).

79 Rist, S., Baun, A. & Hartmann, N. B. Ingestion of micro- and nanoplastics in *Daphnia magna* - quantification of body burdens and assessment of feeding rates and reproduction. *Environmental pollution* **228**, 398-407 (2017).

80 Frankel, R., Ekvall, M. T., Kelpsiene, E., Hansson, L.-A. & Cedervall, T. Controlled protein mediated aggregation of polystyrene nanoplastics does not reduce toxicity towards *Daphnia magna*. *Environmental Science: Nano* (2020).

81 Chae, Y., Kim, D., Kim, S. W. & An, Y.-J. Trophic transfer and individual impact of nano-sized polystyrene in a four-species freshwater food chain. *Scientific Reports* **8**, 284 (2018).

82 Blonç, M. *et al.* Evaluation of a chronic exposure to nanoplastics in goldfish (*Carassius auratus*): Analytical validation of automated assays for the measurement of biochemical markers. *Ecological Indicators* **147**, 109966 (2023).

83 Brandts, I. *et al.* Nanoplastics are bioaccumulated in fish liver and muscle and cause DNA damage after a chronic exposure. *Environmental Research* **212**, 113433 (2022).

84 Ekvall, M. T. *et al.* Size fractionation of high-density polyethylene breakdown nanoplastics reveals different toxic response in *Daphnia magna*. *Scientific Reports* **12**, 3109 (2022).

85 Nasser, F. & Lynch, I. Secreted protein eco-corona mediates uptake and impacts of polystyrene nanoparticles on *Daphnia magna*. *Journal of Proteomics* **137**, 45-51 (2016).

86 Meng, Z., Recoura-Massaquant, R., Chaumot, A., Stoll, S. & Liu, W. Acute toxicity of nanoplastics on *Daphnia* and *Gammarus* neonates: Effects of surface charge, heteroaggregation, and water properties. *Science of The Total Environment* **854**, 158763 (2023).

87 Heinlaan, M. *et al.* Hazard evaluation of polystyrene nanoplastic with nine bioassays did not show particle-specific acute toxicity. *Science of The Total Environment* **707**, 136073 (2020).

88 Lin, W. *et al.* Investigating the toxicities of different functionalized polystyrene nanoplastics on *Daphnia magna*. *Ecotoxicol Environ Saf* **180**, 509-516 (2019).

89 Vaz, V. P., Nogueira, D. J., Vicentini, D. S. & Matias, W. G. Can the sonication of polystyrene nanoparticles alter the acute toxicity and swimming behavior results for *Daphnia magna*? *Environmental Science and Pollution Research* **28**, 14192-14198 (2021).

90 Pochelon, A., Stoll, S. & Slaveykova, V. I. Polystyrene nanoplastic behavior and toxicity on crustacean *Daphnia magna*: media composition, size, and surface charge effects. *Environments* **8**, 101 (2021).

91 Liu, Z. *et al.* Age-dependent survival, stress defense, and AMPK in *Daphnia pulex* after short-term exposure to a polystyrene nanoplastic. *Aquatic Toxicology* **204**, 1-8 (2018).

92 Liu, Z. *et al.* Polystyrene nanoplastic exposure induces immobilization, reproduction, and stress defense in the freshwater cladoceran *Daphnia pulex*. *Chemosphere* **215**, 74-81 (2019).

93 Liu, Z. *et al.* Polystyrene nanoplastic induces oxidative stress, immune defense, and glycometabolism change in *Daphnia pulex*: Application of transcriptome profiling in risk assessment of nanoplastics. *Journal of Hazardous Materials* **402**, 123778 (2021).

94 Wu, D. *et al.* Molecular characterisation of cytochrome P450 enzymes in waterflea (*Daphnia pulex*) and their expression regulation by polystyrene nanoplastics. *Aquatic Toxicology* **217**, 105350 (2019).

95 Liu, Z. *et al.* Polystyrene nanoplastic induces ROS production and affects the MAPK-HIF-1/NFkB-mediated antioxidant system in *Daphnia pulex*. *Aquatic Toxicology* **220**, 105420 (2020).

96 Zhang, W. *et al.* Transcriptional response provides insights into the effect of chronic polystyrene nanoplastic exposure on *Daphnia pulex*. *Chemosphere* **238**, 124563 (2020).

97 Liu, Z. *et al.* Two sigma and two mu class genes of glutathione S-transferase in the waterflea *Daphnia pulex*: Molecular characterization and transcriptional response to nanoplastic exposure. *Chemosphere* **248**, 126065 (2020).

98 Liu, Z. *et al.* Development of an adverse outcome pathway for nanoplastic toxicity in *Daphnia pulex* using proteomics. *Science of The Total Environment*, 144249 (2020).

99 Ma, C., Liu, X. & Zuo, D. Cloning and characterization of AMP-activated protein kinase genes in *Daphnia pulex*: Modulation of AMPK gene expression in response to polystyrene nanoparticles. *Biochemical and Biophysical Research Communications* **583**, 114-120 (2021).

100 Liu, Z. *et al.* Effects of nanoplastics at predicted environmental concentration on *Daphnia pulex* after exposure through multiple generations. *Environmental Pollution* **256**, 113506 (2020).

101 Kelpsiene, E., Cedervall, T. & Malmendal, A. Metabolomics-based analysis in *Daphnia magna* after exposure to low environmental concentrations of polystyrene nanoparticles. *Environmental Science: Nano* (2023).

102 ECHA plastic additives initiative. Supplementary information on scope and methods. *https://echa.europa.eu/documents/10162/17228/plastic_additives_supplementary_en.pdf/79bea2d6-8e45-f38c-a318-7d7e812890a1* (2019).

103 Hahladakis, J. N., Velis, C. A., Weber, R., Iacovidou, E. & Purnell, P. An overview of chemical additives present in plastics: Migration, release, fate and environmental impact during their use, disposal and recycling. *Journal of hazardous materials* **344**, 179-199 (2018).

104 Gunaalan, K., Fabbri, E. & Capolupo, M. The hidden threat of plastic leachates: A critical review on their impacts on aquatic organisms. *Water Research* **184**, 116170 (2020).

105 Sridharan, S. *et al.* The polymers and their additives in particulate plastics: What makes them hazardous to the fauna? *Science of The Total Environment* **824**, 153828 (2022).

106 Hermabessiere, L. *et al.* Occurrence and effects of plastic additives on marine environments and organisms: a review. *Chemosphere* **182**, 781-793 (2017).

107 Grindler, N. M. *et al.* Exposure to phthalate, an endocrine disrupting chemical, alters the first trimester placental methylome and transcriptome in women. *Scientific reports* **8**, 6086 (2018).

108 ECHA, E. C. A. Phthalates.

109 Schrank, I. *et al.* Effects of microplastic particles and leaching additive on the life history and morphology of *Daphnia magna*. *Environmental Pollution* **255**, 113233 (2019).

110 Galloway, T. S., Cole, M. & Lewis, C. Interactions of microplastic debris throughout the marine ecosystem. *Nature ecology & evolution* **1**, 1-8 (2017).

111 Cao, J. *et al.* Coronas of micro/nano plastics: a key determinant in their risk assessments. *Particle and Fibre Toxicology* **19**, 55 (2022).

112 Chakraborty, D., Giri, S., Natarajan, L., Chandrasekaran, N. & Mukherjee, A. Recent advances in understanding the facets of eco-corona on engineered nanomaterials. *Journal of the Indian Institute of Science* **102**, 621-637 (2022).

113 Cedervall, T. *et al.* Understanding the nanoparticle–protein corona using methods to quantify exchange rates and affinities of proteins for nanoparticles. *Proceedings of the National Academy of Sciences* **104**, 2050-2055 (2007).

114 Lima, T., Bernfur, K., Vilanova, M. & Cedervall, T. Understanding the lipid and protein corona formation on different sized polymeric nanoparticles. *Scientific reports* **10**, 1-9 (2020).

115 Nel, A. E. *et al.* Understanding biophysicochemical interactions at the nano-bio interface. *Nature materials* **8**, 543-557, doi:10.1038/nmat2442 (2009).

116 Chetwynd, A. J. & Lynch, I. The rise of the nanomaterial metabolite corona, and emergence of the complete corona. *Environmental Science: Nano* **7**, 1041-1060 (2020).

117 Lynch, I. & Dawson, K. A. Protein-nanoparticle interactions. *Nano Today* **3**, 40-47 (2008).

118 Miceli, E., Kar, M. & Calderón, M. Interactions of organic nanoparticles with proteins in physiological conditions. *Journal of Materials Chemistry B* **5**, 4393-4405 (2017).

119 Tenzer, S. *et al.* Rapid formation of plasma protein corona critically affects nanoparticle pathophysiology. *Nature nanotechnology* **8**, 772-781 (2013).

120 Ritz, S. *et al.* Protein corona of nanoparticles: distinct proteins regulate the cellular uptake. *Biomacromolecules* **16**, 1311-1321 (2015).

121 Wheeler, K. E. *et al.* Environmental dimensions of the protein corona. *Nature Nanotechnology* **16**, 617-629 (2021).

122 Lundqvist, M. *et al.* Nanoparticle size and surface properties determine the protein corona with possible implications for biological impacts. *Proceedings of the National Academy of Sciences* **105**, 14265-14270 (2008).

123 Hühn, D. *et al.* Polymer-coated nanoparticles interacting with proteins and cells: focusing on the sign of the net charge. *ACS Nano* **7**, 3253-3263 (2013).

124 Gebauer, J. S. *et al.* Impact of the nanoparticle-protein corona on colloidal stability and protein structure. *Langmuir* **28**, 9673-9679 (2012).

125 Mahmoudi, M. *et al.* Temperature: the “ignored” factor at the nanobio interface. *ACS nano* **7**, 6555-6562 (2013).

126 Dutz, S., Wojahn, S., Gräfe, C., Weidner, A. & Clement, J. H. Influence of sterilization and preservation procedures on the integrity of serum protein-coated magnetic nanoparticles. *Nanomaterials* **7**, 453 (2017).

127 Tenzer, S. *et al.* Nanoparticle size is a critical physicochemical determinant of the human blood plasma corona: a comprehensive quantitative proteomic analysis. *ACS Nano* **5**, 7155-7167 (2011).

128 Lundqvist, M. & Cedervall, T. Three decades of research about the corona around nanoparticles: lessons learned and where to go now. *Small* **16**, 2000892 (2020).

129 Kopac, T. Protein corona, understanding the nanoparticle–protein interactions and future perspectives: A critical review. *International Journal of Biological Macromolecules* **169**, 290-301 (2021).

130 Fleischer, C. C. & Payne, C. K. Nanoparticle–cell interactions: molecular structure of the protein corona and cellular outcomes. *Accounts of chemical research* **47**, 2651-2659 (2014).

131 Vroman, L., Adams, A., Fischer, G. & Munoz, P. Interaction of high molecular weight kininogen, factor XII, and fibrinogen in plasma at interfaces. (1980).

132 Duan, G. *et al.* Protein corona mitigates the cytotoxicity of graphene oxide by reducing its physical interaction with cell membrane. *Nanoscale* **7**, 15214-15224 (2015).

133 Lee, Y. K., Choi, E.-J., Webster, T. J., Kim, S.-H. & Khang, D. Effect of the protein corona on nanoparticles for modulating cytotoxicity and immunotoxicity. *International journal of nanomedicine* **10**, 97 (2015).

134 Lesniak, A. *et al.* Effects of the presence or absence of a protein corona on silica nanoparticle uptake and impact on cells. *ACS Nano* **6**, 5845-5857 (2012).

135 Khort, A. *et al.* Influence of natural organic matter on the transformation of metal and metal oxide nanoparticles and their ecotoxic potency in vitro. *NanoImpact* **25**, 100386 (2022).

136 Docter, D. *et al.* The nanoparticle biomolecule corona: lessons learned–challenge accepted? *Chemical Society Reviews* **44**, 6094-6121 (2015).

137 Pradhan, S. *et al.* Influence of humic acid and dihydroxy benzoic acid on the agglomeration, adsorption, sedimentation and dissolution of copper, manganese, aluminum and silica nanoparticles–A tentative exposure scenario. *PLoS One* **13**, e0192553 (2018).

138 Hedberg, Y. S. *et al.* Nanoparticles of WC-Co, WC, Co and Cu of relevance for traffic wear particles–particle stability and reactivity in synthetic surface water and influence of humic matter. *Environmental pollution* **224**, 275-288 (2017).

139 Lowry, G. V., Gregory, K. B., Apte, S. C. & Lead, J. R. Transformations of nanomaterials in the environment. *Environmental science & technology* **46**, 6893-6899 (2012).

140 Wang, Z., Zhang, L., Zhao, J. & Xing, B. Environmental processes and toxicity of metallic nanoparticles in aquatic systems as affected by natural organic matter. *Environmental Science: Nano* **3**, 240-255 (2016).

141 Hyne, R. V., Pablo, F., Julli, M. & Markich, S. J. Influence of water chemistry on the acute toxicity of copper and zinc to the cladoceran *Ceriodaphnia cf dubia*. *Environmental Toxicology and Chemistry: An International Journal* **24**, 1667-1675 (2005).

142 Clifford, M. & McGeer, J. C. Development of a biotic ligand model for the acute toxicity of zinc to *Daphnia pulex* in soft waters. *Aquatic Toxicology* **91**, 26-32 (2009).

143 Ekvall, M. T. *et al.* Adsorption of bio-organic eco-corona molecules reduces the toxic response to metallic nanoparticles in *Daphnia magna*. *Scientific reports* **11**, 1-11 (2021).

144 Kelpsiene, E. *et al.* The effect of natural biomolecules on yttrium oxide nanoparticles from a *Daphnia magna* survival rate perspective. *Nanotoxicology*, 1-15 (2023).

145 European Bioplastics, nova-Institute. *https://www.european-bioplastics.org/global-bioplastics-production-defies-challenges-by-showing-significant-increase/* (2022).

146 Svensk Dagligvaruhandel. Road map for fossil free competitiveness – food retailers. *https://www.svenskdagligvaruhandel.se/wp-content/uploads/SvDH.-Fossil-free-and-recyclable-plastic-pacakaging-to-2030.Sweden-1.pdf* (2018).

147 Iwata, T. Biodegradable and bio-based polymers: future prospects of eco-friendly plastics. *Angewandte Chemie International Edition* **54**, 3210-3215 (2015).

148 Kubowicz, S. & Booth, A. M. Biodegradability of plastics: challenges and misconceptions. *Environmental Science & Technology* **51**, 12058-12060 (2017).

149 Singhvi, M. S., Zinjarde, S. S. & Gokhale, D. V. Polylactic acid: synthesis and biomedical applications. *Journal of Applied Microbiology* **127**, 1612-1626 (2019).

150 Ainali, N. M. *et al.* Do poly (lactic acid) microplastics instigate a threat? A perception for their dynamic towards environmental pollution and toxicity. *Science of the total environment* **832**, 155014 (2022).

151 Chen, W.-L., Cordero, R., Tran, H. & Ober, C. K. 50th anniversary perspective: Polymer brushes: Novel surfaces for future materials. *Macromolecules* **50**, 4089-4113 (2017).

152 Xu, L., Crawford, K. & Gorman, C. B. Effects of temperature and pH on the degradation of poly (lactic acid) brushes. *Macromolecules* **44**, 4777-4782 (2011).

153 Haider, T. P., Völker, C., Kramm, J., Landfester, K. & Wurm, F. R. Plastics of the future? The impact of biodegradable polymers on the environment and on society. *Angewandte Chemie International Edition* **58**, 50-62 (2019).

154 Liu, X. *et al.* Effects comparison between the secondary nanoplastics released from biodegradable and conventional plastics on the transfer of antibiotic resistance genes between bacteria. *Environmental Pollution* **317**, 120680 (2023).

155 Green, D. S. Effects of microplastics on European flat oysters, *Ostrea edulis* and their associated benthic communities. *Environmental Pollution* **216**, 95-103 (2016).

156 Green, D. S., Colgan, T. J., Thompson, R. C. & Carolan, J. C. Exposure to microplastics reduces attachment strength and alters the haemolymph proteome of blue mussels (*Mytilus edulis*). *Environmental Pollution* **246**, 423-434 (2019).

157 Zhang, X. *et al.* Photolytic degradation elevated the toxicity of polylactic acid microplastics to developing zebrafish by triggering mitochondrial dysfunction and apoptosis. *Journal of Hazardous Materials* **413**, 125321 (2021).

158 Chagas, T. Q. *et al.* Multiple endpoints of polylactic acid biomicroplastic toxicity in adult zebrafish (*Danio rerio*). *Chemosphere* **277**, 130279 (2021).

159 Rosli, N. A., Karamanlioglu, M., Kargarzadeh, H. & Ahmad, I. Comprehensive exploration of natural degradation of poly (lactic acid) blends in various degradation media: a review. *International journal of biological macromolecules* **187**, 732-741 (2021).

160 Ebert, D. Introduction to *Daphnia* biology. *Ecology, Epidemiology and Evolution of Parasitism in Daphnia*, 5-18 (2005).

161 Ebert, D. *Daphnia* as a versatile model system in ecology and evolution. *EvoDevo* **13**, 16 (2022).

162 Geller, W. & Müller, H. The filtration apparatus of Cladocera: filter mesh-sizes and their implications on food selectivity. *Oecologia* **49**, 316-321 (1981).

163 Rist, S., Baun, A. & Hartmann, N. B. Ingestion of micro-and nanoplastics in *Daphnia magna*–quantification of body burdens and assessment of feeding rates and reproduction. *Environmental pollution* **228**, 398-407 (2017).

164 Jemec, A., Horvat, P., Kunej, U., Bele, M. & Kržan, A. Uptake and effects of microplastic textile fibers on freshwater crustacean *Daphnia magna*. *Environmental Pollution* **219**, 201-209 (2016).

165 Davis, A., Nasser, F., Lead, J. R. & Shi, Z. Development and application of a ratiometric nanosensor for measuring pH inside the gastrointestinal tract of zooplankton. *Environmental Science: Nano* **7**, 1652-1660 (2020).

166 Powers, K. W. *et al.* Research strategies for safety evaluation of nanomaterials. Part VI. Characterization of nanoscale particles for toxicological evaluation. *Toxicological Sciences* **90**, 296-303 (2006).

167 Filipe, V., Hawe, A. & Jiskoot, W. Critical evaluation of nanoparticle tracking analysis (NTA) by NanoSight for the measurement of nanoparticles and protein aggregates. *Pharm Res* **27**, 796-810 (2010).

168 Jia, Z., Li, J., Gao, L., Yang, D. & Kanaev, A. Dynamic light scattering: a powerful tool for in situ nanoparticle sizing. *Colloids and Interfaces* **7**, 15 (2023).

169 Minelli, C. *et al.* Measuring the size and density of nanoparticles by centrifugal sedimentation and flotation. *Analytical Methods* **10**, 1725-1732 (2018).

170 Naiim, M. *et al.* Multiangle dynamic light scattering for the improvement of multimodal particle size distribution measurements. *Soft matter* **11**, 28-32 (2015).

171 Gilroy, E. L., Hicks, M. R., Smith, D. J. & Rodger, A. Viscosity of aqueous DNA solutions determined using dynamic light scattering. *Analyst* **136**, 4159-4163 (2011).

172 Bhattacharjee, S. DLS and zeta potential – What they are and what they are not? *Journal of Controlled Release* **235**, 337-351 (2016).

173 Worldwide, M. I. Dynamic light scattering, common terms defined. *Inform white paper. Malwern Instruments Limited*, 1-6 (2011).

174 Filipe, V., Hawe, A. & Jiskoot, W. Critical evaluation of nanoparticle tracking analysis (NTA) by NanoSight for the measurement of nanoparticles and protein aggregates. *Pharm Res* **27**, 796-810 (2010).

175 Jiang, J., Oberdörster, G. & Biswas, P. Characterization of size, surface charge, and agglomeration state of nanoparticle dispersions for toxicological studies. *Journal of Nanoparticle Research* **11**, 77-89 (2009).

176 Clogston, J. D. & Patri, A. K. Zeta potential measurement. *Characterization of nanoparticles intended for drug delivery*, 63-70 (2011).

177 Freitas, C. & Müller, R. H. Effect of light and temperature on zeta potential and physical stability in solid lipid nanoparticle (SLN™) dispersions. *International journal of pharmaceutics* **168**, 221-229 (1998).

178 Campanale, C., Savino, I., Massarelli, C. & Uricchio, V. F. Fourier transform infrared spectroscopy to assess the degree of alteration of artificially aged and environmentally weathered microplastics. *Polymers* **15**, 911 (2023).

179 Petit, S. Fourier transform infrared spectroscopy. *Developments in Clay Science* **1**, 909-918 (2006).

180 Michen, B. *et al.* Avoiding drying-artifacts in transmission electron microscopy: Characterizing the size and colloidal state of nanoparticles. *Scientific Reports* **5**, 9793 (2015).

181 Kelpsiene, E. *et al.* Protein binding on acutely toxic and non-toxic polystyrene nanoparticles during filtration by *Daphnia magna*. *Environmental Science: Nano* (2022).

182 Lenz, R., Enders, K. & Nielsen, T. G. Microplastic exposure studies should be environmentally realistic. *Proceedings of the National Academy of Sciences* **113**, 4121-4122 (2016).

183 OECD. *Test No. 202: Daphnia sp. Acute Immobilisation Test.* (2004).

184 Burns, C. W. The relationship between body size of filter-feeding Cladocera and the maximum size of particle ingested. *Limnology and Oceanography* **13**, 675-678 (1968).

185 Gophen, M. & Geller, W. Filter mesh size and food particle uptake by *Daphnia*. *Oecologia* **64**, 408-412 (1984).

186 Lampert, W. & Brendelberger, H. Strategies of phenotypic low-food adaptation in *Daphnia*: Filter screens, mesh sizes, and appendage beat rates. *Limnology and Oceanography* **41**, 216-223 (1996).

187 *OECD Test No. 211: Daphnia magna reproduction test https://read.oecd-ilibrary.org/environment/test-no-211-daphnia-magna-reproduction-test_9789264185203-en#page1*. (2012).

188 Pacheco, A., Martins, A. & Guilhermino, L. Toxicological interactions induced by chronic exposure to gold nanoparticles and microplastics mixtures in *Daphnia magna*. *Science of the total environment* **628**, 474-483 (2018).

189 Liu, Y. *et al.* Effects of polyvinyl chloride microplastics on reproduction, oxidative stress and reproduction and detoxification-related genes in *Daphnia magna*. *Comparative Biochemistry and Physiology Part C: Toxicology & Pharmacology* **254**, 109269 (2022).

190 Baun, A., Hartmann, N. B., Grieger, K. & Kusk, K. O. Ecotoxicity of engineered nanoparticles to aquatic invertebrates: a brief review and recommendations for future toxicity testing. *Ecotoxicology* **17**, 387-395 (2008).

191 Baun, A., Sørensen, S. N., Rasmussen, R., Hartmann, N. B. & Koch, C. B. Toxicity and bioaccumulation of xenobiotic organic compounds in the presence of aqueous suspensions of aggregates of nano-C60. *Aquatic Toxicology* **86**, 379-387 (2008).

192 Murray, F. & Cowie, P. R. Plastic contamination in the decapod crustacean *Nephrops norvegicus* (Linnaeus, 1758). *Marine pollution bulletin* **62**, 1207-1217 (2011).

193 Skjolding, L. M. *et al.* Aquatic ecotoxicity testing of nanoparticles—the quest to disclose nanoparticle effects. *Angewandte Chemie International Edition* **55**, 15224-15239 (2016).

194 Rosenkranz, P., Chaudhry, Q., Stone, V. & Fernandes, T. F. A comparison of nanoparticle and fine particle uptake by *Daphnia magna*. *Environmental toxicology and chemistry* **28**, 2142-2149 (2009).

195 Kaur, J. *et al.* Label-free detection of polystyrene nanoparticles in *Daphnia magna* and assessment of barrier integrity using an in vitro intestinal model. *Nanoscale Advances* **5**, 3453-3462 (2023).

196 Nagato, E. G., Simpson, A. J. & Simpson, M. J. Metabolomics reveals energetic impairments in *Daphnia magna* exposed to diazinon, malathion and bisphenol-A. *Aquatic Toxicology* **170**, 175-186 (2016).

197 Lane, D. *et al.* Selective amino acid-only *in vivo* NMR: a powerful tool to follow stress processes. *ACS Omega* **4**, 9017-9028 (2019).

198 Tattoli, I. *et al.* Amino acid starvation induced by invasive bacterial pathogens triggers an innate host defense program. *Cell Host & Microbe* **11**, 563-575 (2012).

199 Zhang, X. *et al.* Innate immune responses and metabolic alterations of mud crab (*Scylla paramamosain*) in response to *Vibrio parahaemolyticus* infection. *Fish & Shellfish Immunology* **87**, 166-177 (2019).

200 Houbrechts, A. M. *et al.* Age-dependent changes in glucose homeostasis in male deiodinase type 2 knockout zebrafish. *Endocrinology* **160**, 2759-2772 (2019).

201 Arslan, K. *et al.* Engineering *Acetobacterium woodii* for the production of isopropanol and acetone from carbon dioxide and hydrogen. *Biotechnology Journal* **17**, 2100515 (2022).

202 Saptarshi, S. R., Duschl, A. & Lopata, A. L. Interaction of nanoparticles with proteins: relation to bio-reactivity of the nanoparticle. *Journal of nanobiotechnology* **11**, 1-12 (2013).

203 Li, S. A. *et al.* Immunohistochemical localization of Klotho protein in brain, kidney, and reproductive organs of mice. *Cell structure and function* **29**, 91-99 (2004).

204 Dhar, P., Tarafder, D., Kumar, A. & Katiyar, V. Thermally recyclable polylactic acid/cellulose nanocrystal films through reactive extrusion process. *Polymer* **87**, 268-282 (2016).

205 Lopera-Valle, A. & Elias, A. Amine responsive poly (lactic acid)(PLA) and succinic anhydride (SAh) graft-polymer: synthesis and characterization. *Polymers* **11**, 1466 (2019).

206 Kalogerakis, N. *et al.* Microplastics generation: onset of fragmentation of polyethylene films in marine environment mesocosms. *Frontiers in Marine Science* **4** (2017).

207 Kelpsiene, E., Rydberg, M., Ekvall, M. T., Lundqvist, M. & Cedervall, T. Prolonged survival time of *Daphnia magna* exposed to polylactic acid breakdown nanoplastics. *PLOS ONE* **18**, e0290748 (2023).

208 Zettler, E. R., Mincer, T. J. & Amaral-Zettler, L. A. Life in the "Plastisphere": microbial communities on plastic marine debris. *Environmental Science & Technology* **47**, 7137-7146 (2013).

209 Lagarde, F. *et al.* Microplastic interactions with freshwater microalgae: hetero-aggregation and changes in plastic density appear strongly dependent on polymer type. *Environmental pollution* **215**, 331-339 (2016).

210 Fazey, F. M. C. & Ryan, P. G. Biofouling on buoyant marine plastics: An experimental study into the effect of size on surface longevity. *Environmental Pollution* **210**, 354-360 (2016).

211 Romera-Castillo, C., Pinto, M., Langer, T. M., Álvarez-Salgado, X. A. & Herndl, G. J. Dissolved organic carbon leaching from plastics stimulates microbial activity in the ocean. *Nature communications* **9**, 1430 (2018).

Scientific Publications

Paper I

SCIENTIFIC REPORTS
nature research

OPEN

Long-term exposure to nanoplastics reduces life-time in *Daphnia magna*

Egle Kelpsiene[1,3*], Oscar Torstensson[1], Mikael T. Ekvall[2,3], Lars-Anders Hansson[2,3] & Tommy Cedervall[1,3]

Plastics are widely used in todays society leading to an accelerating amount of plastic waste entering natural ecosystems. Over time these waste products degrade to micro- and, eventually, nanoplastic particles. Therefore, the break-down of plastics may become a critical threat to aquatic ecosystems and several short term studies have demonstrated acute toxicity of nanoplastics on aquatic organisms. However, our knowledge about effects of chronic or life-time exposure on freshwater invertebrates remains elusive. Here, we demonstrate results from life-time exposure (103 days) of a common freshwater invertebrate, *Daphnia magna*, exposed to sub-lethal concentrations of polystyrene nanoparticles. 53 nm positively charged aminated polystyrene particles were lethal at concentration of 0.32 mg/L which is two magnitudes lower than previously used concentrations in short-term (24 h) tests. At this concentration the life-time of individuals was shortened almost three times. Negatively charged carboxylated 26 and 62 nm polystyrene particles, previously demonstrated to be non-toxic at 25 and 50 mg/L concentrations in short-term tests, were toxic to *D. magna* at all concentrations used in our long-term study. Although total reproductive output was not significantly affected at increasing concentrations of polystyrene nanoparticles, there was a decreasing trend in the number of offspring over their life-time. Hence, in order to understand how the potential future environmental problem of nanoplastic particles may affect biota, long-term or life-time studies resembling environmental concentrations should be performed in order to provide information for predictions of future scenarios in natural aquatic environments.

Plastic materials are of remarkable benefit for modern society due to their low price, easy manufacturing and practical function in a multitude of daily used products[1]. At a global scale, plastic production has increased tremendously over the past years[2], and will likely continue increasing. Lebreton *et al.*[3] estimated that between 1.15 and 2.41 million tonnes of plastic waste enter oceans every year. Plastics can degrade into a wide range of sizes, including micro- (<5 mm) and nano-sized (<100 nm) particles. Biological degradation[4], exposure to ultraviolet radiation, and abrasion[5] are processes taking place under natural conditions. Nanoplastics in nature has in one case been reported[6] and the presence of styrene oligomers[7,8] indicates continuing degradation of polystyrene in nature. Furthermore, ordinary polystyrene products submitted to mechanical forces[9] or ultraviolet radiation[10] in laboratory conditions release nanosized particles. Pollution by micro- and nanoplastics constitutes a potential threat to aquatic ecosystems[11,12]. Due to their small size, plastic particles might be ingested by organisms at the lower end of the food chain and can be thansferred by feeding to top consumers[13,14]. Several studies have shown that plastic particles of various sizes can be ingested by aquatic organisms causing tissue damage[15] or even death[16]. Therefore, plastic pollution in aquatic environments and its potential impact on aquatic life has recently been recognized as an issue of considerable concern for society, as well as for ecosystem functioning[16].

Although many studies addressing microplastic pollution have focused on marine environments[17,18], recent reports have shown that microplastics can also be found in freshwater ecosystems[19,20]. Previous studies have reported microplastic ingestion by freshwater invertebrates such as tubificid worms[21] and amphipod crustaceans[22]. Previously it has been observed that ingestion of nanoplastic particles may disturb fish feeding behavior and alter their metabolism[23–25], as well as induce oxidative stress and tissue damage[26,27].

[1]Department of Biochemistry and Structural Biology, Lund University, Lund University, P.O. Box 118, SE-221 00, Lund, Sweden. [2]Department of Biology/Aquatic ecology, Lund University, SE-223 62, Lund, Sweden. [3]NanoLund, Lund University, Box 118, SE-221 00, Lund, Sweden. *email: egle.kelpsiene@biochemistry.lu.se

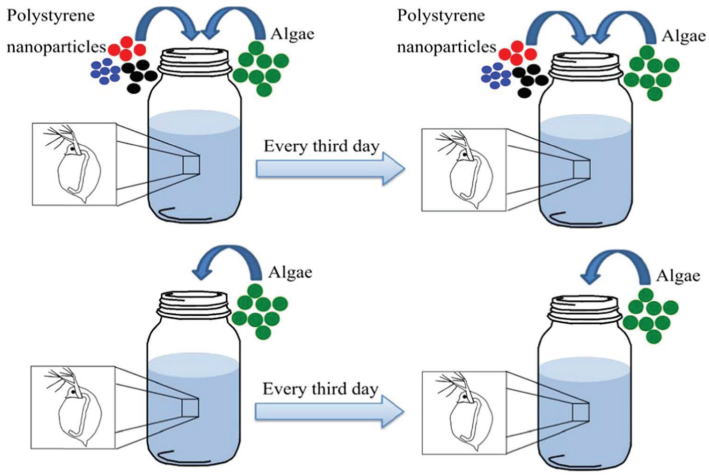

Figure 1. Schematic representation of long-term toxicity test. In total, there were ten replicates in each treatment. During the exposure to polystyrene nanoparticles, alive *Daphnia magna* individuals were transferred every third day to 100 mL glass beakers with 80 mL total volume of fresh medium, containing 2.5 mL of food (algae), with (treatment) or without (control) particles. Nanoparticles were dialyzed prior the experiments and particle sizes were measured during exposure using DLS. Algae concentration and water pH values were measured every time *D. magna* was transferred.

Several ecotoxicological studies have used the freshwater crustacean *Daphnia magna* as study organism[28–31]. *D. magna* is a filter feeder and plays a key role in freshwater food chains as a food source for many aquatic organisms[32]. Previous studies have shown that *D. magna* can ingest nano- and microplastic particles ranging in size from 20 nm to 5μm[28,30] and that *D. magna* show reduced reproduction after 21 days of exposure to 70 nm polystyrene particles[33]. Exposure to microplastics can also alter feeding behavior[31], reduce growth rate or lead to immobilization in *D. magna*[34].

The small size of plastic particles appears to be an important factor behind toxicity[24,29]. Mattsson *et al.*[24] showed that survival of *D. magna* was significantly affected after acute exposure to concentrations ranging from 75 to 150 mg/L of 52 nm aminated polystyrene nanoparticles. Similarly, after exposure to 100 mg/L of positively and negatively charged polystyrene particles, *D. magna* neonates were all immobilized after 24 h exposure[29]. Additionally, exposure to 70 nm polystyrene particles negatively affected reproduction and body size of *D. magna* at concentrations of 0.22 and 103 mg/L[33], and 52 nm polystyrene nanoparticles, at a concentration of 5 mg/L, reduced hatching rate and caused abnormal embryo development in *D. galeata*[35].

Despite several acute toxicity tests showing negative effects on freshwater and marine zooplankton[28,34,36,37], surprisingly little is known about the long-term biological and ecological effects of nanoplastics. Therefore, the aim of our study was to address the potential effects on life history traits (survival and reproduction) in *D. magna* to life-time exposure to three smallest commercially available polystyrene particles sizes.

Results and Discussion

It has previously been shown in acute 24 h tests that small (50 to 60 nm) positively charged aminated polystyrene nanoparticles (PS-NH_2) are the most toxic particles among the polystyrene nanoparticles tested on *D. magna*[24]. Therefore, 53 nm PS-NH_2 nanoparticles were chosen in the present study to determine the lowest concentrations of nanoparticles observed causing mortality of *D. magna* in life-time exposure. Two to five day-old *D. magna* were isolated and exposed to polystyrene nanoparticles (Fig. 1) throughout their entire life-time, which for the oldest animal was 103 days. A concentration of 0.32 mg/L was chosen based from preliminary studies with aminated polystyrene nanoparticles (data not shown). In order to compare differently charged nanoparticles of specific surface areas, we increased concentrations for 62 and 26 nm carboxylic modified particles.

D. magna individuals exposed to 0.32 mg/L of 53 nm PS-NH_2 showed an increased mortality ($\chi^2_{(1)} = 10.19$, $p < 0.01$) compared to the control group, while lower concentrations (0.032 and 0.0032 mg/L, Fig. 2) did not have any significant effects ($\chi^2_{(1)} = 0.89$ and 0.089, respectively, $p > 0.05$, Fig. 2). The lowest lethal concentration in the present study (0.32 mg/L) was 78 times lower compared to the lowest lethal concentration (25 mg/L) previously used in acute tests[24].

We also addressed the question if polystyrene nanoparticles that did not induce mortality in acute test[24] is toxic at long-term (life-time) exposure. Negatively charged carboxylated polystyrene nanoparticles (PS-COOH) at the sizes 26 and 62 nm have been shown to be non-toxic in 24 h acute tests at concentrations up to 400 mg/L[24].

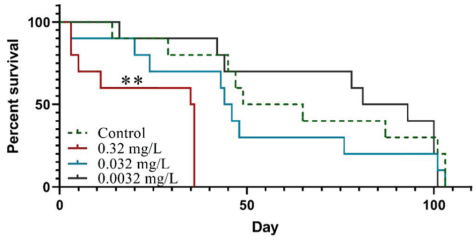

Figure 2. Survival of *Daphnia magna* exposed to different concentrations of 53 nm PS-NH_2 throughout their life-time. Asterisk indicates significant difference compared to the control group estimated over the whole study period, $^{**}p < 0.01$.

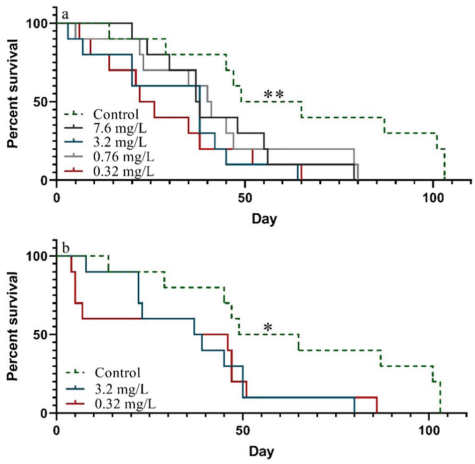

Figure 3. Survival of *Daphnia magna* exposed to 62 nm PS-COOH (**a**) and 26 nm PS-COOH (**b**) particles throughout their life-time. Asterisks indicate significant differences throughout the study period compared to the control group, $^{*}p < 0.05$, $^{**}p < 0.01$. Asterisks added on the control group indicate that all treatments were significantly different from the control group.

However, after long term exposure to lower concentrations (7.6, 3.2, 0.76 and 0.32 mg/L) of 62 nm PS-COOH in our study, *D. magna* showed a significant decrease in survival ($\chi^2_{(1)} = 3.85$, 8.03, 4.55 and 6.89, respectively, $p < 0.05$, Fig. 3a). Similarly, *D. magna* showed a significantly reduced survival rate than in the control when exposed to both 3.2 and 0.32 mg/L of 26 nm PS-COOH ($\chi^2_{(1)} = 4.51$ and 5.04, respectively, $p < 0.05$, Fig. 3b). For none of the sizes sub-lethal concentrations were reached and we may therefore conclude that although these carboxylated polystyrene particles were not considered toxic at short-term 24 h exposure[24], they are indeed lethal at similar concentrations as the aminated particles at prolonged exposure.

Interestingly, there was an apparent reversed concentration dependency in survival between the lowest (0.32 mg/L) and highest (7.6 mg/L) concentrations of 62 nm PS-COOH. It could be speculated, especially as the polystyrene nanoparticles are mixed with the algae, that the exposure scenario was influenced by differences in nanoparticle concentrations, e.g. aggregation and/or faster sedimentation. Sedimentation was shown to be an important factor affecting exposure scenarios in a life-time test evaluating the effects of tungsten carbide nanoparticles[38]. However, in the present study, no sedimentation was observed over 48 h at a particle concentration of 7.6 mg/L mixed together with algae (Fig. S1). Furthermore, no particle aggregation, measured by dynamic light scattering (DLS), was observed in neither the lowest, nor the highest concentrations (Table S1). Another possible difference in exposure scenario is that the binding of organic molecules to the particle surfaces changes the toxicity of the particles. This effect has been shown for polystyrene particles pre-incubated in algae and in media containing molecules secreted from *D. magna*[29,33]. Increasing the particle concentration from 0.32 to 7.6 mg/L

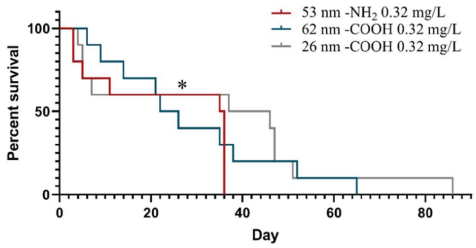

Figure 4. Comparison of *Daphnia magna* survival during life-time exposure to 53 nm PS-NH_2, 62 nm PS-COOH and 26 nm PS-COOH at 0.32 mg/L. Asterisk indicates significant difference compared to the control group throughout the study period, $*p < 0.05$.

causes an increase in added particle surface area from 2.4×10^{11} to 56.4×10^{11} µm^2 which may affect which type and how much organic material is bound to the particles.

A comparison between the effect of 53 nm PS-NH_2, 62 nm PS-COOH and 26 nm PS-COOH at 0.32 mg/L, revealed a significant difference in the survival of *D. magna* between 53 nm -NH_2 and 26 nm -COOH treatments ($\chi^2_{(1)} = 3.88$, $p < 0.05$, Fig. 4). This implies that although the PS-COOH was shown to be toxic in the life-time experiments, but not in acute tests[24], there is still a charge dependent toxicity. Generally, the positively charged PS-NH_2 have been shown to be more toxic to *D. magna*, which might be due to a stronger interaction with the negatively charged *Daphnia* cell membrane[29]. It has also been shown that 50 nm PS-NH_2 particle induces apoptosis in a variety of cells, while negatively charged nanoplastic particles did not have a significant effect[39].

The accumulation of polystyrene nanoparticles in the body of *D. magna* has previously been demonstrated using fluorescent nanoparticles[29], including the uptake of 20 and 70 nm particles[25,40], as well as the accumulated body burden after 21 days exposure to 100 nm fluorescent polystyrene particles[37]. However, no data is available for the accumulation of non-fluorescent polystyrene nanoparticles. In order to document any microscopic changes during the life-time exposure, microscopic images were taken after death of several randomly chosen *D. magna* individuals (n = 3 for each treatment) that died after 30 to 100 days of exposure to different concentrations and sizes of PS-NH_2 and PS-COOH. In some of the *D. magna* exposed to 53 nm PS-NH_2 and 62 nm PS-COOH the gut contents were blackish (Fig. S2-B-C), which was not seen in individuals exposed to 26 nm PS-COOH (Fig. S2. D). These observations might suggest an accumulation of nanoplastic particles in some of the exposed organisms. This was not observed in any of the photographed individuals from the control group, where the guts instead had greenish contents from algal feeding (Fig. S2. A). Accumulation of nanoplastics in the gut of several organisms has previously been observed. For example, Torre *et al.*[41] noted that after 48 h exposure negatively charged particles were accumulated in the digestive tract of sea urchin embryos, whereas positively charged nanoplastic particles were more dispersed in the gut. Nanoplastic particles aggregates have also been observed in *D. galeata* exposed to 52 nm polystyrene nanoparticles[35]. Similarly, Jemec *et al.*[28] showed that polyethylene terephthalate textile microfibers were present in the gut of tested *D. magna* after 48 h exposure. Microplastic particles were also seen in the gut of exposed *D. magna* after 24 h test to particle concentrations of 12.5–400 mg/L, while the guts of control animals were greenish[34].

In our study, the total number of offspring produced during the whole exposure time in treatments and the control group were not significantly different, neither by nanoparticle size nor concentration used within the same time period ($p > 0.05$ one-way ANOVA, Table S2). Similary, Rist *et al.*[37] showed that reproduction was not effected after 21-day exposure to micro- and nanoplastic particles. However, at increasing concentrations of polystyrene nanoparticles, there was a decreasing trend in the number of offspring over their life-time (Table S3). Similarly, Besseling *et al.*[33] also observed that increasing concentrations reduced the number of *D. magna* offspring. *D. magna* exposed to 0.1 mg/L of 1–5 µm microplastics of polymer microspheres for 21-day showed a significant reduction in reproduction[42]. Rist *et al.*[37] showed that there was no difference in time to first offspring when *D. magna* were exposed to micro- and nanoplastic particles for 21 days, whereas Pacheco *et al.*[43] observed a delay in the first brood release in *D. magna* after exposure to 1–5 µm microplastics. Likewise, Ekvall *et al.*[38] showed a significant delay in time to first brood in *D. magna* exposed to tungsten carbide nanoparticles.

The majority of the published studies focus on acute, short-term, tests at high plastic particle concentrations[24,29,34], whereas long-term toxicity studies on nanoplastics are rare, despite long-term, even life-time, exposure to low concentrations is the rule as nanoparticles enter natural ecosystems. Therefore, our understanding on how life-time exposure to nanoplastic particles affect organisms in aquatic food chains still remains elusive. Potential effects on aquatic organisms, such as zooplankton, may have considerable consequences for the function of aquatic food webs in which these organisms play a key role. In natural environments aquatic organisms are exposed to different sizes of plastic particles during their whole life-span. Our life-time experimental set-up does not only demonstrate toxicity of nanoplastic particles at relatively low concentrations, but also reveals toxicity of nanoplastics that are apparently non-toxic in standardized 24 or 48 h acute tests even at very high concentrations. Furthermore, in many cases mortality occurs after the standardized long-term 21-day tests. This clearly suggests that routine, standard test times may not be enough to assess the severity of plastic particles in our environment. Hence, by introducing life-time exposure tests we were here able to identify lethal effects at concentrations almost

Surface modification	Diameter size (nm)	Concentration (mg/L)	Specific surface area (μm^2/mg)	Particles/mL (at concentration of 0.32 mg/L)	Surface charge
Aminated (-NH_2)	53	0.32, 0.032, 0.0032	1.11×10^{11}	3.91×10^9	Positive
Carboxylated (-COOH)	26	3.2, 0.32	2.21×10^{11}	3.31×10^{10}	Negative
	62	7.6, 3.2, 0.76, 0.32	9.29×10^{10}	2.44×10^9	

Table 1. Characteristics for particles used.

two magnitudes lower than previously shown[29]. Moreover, mortality may not be optimal to assess the lowest concentration of nanoplastic particles that will negatively affect the environment. Slow uptake of nanoplastics at low concentrations allow for accumulation of particles by the individuals, whereas high concentrations of nanoplastics in acute tests may rip off tissue or deplete the digestive system of neseccary enzymes[44–46]. In the future there is a need for mechanistic studies of the long-term toxicity in order to be able to properly assess the environmental risk, as well as the risk of different kinds of plastic particles.

Although the relevant concentrations of nanoplastic particles have, due to methodological constraints, not been determined, we here use relatively low concentrations of nanoplastic. We conclude that long-term exposure to low concentrations of nanoplastics material may provide considerably different outcomes with respect to toxicity than short-term, acute tests at high concentrations. Since long-term, or even life-time exposures may even already be ongoing in many regions of the world, our results have considerable implications for our use and manufacturing of plastic materials.

Material and Methods

Study organisms. The *Daphnia magna* culture used originates from Lake Bysjön, southern Sweden (55°40′31.3″N 13°32′41.9″E), and has been kept in the laboratory for several hundred generations. The culture was fed three times per week with an algae diet mainly composed of the green algae *Scenedesmus* sp. The algal culture was filtered once a week through 20 μm mesh filter to remove larger algal species, such as cyanobacteria, from the culture and fed with 250 μL of liquid plant nutrient, of which 100 mL contains 5.1 g nitrogen, 1.0 g phosphorus and microelements. All cultures were maintained at 18 °C at a 8:16 h light/dark photoperiod.

Nanoparticles preparation and characterization. The smallest commercially available positively (aminated, diameter size of 53 nm) and negatively charged (carboxylated, diameter sizes of 26 and 62 nm) polystyrene particles were purchased from Bangs Laboratories Inc. (www.bangslabs.com). Prior to the start of the experiments, particles were diluted to 10 mg/mL and dialyzed in Standard RC Tubing, Dialysis Membrane (MWCO: 3.5 kD) for 24 h in 10 L of MilliQ water. Water was changed at least 4 times during the dialysis, which was performed to separate the nanoparticles from the solvent creating a stock solution suitable for toxicity testing of nanoparticles. The particle sizes were measured in triplicates using DLS on DynaPro Plate Reader II (Wyatt instruments, USA) directly after dialysis and every third day during experiments to ensure that particle sizes did not change during the study. No changes in particles sizes were observed during the experiment (Table S4.1-3). To quantify particle sedimentation rate, absorbance of particle suspension mixed with algae cells was measured. 1 mL of the medium solution was added to a quartz cuvette and the absorbance was measured at 200–250 nm by a flash light through a fixed point, 0.8 mm in diameter, during 48 h using a ProbeDrum spectrophotometer (Probation Labs, Lund, Sweden). We recorded no change in absorbance, suggesting that sedimentation did not occur (Fig. S1).

Exposure to nanoparticles. A life-long experiment (the median life-time for a control group was 64.3 ± 32.5 days) on *D. magna* was performed to analyze effects on life history traits (survival and reproduction) when exposed to different concentrations of polystyrene particles of three different sizes (Table 1). Different concentrations were chosen to determine the lowest concentration of polystyrene nanoparticles causing mortality in *D. magna*. Two-five days old *D. magna* individuals from the same population were isolated and randomly assigned to the different groups. Gender determination was not possible since handling and microscopic examination induced high mortality at this early age. Each individual was put in a 100 mL uncovered glass beaker with 80 mL total volume ($n = 10$ for each treatment), filled with tap water which had been aerated for 24 h prior to the start of the experiment in order to increase the oxygen level. Aeration was repeated prior to the medium exchange. During the exposure to nanoplastic particles, alive *D. magna* individuals were gently transferred to fresh medium by using a 1 mL plastic pipette with a removed tip to reduce handling stress, every third day. The fresh medium contained 2.5 mL of food (algae), with (treatment) or without (control) nanoparticles (Fig. 1). Water with nanoplastic particles was mixed thoroughly each time before adding it to exposure jars to ensure that particle number did not vary between samples. Experimental cultures were maintained at 18 °C at a 8:16 h light/dark photoperiod.

Algae stock culture was filtered through 20 μm mesh filter, diluted with tap water to keep algae concentration stable throughout the experiment (Table S5). The concentration of algae (chlorophyll *a*) in the stock culture was assessed in triplicates prior to transferring *D. magna* to fresh medium using AlgaeLabAnalyser (bbe Moldaenke, GmbH). 2.5 mL of this algae culture was then added to *D. magna* individuals each time individuals were transferred. The tap water was aerated 24 h prior individuals transfer and used to make new particle containing media, and control group (fresh and 3 days old) samples. The pH remained stable in all samples during the experiment (Fig. S3). To document any morphological changes in the exposed animals, photos were taken using a stereo microscope (Olympus SZX7) of randomly chosen *D. magna* individuals that died after 30 to 100 days of exposure

to different concentrations, charges and sizes of nanoparticles. At least three photos were taken for each treatment during the experiment. The survival rate of *D. magna* was checked daily, while reproduction rate was checked every third day. Offspring were counted and removed from glass beakers every third day.

Statistical analysis. Kaplan Meier survival curves analysis were performed using statistical computing software GraphPad Prism version 8.0.0 (224) for Windows, GraphPad Software, Inc., www.graphpad.com, and one-way ANOVA was used to test for differences in reproduction output in R version 3.6.1, www.r-project.org.

Received: 16 December 2019; Accepted: 22 March 2020;
Published online: 06 April 2020

References

1. Andrady, A. L. & Neal, M. A. Applications and societal benefits of plastics. *Philosophical transactions of the Royal Society of London. Series B, Biological sciences* **364**, 1977–1984, https://doi.org/10.1098/rstb.2008.0304 (2009).
2. Plastics – the Facts 2019. An analysis of European plastics production, demand and waste data. plasticseurope https://www.plasticseurope.org/application/files/9715/7129/9584/FINAL_web_version_Plastics_the_facts2019_14102019.pdf (2019).
3. Lebreton, L. C. M. *et al*. River plastic emissions to the world's oceans. *Nature Communications* **8**, 15611, https://doi.org/10.1038/ncomms15611 (2017).
4. Andrady, A. L. Microplastics in the marine environment. *Marine Pollution Bulletin* **62**, 1596–1605, https://doi.org/10.1016/j.marpolbul.2011.05.030 (2011).
5. Barnes, D. K. A., Galgani, F., Thompson, R. C. & Barlaz, M. Accumulation and fragmentation of plastic debris in global environments. *Philosophical Transactions of the Royal Society B: Biological Sciences* **364**, 1985–1998, https://doi.org/10.1098/rstb.2008.0205 (2009).
6. Ter Halle, A. *et al*. Nanoplastic in the North Atlantic Subtropical Gyre. Environmental Science &. *Technology* **51**, 13689–13697, https://doi.org/10.1021/acs.est.7b03667 (2017).
7. Kwon, B. G. *et al*. Monitoring of styrene oligomers as indicators of polystyrene plastic pollution in the North-West Pacific Ocean. *Chemosphere* **180**, 500–505, https://doi.org/10.1016/j.chemosphere.2017.04.060 (2017).
8. Kwon, B. G. *et al*. Regional distribution of styrene analogues generated from polystyrene degradation along the coastlines of the North-East Pacific Ocean and Hawaii. *Environmental Pollution* **188**, 45–49, https://doi.org/10.1016/j.envpol.2014.01.019 (2014).
9. Ekvall, M. T. *et al*. Nanoplastics formed during the mechanical breakdown of daily-use polystyrene products. *Nanoscale Advances* **1**, 1055–1061 (2019).
10. Lambert, S. & Wagner, M. Characterisation of nanoplastics during the degradation of polystyrene. *Chemosphere* **145**, 265–268, https://doi.org/10.1016/j.chemosphere.2015.11.078 (2016).
11. Koelmans, A. A. *et al*. Risks of Plastic Debris: Unravelling Fact, Opinion, Perception, and Belief. *Environmental Science & Technology* **51**, 11513–11519, https://doi.org/10.1021/acs.est.7b02219 (2017).
12. Koelmans, A. A., Besseling, E. & Shim, W. J. In Marine anthropogenic litter 325-340 (Springer, Cham, 2015).
13. Chae, Y., Kim, D., Kim, S. W. & An, Y.-J. Trophic transfer and individual impact of nano-sized polystyrene in a four-species freshwater food chain. *Scientific reports* **8**, 284, https://doi.org/10.1038/s41598-017-18849-y (2018).
14. Setälä, O., Fleming-Lehtinen, V. & Lehtiniemi, M. Ingestion and transfer of microplastics in the planktonic food web. *Environmental Pollution* **185**, 77–83, https://doi.org/10.1016/j.envpol.2013.10.013 (2014).
15. Rajkumar, K. S., Kanipandian, N. & Thirumurugan, R. Toxicity assessment on haemotology, biochemical and histopathological alterations of silver nanoparticles-exposed freshwater fish Labeo rohita. *Applied Nanoscience* **6**, 19–29, https://doi.org/10.1007/s13204-015-0417-7 (2016).
16. de Sá, L. C., Oliveira, M., Ribeiro, F., Rocha, T. L. & Futter, M. N. Studies of the effects of microplastics on aquatic organisms: What do we know and where should we focus our efforts in the future? *Science of The Total Environment* **645**, 1029–1039, https://doi.org/10.1016/j.scitotenv.2018.07.207 (2018).
17. Derraik, J. G. B. The pollution of the marine environment by plastic debris: a review. *Marine Pollution Bulletin* **44**, 842–852, https://doi.org/10.1016/S0025-326X(02)00220-5 (2002).
18. Barboza, L. G. A. *et al*. In *World Seas: an Environmental Evaluation (Second Edition)* (ed. Charles Sheppard) 329–351 (Academic Press, 2019).
19. Baldwin, A. K., Corsi, S. R. & Mason, S. A. Plastic Debris in 29 Great Lakes Tributaries: Relations to Watershed Attributes and Hydrology. *Environmental Science & Technology* **50**, 10377–10385, https://doi.org/10.1021/acs.est.6b02917 (2016).
20. Leslie, H. A., Brandsma, S. H., van Velzen, M. J. M. & Vethaak, A. D. Microplastics en route: Field measurements in the Dutch river delta and Amsterdam canals, wastewater treatment plants, North Sea sediments and biota. *Environment International* **101**, 133–142, https://doi.org/10.1016/j.envint.2017.01.018 (2017).
21. Hurley, R. R., Woodward, J. C. & Rothwell, J. J. Ingestion of Microplastics by Freshwater Tubifex Worms. *Environmental Science & Technology* **51**, 12844–12851, https://doi.org/10.1021/acs.est.7b03567 (2017).
22. Redondo-Hasselerharm, P. E., Falahudin, D., Peeters, E. T. H. M. & Koelmans, A. A. Microplastic Effect Thresholds for Freshwater Benthic Macroinvertebrates. *Environmental Science & Technology* **52**, 2278–2286, https://doi.org/10.1021/acs.est.7b05367 (2018).
23. Mattsson, K. *et al*. Altered Behavior, Physiology, and Metabolism in Fish Exposed to Polystyrene Nanoparticles. *Environmental Science & Technology* **49**, 553–561, https://doi.org/10.1021/es5053655 (2015).
24. Mattsson, K. *et al*. Brain damage and behavioural disorders in fish induced by plastic nanoparticles delivered through the food chain. *Scientific Reports* **7**, 11452, https://doi.org/10.1038/s41598-017-10813-0 (2017).
25. Cedervall, T., Hansson, L.-A., Lard, M., Frohm, B. & Linse, S. Food Chain Transport of Nanoparticles Affects Behaviour and Fat Metabolism in Fish. *Plos One* **7**, e32254, https://doi.org/10.1371/journal.pone.0032254 (2012).
26. Greven, A.-C. *et al*. Polycarbonate and polystyrene nanoplastic particles act as stressors to the innate immune system of fathead minnow (Pimephales promelas). *Environmental Toxicology and Chemistry* **35**, 3093–3100, https://doi.org/10.1002/etc.3501 (2016).
27. Lu, Y. *et al*. Uptake and Accumulation of Polystyrene Microplastics in Zebrafish (Danio rerio) and Toxic Effects in Liver. *Environmental Science & Technology* **50**, 4054–4060, https://doi.org/10.1021/acs.est.6b00183 (2016).
28. Jemec, A., Horvat, P., Kunej, U., Bele, M. & Kržan, A. Uptake and effects of microplastic textile fibers on freshwater crustacean Daphnia magna. *Environmental Pollution* **219**, 201–209, https://doi.org/10.1016/j.envpol.2016.10.037 (2016).
29. Nasser, F. & Lynch, I. Secreted protein eco-corona mediates uptake and impacts of polystyrene nanoparticles on Daphnia magna. *Journal of Proteomics* **137**, 45–51, https://doi.org/10.1016/j.jprot.2015.09.005 (2016).
30. Frydkjær, C. K., Iversen, N. & Roslev, P. Ingestion and Egestion of Microplastics by the Cladoceran Daphnia magna: Effects of Regular and Irregular Shaped Plastic and Sorbed Phenanthrene. *Bulletin of Environmental Contamination and Toxicology* **99**, 655–661, https://doi.org/10.1007/s00128-017-2186-3 (2017).
31. Ogonowski, M., Schür, C., Jarsén, Å. & Gorokhova, E. The Effects of Natural and Anthropogenic Microparticles on Individual Fitness in Daphnia magna. *Plos One* **11**, e0155063, https://doi.org/10.1371/journal.pone.0155063 (2016).

32. Ebert, D. Ecology, epidemiology, and evolution of parasitism in Daphnia, http://www.ncbi.nlm.nih.gov/entrez/query.fcgi?db=Books (2005).
33. Besseling, E., Wang, B., Lürling, M. & Koelmans, A. A. Nanoplastic Affects Growth of S. obliquus and Reproduction of D. magna. *Environmental Science & Technology* **48**, 12336–12343, https://doi.org/10.1021/es503001d (2014).
34. Rehse, S., Kloas, W. & Zarfl, C. Short-term exposure with high concentrations of pristine microplastic particles leads to immobilisation of Daphnia magna. *Chemosphere* **153**, 91–99, https://doi.org/10.1016/j.chemosphere.2016.02.133 (2016).
35. Cui, R., Kim, S. W. & An, Y.-J. Polystyrene nanoplastics inhibit reproduction and induce abnormal embryonic development in the freshwater crustacean Daphnia galeata. *Scientific Reports* **7**, 12095, https://doi.org/10.1038/s41598-017-12299-2 (2017).
36. Kim, D., Chae, Y. & An, Y.-J. Mixture Toxicity of Nickel and Microplastics with Different Functional Groups on Daphnia magna. *Environmental Science & Technology* **51**, 12852–12858, https://doi.org/10.1021/acs.est.7b03732 (2017).
37. Rist, S., Baun, A. & Hartmann, N. B. Ingestion of micro- and nanoplastics in Daphnia magna – Quantification of body burdens and assessment of feeding rates and reproduction. *Environmental Pollution* **228**, 398–407, https://doi.org/10.1016/j.envpol.2017.05.048 (2017).
38. Ekvall, M. T., Hedberg, J., Odnevall Wallinder, I., Hansson, L.-A. & Cedervall, T. Long-term effects of tungsten carbide (WC) nanoparticles in pelagic and benthic aquatic ecosystems. *Nanotoxicology* **12**, 79–89, https://doi.org/10.1080/17435390.2017.1421274 (2018).
39. Anguissola, S., Garry, D., Salvati, A., O'Brien, P. J. & Dawson, K. A. High Content Analysis Provides Mechanistic Insights on the Pathways of Toxicity Induced by Amine-Modified Polystyrene Nanoparticles. *Plos One* **9**, e108025, https://doi.org/10.1371/journal.pone.0108025 (2014).
40. Rosenkranz, P., Chaudhry, Q., Stone, V. & Fernandes, T. F. A comparison of nanoparticle and fine particle uptake by Daphnia magna. *Environmental Toxicology and Chemistry* **28**, 2142–2149, https://doi.org/10.1897/08-559.1 (2009).
41. Della Torre, C. *et al*. Accumulation and Embryotoxicity of Polystyrene Nanoparticles at Early Stage of Development of Sea Urchin Embryos Paracentrotus lividus. *Environmental Science & Technology* **48**, 12302–12311, https://doi.org/10.1021/es502569w (2014).
42. Martins, A. & Guilhermino, L. Transgenerational effects and recovery of microplastics exposure in model populations of the freshwater cladoceran Daphnia magna Straus. *Science of The Total Environment* **631–632**, 421–428, https://doi.org/10.1016/j.scitotenv.2018.03.054 (2018).
43. Pacheco, A., Martins, A. & Guilhermino, L. Toxicological interactions induced by chronic exposure to gold nanoparticles and microplastics mixtures in Daphnia magna. *Science of The Total Environment* **628–629**, 474–483, https://doi.org/10.1016/j.scitotenv.2018.02.081 (2018).
44. Jin, Y. *et al*. Polystyrene microplastics induce microbiota dysbiosis and inflammation in the gut of adult zebrafish. *Environmental Pollution* **235**, 322–329, https://doi.org/10.1016/j.envpol.2017.12.088 (2018).
45. Lu, L., Wan, Z., Luo, T., Fu, Z. & Jin, Y. Polystyrene microplastics induce gut microbiota dysbiosis and hepatic lipid metabolism disorder in mice. *Science of The Total Environment* **631–632**, 449–458, https://doi.org/10.1016/j.scitotenv.2018.03.051 (2018).
46. Jin, Y., Lu, L., Tu, W., Luo, T. & Fu, Z. Impacts of polystyrene microplastic on the gut barrier, microbiota and metabolism of mice. *Science of The Total Environment* **649**, 308–317, https://doi.org/10.1016/j.scitotenv.2018.08.353 (2019).

Acknowledgements

Funding for the present study was provided by Swedish Council for the Environment (FORMAS), the Swedish Research Council (VR), the Swedish Environmental Protection Agency and the MISTRA program Environmental Nanosafety. Open access funding provided by Lund University.

Author contributions

E.K., O.T., M.T.E., L.-A.H. and T.C. were involved in the planning and designing the study. E.K. and O.T. performed experiments and contributed equally to this work. All authors were involved in the evaluation of the data. E.K. wrote the first version of the manuscript and all authors commented on the manuscript.

Competing interests

The authors declare no competing interests.

Additional information

Supplementary information is available for this paper at https://doi.org/10.1038/s41598-020-63028-1.

Correspondence and requests for materials should be addressed to E.K.

Reprints and permissions information is available at www.nature.com/reprints.

Publisher's note Springer Nature remains neutral with regard to jurisdictional claims in published maps and institutional affiliations.

Supplementary Information

Long-term exposure to nanoplastics reduces life-time in *Daphnia magna*

Egle Kelpsiene[1,3*], Oscar Torstensson[1], Mikael T. Ekvall[2,3], Lars-Anders Hansson[2,3], and Tommy Cedervall[1,3]

[1]*Department of Biochemistry and Structural Biology, Lund University, Lund University, P.O. Box 118, SE-221 00 Lund, Sweden*

[2]*Department of Biology/Aquatic ecology, Lund University, SE-223 62 Lund, Sweden*

[3]*NanoLund, Lund University, Box 118, SE-221 00 Lund, Sweden*

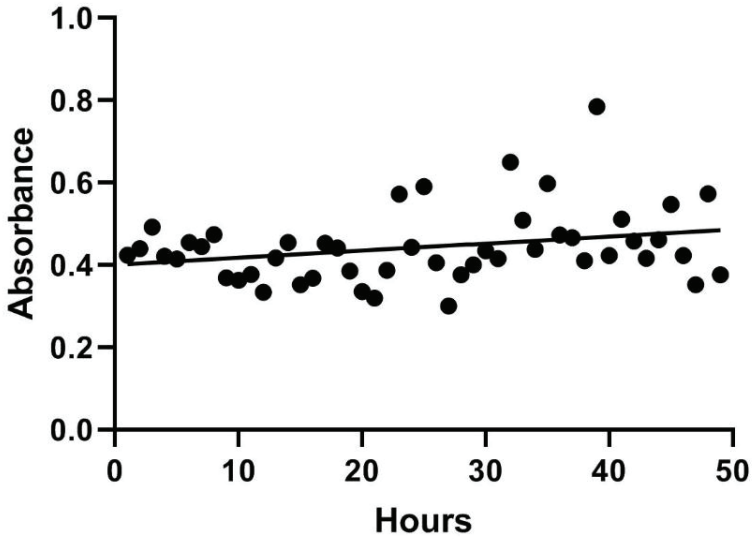

Fig. S1. Absorbance of 62 nm PS-COOH (7.6 mg/L) particle mixed together with algae over 48 h. Absorbance was measured at 200-250 nm as polystyrene has a strong absorbance maximum at 230 nm. No change in absorbance indicates that particle sedimentation did not occur. Sedimentation was measured only for the highest concentrations of 62 nm PS-COOH as an apparent reversed concentration dependency was noticed in survival of *Daphnia magna*. The sedimentation velocity for polystyrene nanoparticles would be more than 10 000 years, which is calculated according to an equation which includes depth of solution, viscosity of solution, radius of particle, density of particle, density of solution, the acceleration due to gravity.

Table S1. Radius and % polydispersity of 0.32 and 7.6 mg/L of 62 nm of PS-COOH after 48 h measured in triplicates by DLS. No particle aggregation was observed in measured concentrations. Aggregation was measured for the lowest and highest concentrations of 62 nm PS-COOH as an apparent reversed concentration dependency was noticed in survival.

Concentration (mg/L)	Radius (nm)	% DP
0.32	37.087	20.7
	48.751	7.1
	36.312	22.1
7.6	27.206	14.2
	28.368	12.3
	27.141	12.4

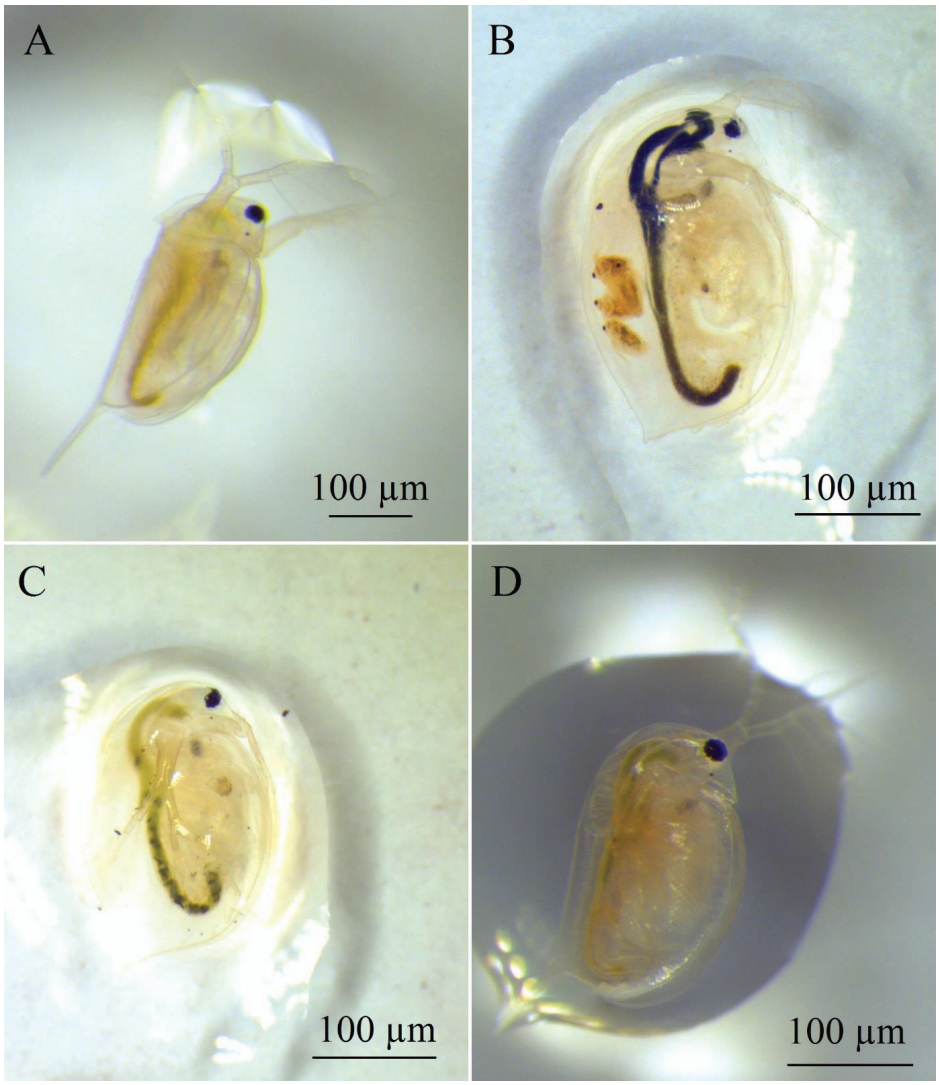

Fig. S2. *Daphnia magna* individuals in the control group (A) and after exposure to differently charged and differently sized polystyrene nanoparticles (53 nm PS-NH_2, B; 62 nm PS-COOH, C; 26 nm PS-COOH, D). Localized accumulation and blackish guts were seen in *D. magna* after exposure to 53 nm PS-NH_2 (B) and 62 nm PS-COOH (C). This was not seen in the control group. Pictures were taken for randomly chosen individuals after death, at least three

images were taken from each treatment. Individuals were photographed after 30 to 100 days of exposure.

Table S2. Mean number of offspring produced by *D. magna* replicates (N ≤ 10, as not all replicates were females) in the control group and exposed to 53 nm PS-NH_2, 62 nm PS-COOH, and 26 nm PS-COOH. The first brood was observed in all groups after 9 days from the beginning of the experiment. Empty vials indicate that there were no alive individuals left. Offspring were counted and removed from glass beakers every third day. Mean values were calculated together with standard deviation.

Day		9	12	15	18	21	24	27
Control		3.13±4.32	7.5±5.26	7±6.56	3.71±2.56	-	1±1.41	-
53 nm -NH_2	0.32 mg/L	3.6±3.78	8.25±5.91	6.75±6.8	3.75±2.5	0.5±1	0.25±0.5	2.25±1.71
	0.032 mg/L	2.22±3.42	6.67±5.98	8.22±5.4	3.44±2.92	0.63±1.19	1.57±1.9	-
	0.0032 mg/L	3.44±4.22	5.56±5.55	5.13±5.54	2.38±3.46	-	0.63±1.77	-
62 nm - COOH	7.6 mg/L	1.33±4	6.56±6.29	7.44±5.81	3±2.83	0.5±1.41	1.86±1.77	-
	3.2 mg/L	6.75±4.99	7.25±8.46	3.75±7.5	4.75±3.3	0.75±1.5	-	-
	0.76 mg/L	1±2.83	5.38±5.13	10±5.35	3±3.34	0.29±0.76	2±1.41	-
	0.32 mg/L	2.25±4.3	9.38±5.26	7.57±4.08	2.43±3.55	1.67±2.66	2±1.41	-

26 nm - COOH	3.2 mg/L	1.14±3.02	5±5.29	9.71±5.41	3.71±2.56	-	-	0.2±0.45
	0.32 mg/L	1.6±3.58	9.2±4.76	10.8±2.49	2±2.83	1.2±1.79	3.2±2.28	-
Day		30	33	36	39	42	45	48
Control		9.43±6.16	4.43±4.16	0.43±1.13	0.43±0.79	-	6±3.22	10.5±5.8
53 nm -NH_2	0.32 mg/L	4.5±5.26	8.25±6.99					
	0.032 mg/L	7.14±5.79	5.29±4.39	3.57±3.1	1.57±1.8	-	3±3.94	4.33±4.04
	0.0032 mg/L	7.38±4.63	5.38±4.96	1.75±3.41	0.38±0.52	-	0.57±1.51	2.14±3.93
62 nm - COOH	7.6 mg/L	8.67±5.05	1.5±2.35	3.6±3.58	0.4±0.89	-	-	-
	3.2 mg/L	11±1.63	3±3.83	0.75±1.5	1.8±2.49			
	0.76 mg/L	4.5±3.89	3.5±4.18	1.8±2.49				
	0.32 mg/L	7±1.41	2.75±5.5	4±3.16	1±1.41	-	-	-
26 nm - COOH	3.2 mg/L	8.6±4.98	4±3.94	2±2.83	3.75±0.5	1±2	6.67±4.73	8±9.54
	0.32 mg/L	7±5.87	5±4.24	1±2	1.75±2.06	1±2	6.5±1	7
Day		51	54	57	60	63	66	69

Control		-	15.25±4.03	8.75±4.11	-	1.5±1.73	-	2.67±2.52
53 nm -NH_2	0.32 mg/L							
	0.032 mg/L	0.33±0.58	15.67±8.08	4±3.61	-	1.33±1.53	-	1±1.73
	0.0032 mg/L	9.43±10.98	1.57±2.82	4±3.21	0.14±0.38	0.43±1.13	4±5.13	3.14±3.93
62 nm - COOH	7.6 mg/L	-	2±2.83					
	3.2 mg/L							
	0.76 mg/L							
	0.32 mg/L	-	-	-	1			
26 nm - COOH	3.2 mg/L	-	16	7	-	1	-	-
	0.32 mg/L							
Day		72	75	78	81	84	87	90
Control		-	2.67±4.62	1.33±2.31	-	-	3.33±2.89	1±1.41
53 nm -NH_2	0.32 mg/L							
	0.032 mg/L	-	1.5±2.12	3±1.41	-	-	-	2±2.83

	0.0032 mg/L	0.29±0.76	0.43±1.13	2.86±3.18	-	-	1.5±2.51	2.83±2.79
62 nm - COOH	7.6 mg/L							
	3.2 mg/L							
	0.76 mg/L							
	0.32 mg/L							
26 nm - COOH	3.2 mg/L	1	9	-				
	0.32 mg/L							
Day		93	96	99	102			
Control		-	-	3.5±4.95	-			
53 nm -NH_2	0.32 mg/L							
	0.032 mg/L	1±1.41						
	0.0032 mg/L	-	2±3.94	2±3.46				
	7.6 mg/L							

62 nm - COOH	3.2 mg/L							
	0.76 mg/L							
	0.32 mg/L							
26 nm - COOH	3.2 mg/L							
	0.32 mg/L							

50

51 **Table S3**. Reproduction efficiency in treated groups. There were no significant differences in
52 reproduction efficiency between treated individuals compared to the control group within the
53 same time period. Reproduction efficiency was calculated by dividing total number of
54 offspring by number of females and survived days.

Treatment		Total number of offspring	Last survival day	Reproduction efficiency
53 nm -NH_2	0.0032 mg/L	505	99	0.63
	0.032 mg/L	453	99	0.51
	0.32 mg/L	156	33	1.18
62 nm -COOH	0.32 mg/L	241	45	0.67
	0.76 mg/L	256	39	0.72
	3.2 mg/L	156	39	1
	7.6 mg/L	267	57	0.52

26 nm -COOH	0.32 mg/L	248	48	1.03
	3.2 mg/L	308	75	0.59
Control		489	103	0.59

55

56 **Table S4.1**. 53 nm PS-NH_2 diameter size (nm) and % polydispersity measured in triplicates
57 by DLS. Measurements were taken direct after particle dialysis (Day 0), and every third day
58 during the exposure to ensure that particle size remained stable. Mean values were calculated
59 together with standard deviation.

Day	0	3	6	9	12	15	18
Diameter (nm)	50.12±4.19	49.52±0.22	50.23±1.81	50.86±2.06	49.91±1.16	48.64±0.93	48.29±0.99
% DP	14.23±2.72	12.5±0.2	16.5±7.51	18.8±8.15	13.07±1.55	12.57±2.05	13.4±0.72
Day	21	24	27	30	33	36	39
Diameter (nm)	49.21±0.61	49.85±0.46	48.85±4.99	48.00±0.53	48.16±0.65	48.62±0.45	48.76±0.33
% DP	16.43±6.44	12.07±0.23	22.63±1.07	13.67±0.67	12.13±1.32	13.6±0.44	13.07±1.93
Day	42	45	48	51	54	57	60
Diameter (nm)	48.95±0.78	48.36±0.63	49.18±0.12	47.78±1.34	42.96±1.08	48.80±0.42	49.69±0.50
% DP	14.67±0.71	13.07±1.15	13.2±0.72	13.03±2.70	4.53±7.85	14.43±2.27	11.27±2.55
Day	63	66	69	72	75	78	81

Diameter (nm)	49.10±0.50	47.89±0.58	48.49±0.72	48.36±0.13	49.58±0.46	49.32±0.45	48.71±0.49
% DP	14.27±2.37	12.63±0.89	15.87±2.20	15.2±1.83	13.37±1.76	17.77±2.51	15.13±0.81
Day	84	87	90	93	96	99	102
Diameter (nm)	50.83±1.04	49.04±1.12	51.12±0.62	51.29±0.12	42.31±4.83	45.21±0.56	49.09±1.14
% DP	16.87±1.05	16.6±1.57	16.27±1.08	17.4±0.36	21.07±4.92	17.9±3.00	12.6±2.07

60

61 **Table S4.2**. 62 nm PS-COOH diameter size (nm) and % polydispersity measured in
62 triplicates by DLS. Measurements were taken direct after particle dialysis (Day 0), and every
63 third day during the exposure to ensure that particle size remained stable. Mean values were
64 calculated together with standard deviation.

Day	0	3	6	9	12	15	18
Diameter (nm)	58.19±0.14	58.90±0.57	57.17±2.77	53.78±4.52	55.08±3.87	53.66±3.39	57.39±0.37
% DP	8.27±1.01	8.5±1.21	12.23±5.09	18±5.14	11.43±3.39	13.83±4.53	9.2±1.18
Day	21	24	27	30	33	36	39
Diameter (nm)	58.48±0.83	59.06±0.81	55.57±3.75	58.49±1.11	56.86±2.63	57.21±0.48	57.67±0.08
% DP	9.23±1.32	8.77±0.85	12.23±7.25	10.07±0.71	12.87±6.31	10.07±1.07	10.63±1.59

Day	42	45	48	51	54	57	60
Diameter (nm)	58.13±0.83	58.02±1.82	57.66±0.55	58.01±0.64	55.64±1.11	56.71±1.66	55.76±1.18
% DP	9.5±1.15	12.97±4.66	9.1±1.65	8.33±1.32	11.73±2.64	9.87±1.95	4.63±2.02
Day	63	66	69	72	75	78	
Diameter (nm)	57.01±1.36	50.62±0.18	57.66±0.72	57.99±1.73	57.21±0.41	58.05±0.37	
% DP	6.7±2.23	9.73±2.14	9.23±0.51	7.23±3.29	11.87±0.06	8.77±1.4	

Table S4.3. 26 nm PS-COOH diameter size (nm) and % polydispersity measured in triplicates by DLS. Measurements were taken direct after particle dialysis (Day 0), and every third day during the exposure to ensure that particle size remained stable. Mean values were calculated together with standard deviation.

Day	0	3	6	9	12	15	18
Diameter (nm)	26.05±1.65	25.43±0.31	25.44±0.29	25.95±0.23	25.59±0.45	25.26±0.06	25.75±0.18
% DP	14.53±1.99	16.87±1.95	16±2.42	17.87±1.63	16.27±2.11	15.47±1.25	15.43±1.01
Day	21	24	27	30	33	36	39
Diameter (nm)	25.39±0.39	25.4±0.61	25.12±0.56	24.9±0.06	25.39±0.23	24.76±0.24	25.18±0.33

% DP	17.13±2.15	16.5±1.47	14.37±2.15	13.37±0.47	15.2±0.61	14.1±0.17	16.13±3.93
Day	42	45	48	51	54	57	60
Diameter (nm)	25.15±0.53	25.29±0.49	24.98±0.42	25.56±0.06	25.61±0.61	24.79±0.57	25.54±0.39
% DP	15.53±3.72	14.97±1.89	13.97±0.75	16.2±2.51	16.07±4.38	13.1±5.3	14.9±2.55
Day	63	66	69	72	75	78	81
Diameter (nm)	25.51±0.24	25.31±0.28	25.14±0.18	25.19±0.15	24.99±0.06	25.4±0.12	24.92±0.23
% DP	15.93±1.05	15.47±1.72	14.37±1.59	13.57±1.08	14.53±1.00	15.93±4.13	13.7±0.36
Day	84	87					
Diameter (nm)	25.29±0.41	25.27±0.56					
% DP	14.73±0.78	16.23±0.96					

Table S5. Total algae and green algae concentrations used during the exposure to polystyrene nanoparticles. Data presented as mean values calculated together with standard deviation.

Day	0	3	6	9	12	15
Total algae conc. (µg/L)	542.17±14.26	531.45±10.25	545.01±8.20	530.57±0.93	544.98±0.41	549.06±3.32

Green algae conc. (µg/L)	65.38±10.20	59.07±5.68	65.30±5.56	150.42±11.25	438.21±0.65	344.42±2.39
Day	18	21	24	27	30	33
Total algae conc. (µg/L)	516.59±3.14	532.38±3.86	558.89±2.27	485.58±5.614	593.32±2.22	513.47±1.75
Green algae conc. (µg/L)	408.89±0.87	206.96±13.67	375.82±1.35	258.19±3.77	315.42±2.27	232.88±2.37
Day	36	39	42	45	48	51
Total algae conc. (µg/L)	519.39±1.36	490.15±4.51	550.17±6.28	549.13±9.56	545.01±4.08	429.51±0.73
Green algae conc. (µg/L)	302.63±1.56	184.01±15.55	71.76±4.01	68.80±5.45	70.28±2.69	95.41±9.30
Day	54	57	60	63	66	70
Total algae conc. (µg/L)	539.95±1.91	478.75±1.27	640.67±2.70	498.41±0.84	553.29±3.82	500.59±0.91
Green algae conc. (µg/L)	169.92±17.14	183.22±7.45	229.74±2.49	179.92±6.48	291.48±19.90	132.43±17.93
Day	73	76	79	81	84	87
Total algae conc. (µg/L)	567.35±0.82	345.56±8.57	459.2±0.84	446.77±0.67	521.05±1.69	595.65±2.91
Green algae conc. (µg/L)	240.95±8.56	330.92±6.75	287.02±5.46	134.27±9.58	358.92±9.99	96.55±1.38
Day	90	93	96	99		
Total algae conc. (µg/L)	657.29±1.75	568.2±1.67	566.94±5.31	375.19±1.11		

Green algae conc. (µg/L)	190.82±4.96	449.25±0.99	422.02±4.35	235.80±1.28		

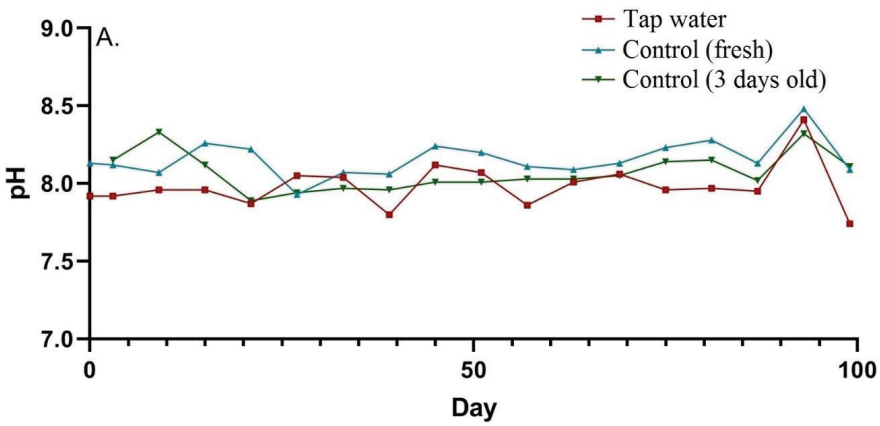

Fig. S3. pH during the exposure polystyrene nanoparticles. Tap water was aerated for 24 h prior to the start of the experiment and every time before the medium exchange.

Paper II

Environmental Science Nano

ROYAL SOCIETY OF CHEMISTRY

PAPER

View Article Online
View Journal | View Issue

Cite this: *Environ. Sci.: Nano*, 2023, **10**, 1858

Metabolomics-based analysis in *Daphnia magna* after exposure to low environmental concentrations of polystyrene nanoparticles†

Egle Kelpsiene, [ab] Tommy Cedervall *[ab] and Anders Malmendal [c]

Received 3rd March 2023,
Accepted 22nd May 2023

DOI: 10.1039/d3en00142c

rsc.li/es-nano

Larger plastic pieces break down into micro- and eventually nano-sized plastics. This makes nanoplastics ubiquitous in the environment, giving rise to great concern for its effect on biota. Many studies use polystyrene nanoparticles (PS-NPs) as a model for nanoplastics, showing a negative impact on various organisms, but the molecular effects are yet not fully explored. Here we applied ^{1}H nuclear magnetic resonance (NMR) metabolomics to characterize the metabolic changes in *Daphnia magna* during long-term (37 days) exposure to low concentrations of positively and negatively charged (aminated and carboxylated) PS-NPs. We show that exposure to PS-NPs at concentrations down to 3.2 μg L^{-1} affected amino acid metabolism and the bacterial metabolite isopropanol in *D. magna*. These effects were largely independent of particle concentration and surface charge. The results highlight the importance of (1) performing chronic exposures under low concentrations and (2) further investigation of particles with different surface charges.

Environmental significance

Nano-sized particles are ubiquitous; therefore, adversary effects of nanoparticles (NPs) have attracted both societal and scientific attention. Polystyrene (PS) is one of the most used plastics, wherefore PS NPs as model particles have been widely used in the toxicity studies in various organisms. Yet molecular mechanism behind these particles is not fully understood. Metabolomics-based studies allow identification of physiological changes in the organisms in response to pollutants even at low concentrations. The present study shows that daphnids metabolism is affected by PS NPs at 3.2 μg L^{-1} after two days exposure. The effect remains throughout the whole experiment (37 days). Therefore, chronic exposures at low concentrations should be priority when it comes to the toxicity studies to get broader understanding about nanoplastics effects to aquatic biota. The differences between different particle concentrations and between positive and negative surface charges were limited.

Introduction

The global plastic production increased from 1.5 million metric tons to 367 million metric tons between 1950 and 2020.[1] Most plastic is non-biodegradable and, therefore, remains as a waste for many years in the environment.[2] It has been calculated that almost 300 million tons of plastic are consumed each year,[3] of which 60 to 100 million tons are mismanaged and around 90% ends up in waterways, potentially reaching the oceans.[4] An increased levels of plastic production, improper disposal, poor waste management, and low recovery rate, leads to hazardous plastic waste being thrown out into the environment, which has attracted public attention.[5]

Depending on size, plastic debris is mainly classified as macro- (>5 mm), micro- (MPs, <5 mm, >1 μm), and nano-plastic (NPs, <1 μm).[6] NPs can be further divided into primary or intentionally manufactured and secondary or generated by fragmentation of larger plastic pieces.[7] The presence and chemical composition of NPs in seawater samples have been found in the North Atlantic Subtropical Gyre.[8] Additionally, NPs were found and quantified in the surface water samples from lakes and streams in Siberian Arctic tundra (mean 51 μg L^{-1}), a forest landscape in southern Sweden (mean 563 μg L^{-1})[9] and snow in the remote high-altitude Alps, Austria (mean 46.5 μg L^{-1}).[10] There was no PS found in the southern Sweden, however the highest concentrations were observed for polyethylene (PE), followed by polypropylene (PP), polyvinylchloride (PVC) and polyethylene terephthalate (PET).[9] Similarly, no PS was found in high-altitude Alps, however the main polymers were PP

[a] *Department of Biochemistry and Structural Biology, Lund University, P.O. Box 124, SE-221 00 Lund, Sweden. E-mail: tommy.cedervall@biochemistry.lu.se*
[b] *NanoLund, Lund University, P.O. Box 118, SE-221 00, Lund, Sweden*
[c] *Department of Science and Environment, Roskilde University, P.O. Box 260, DK-4000 Roskilde, Denmark*

† Electronic supplementary information (ESI) available. See DOI: https://doi.org/10.1039/d3en00142c

and PET.[10] Whereas, in PS, PE, PP and PVC were found in Siberian Arctic tundra[9] and the surface waters of Italian Subalpine.[11] Breakdown of PS is also evident due to the presence of styrene oligomers in oceans, beaches, and waterways.[8,12,13] The concentration of oligomers was shown to be between 0.17 μg L^{-1} and 4.26 μg L^{-1} in surface waters and 0.31 μg L^{-1} and 4.31 μg L^{-1} in deep waters.[12]

The small size and high surface to volume ratio allow NPs to enter cells and interact with biological molecules more efficiently than larger size particles.[14] Besides the size, particle surface charge also affects the toxicity.[15] Nano-sized (25 nm to 60 nm) carboxylated surface charged PS NPs that were shown not to be toxic in the acute (24 h) exposure to *D. magna*,[16] appeared to be toxic in the life-time (103 days) exposure.[17] In general, 24–48 h acute toxicity exposure scenarios are the most commonly used tests to evaluate the adverse effects on organism's survival.[18] However, acute toxicity tests often use high concentrations of toxicants, whereas pollutants are present at sub-lethal levels in the natural environment.[19] Thus, acute toxicity tests fail to provide insight into how toxicity manifests at sub-lethal levels and gives little information regarding the biochemical mode of action. Therefore, other endpoints are needed to get broader understanding in terms of responses to pollutants at the molecular level.

Omics approaches such as transcriptomics, proteomics, and metabolomics provide a broad overview of the molecular changes underlying physiological processes affected by toxicants.[20] Metabolomics may be defined as the quantitative measurement of the dynamic multiparametric response of a living system to a stimuli or genetic modification.[21] Nuclear magnetic resonance (NMR) metabolomics is a highly reproducible high-throughput approach to metabolome analysis that require minimal sample preparation.[22,23] It is an untargeted technique, that allows detection of many metabolites, and therefore suitable for studies where no prior assumptions have been made.[24] Here we apply NMR metabolomics to study abnormalities in the metabolism associated with toxicity of environmental pollutants.

Metabolomics have previously been used to study the metabolic responses of *D. magna* induced by various toxicants, such as silver (Ag) nitrate and Ag NPs,[25] PE MPs,[26] pharmaceuticals,[27] cadmium,[28] arsenic, copper, lithium,[29] insecticides, or industrial chemicals.[30,31] It has been shown that released Ag^{+} induced disturbance in energy metabolism and oxidative stress,[25] PE MPs downregulated phosphatidylcholine and upregulated phosphatidylethanolamine, as well as induced the degradation of amino acids,[26] copper and lithium altered production of neurotransmitters and impaired energy metabolism[29] to *D. magna*.

D. magna, used in the present study as a model organism, are small (<1–5 mm) freshwater filter-feeder crustaceans which play a key role in food webs.[32] Under laboratory conditions the lifespan of most *Daphnia* species is approximately 60 days.[32] During that time, a daphnid neonate goes through four to six juvenile instars before it produces eggs for the first time after approximately 5–10 days.[32] *Daphnia* species have become important model organisms in both ecology and toxicology studies due to their sensitivity to environmental contaminants.[32] Various adverse effects, such as increased mortality, inhibited reproduction, induced abnormal embryonic development, alterations in swimming pattern, increase in superoxide dismutase activity, caused by PS NPs to *D. magna* have previously been shown.[16,17,33–38] Most of the studies performed acute (24–48 h) toxicity test using high PS NPs concentrations, ranging from 500 μg L^{-1} to 1.5 × 10^{5} μg L^{-1}.[16,33,36,38] Unfortunately, there are not many studies that focus on a long-term exposure at lower concentrations of PS NPs.

Despite the well-known adverse effects caused by NPs, the molecular mechanisms behind PS NPs are largely unknown and, therefore, need to be further investigated. Therefore, this study focuses on the metabolic responses on *D. magna* after a long-term exposure to low environmental concentrations of PS NPs with different surface charge but similar size, by using ^{1}H NMR metabolomics. The study aims to analyze how the metabolome is affected by PS NP type, concentration, and daphnid aging.

Materials and methods

Preparation and characterization of polystyrene nanoparticles

Positively (aminated, PS-NH_2, diameter size of 53 nm, catalog number: PA02N, 9.1% solids) and negatively (carboxylated, PS-COOH, diameter size of 62 nm, catalog number: PC 02003, 10.1% solids) surface charged PS NPs were purchased from Bangs Laboratories Inc. (**https://www.bangslabs.com**). These particles suspension might contain sodium azide, therefore before the experiment, particles were diluted to 10 mg mL^{-1} and dialyzed in Standard RC Tubing, dialysis membrane (MWCO: 3.5 kD) for 72 h in 10 L of MilliQ water. The water was changed after 4 h the first day and once a day on the following days. Dialysis was performed to remove additives from the NPs and to create a stock solution suitable for toxicity testing of NPs. The particle sizes were measured in triplicated using DLS on DynaPro Plate Reader II (Wyatt instruments, USA) 3 days and 2 months after dialysis to ensure that particle aggregation after dialysis did not occur. Zeta potential measurements were performed in MilliQ water (100 mg L^{-1} of NPs) and in tap water at 25 °C using a Zetasizer Nano ZS instrument (Malvern Instruments, Worcestershire, UK). Measurements were repeated three times and averaged for three consecutive analyses of the same sample.

Study organisms

The filter feeder *D. magna* culture used in the present study originates from Lake Bysjön, Southern Sweden (55°40′31.3″N, 13°32′41.9″E) and has been kept in the laboratory for several hundred generations. The culture was fed *ad libitum* 2–3 times per week with an algae diet mainly composed of the

green algae *Scenedesmus* sp. Additionally, there might be blue-green algae in the culture. Before the feeding, the algal culture was filtered through 20 μm mesh filter to remove larger algal species, such as cyanobacteria, from the culture. The algal culture was fed with 250 μL of liquid plant nutrient, containing 5.1 g nitrogen, 1.0 g phosphorus, and microelements per 100 mL. Both *Daphnia* and algal cultures, as well as experimental groups were maintained at 18 °C at an 8 : 16 h light/dark photoperiod.

Exposure to polystyrene nanoparticles

A long-term (37 days) experiment on *D. magna* was performed to analyze the effects on metabolites after exposure to three different environmentally relevant concentrations (320, 32 and 3.2 μg L^{-1}, or 3.91×10^9 particles per mL and 2.44×10^9 for PS-NH_2 and PS-COOH, respectively at concentrations of 320 μg L^{-1}) of PS particles of different surface charge with similar sizes. Two-five days old *D. magna* individuals from the same population were randomly assigned to the different groups. Ten individuals were put into a 100 mL uncovered glass beaker with 80 mL total exposure volume (5 replicates for each treatment, 10 individuals in each replicate). The first batch of samples were fixed after 2 days exposure, whereas the following samples were fixed every 7 days on a similar time of the day. *D. magna* individuals were transferred into Eppendorf tubes and immediately after placed in a mixture of dry ice and 99% acetic acid to quench the metabolism. *D. magna* samples were subsequently lyophilized and stored at −80 °C before further analysis. The remaining *D. magna* individuals were gently transferred to the fresh tap water, containing 5 mL (~500 μg L^{-1}) of food (algae), with (treatment) or without (control) NPs, by using a 1 mL plastic pipette with a removed tip to reduce handling stress. The fresh medium was changed once a week after samples were collected and fixed. The pH was measured for all treatments and remained stable throughout the exposure period (pH 7.19 ± 0.75). Offspring were removed once a week. The reproduction rate was not followed in the present study.

Sample preparation

Immediately before NMR measurements, the samples were rehydrated in 200 μL of 37.5 mM phosphate buffer (pD 6.95) in heavy water (D_2O) by shaking at 800 rpm at 22 °C for 45 min. The buffer contained 0.747 mM of the chemical shift reference (trimethylsilyl)propionic-2,2,3,3-d_4 acid, sodium salt ($TSPd_4$), and 0.05% w/v of sodium azide to prevent bacterial growth.

NMR spectroscopy

The NMR measurements were carried out at 25 °C on a Bruker Avance-III 700 spectrometer (Bruker Biospin, Germany) operating at a ^1H frequency of 700.20 MHz and equipped with a and 5 mm QCI cryoprobe. The ^1H NMR spectra were acquired using a noesygppr1d experiment. The water signal was suppressed by presaturation and a total of 64k data points spanning a spectral width of 30 ppm were collected in 128 transients. The spectra were processed using Topspin (Bruker). An exponential line broadening of 0.5 Hz was applied to the free induction decay prior to Fourier transformation. All spectra were referenced to the $TSPd_4$ signal at 0 ppm, phased, and baseline corrected. The spectra were aligned using icoshift,[39] and the region around the residual water signal (4.84–4.74 ppm) was removed. The spectra were normalized by probabilistic quotient area normalization,[40] and the data were scaled using Pareto scaling[41] and centered.

NMR data analysis

Initially, the whole dataset was subjected to principal component analysis (PCA).[42] Multivariate analysis of variance (MANOVA) was used to determine whether (1) there were significant effects of daphnid aging, as well as the presence, concentration, and type of PS NPs, and (2) to identify the lowest PS NPs concentration that caused a significant metabolite response. For all NP-related properties, the analyses were made at each day. For an effect to be judged as significant the median p-value across ages needed to be <0.001. Then, orthogonal projection to latent structures discriminant analysis (OPLS-DA) models were created to separate the different daphnid aging days for control (without PS NPs) and treatment (*D. magna* exposed to PS-NH_2 or PS-COOH NPs) groups. OPLS-DA models are multivariate models that predict group membership based on multivariate input, in this case, the NMR spectra. The model separates variations due to group membership from other (orthogonal) variations.[43] This allows us to focus on the spectral changes between different types of samples. The OPLS-DA scores used for further analysis were calculated using cross validation, where models were made with randomly chosen groups of samples left out one at a time, after which the scores were calculated for the left-out samples to avoid overfitting. Significant spectral correlations were identified by applying sequential Bonferroni correction ($p < 0.05$) for an assumed total number of 50 metabolites. The correlations were performed in MATLAB (The MathWorks, Natick, MA). Signal assignments were based on chemical shifts using earlier assignments and spectral databases.[44,45] All multivariate analyses were performed using the Simca-P software (Umetrics, Sweden). Aging and PS NP type effects for individual metabolites were calculated using 2-way ANOVA.

Results

Characterization of polystyrene nanoparticles

PS NPs were measured both 3 days and 2 months after dialysis to ensure that NPs did not aggregate during the exposure period. DLS measurements showed the sizes to be slightly lower compared to the information provided by a supplier (46.37 ± 0.49 nm and 50.85 ± 8.74 nm for PS-NH_2 and PS-COOH, respectively), however particle sizes

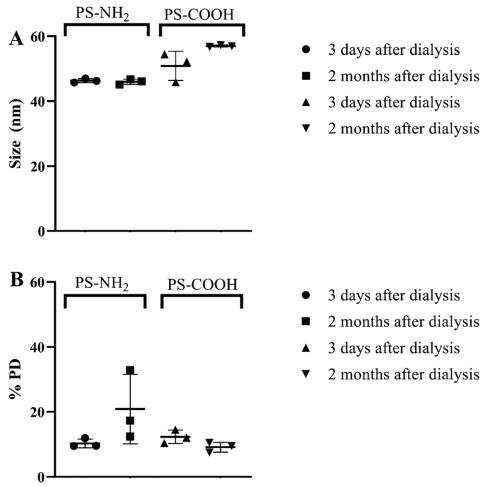

Fig. 1 Characterization of PS NPs used in the present study. Size (A) and polydispersity (PD, B) measurements taken in triplicates by using DLS. Horizontal bars and error bars represent mean values and standard deviations.

remained stable during the exposure period (Fig. 1). Zeta potential analysis showed that PS-NH_2 and PS-COOH NPs (100 mg L^{-1}) in MilliQ water had positive (+26 ± 3 mV) and negative (−37 ± 4 mV) charges, respectively. The *Z*-potential measured in tap water showed similar values (ESI† Fig. S1).

Identification of significant effects of daphnid aging, and the presence, concentration, and type of polystyrene nanoparticles

First, we used MANOVA on the scores from principal component analysis (PCA) to test if there was an effect of the daphnid aging in the control group (without PS NPs). The data shows that there was a significant effect of daphnid age ($p = 7.9 \times 10^{-11}$). Secondly, we tested if there was an effect of presence, concentration, and type of NPs by using MANOVA on the PCA scores at different daphnid ages (Table S1†). This analysis shows an effect of the presence of NPs ($p_{median} = 1.9 \times 10^{-6}$) and this effect is significant even at the lowest (3.2 μg L^{-1}) PS-NP concentration ($p_{median} = 3.8 \times 10^{-4}$). This effect is significant already after 2 days ($p = 6.5 \times 10^{-9}$). On the other hand, there were no significant effects of PS NP concentration or type of PS NPs. Yet, we chose to show data for PS-NH_2 and PS-COOH NPs separately.

Overall changes in the *D. magna* metabolome as a function of daphnid aging

The OPLS-DA model allows us to focus on the effects of daphnid age and exposure to PS NPs on the *D. magna* metabolome (Fig. 2). For untreated (control group) the metabolome changes in one direction until an age of 16 days, displaying an increase in alanine, asparagine, glutamate, glutamine, isoleucine, leucine, lysine, phenyl alanine, tyrosine, valine, lactate, and methionine sulfoxide; and a decrease in glucose, glycogen, nucleic acids, and isopropanol. Then they change in another direction, with increases in glucose, glycogen, and lactate, and at 23 days they turn back again meaning that the metabolome of the 37-day old *D.*

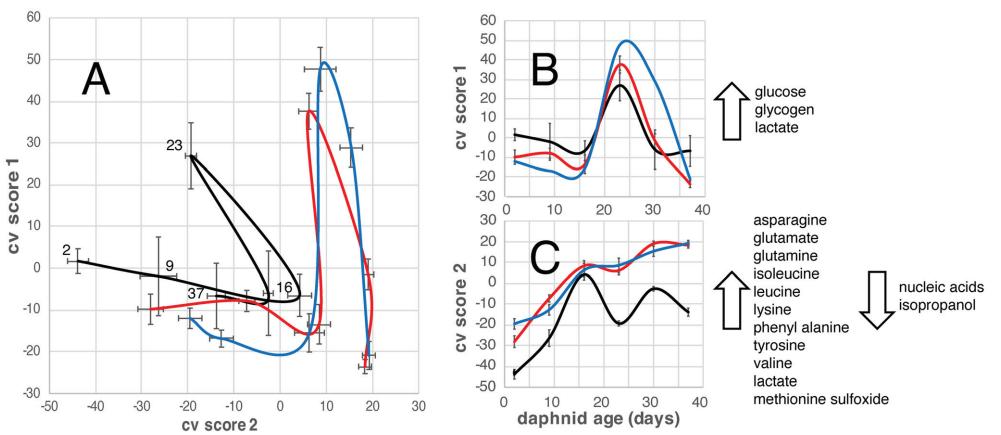

Fig. 2 Cross-validated OPLS-DA scores describing the variation in the metabolome between *D. magna* at different daphnid ages in the absence (control group) of PS NPs (black line), and in the presence of PS-NH_2 (blue line) and PS-COOH (red line) NPs. Fig. 2A shows CV score 1 as a function of CV score 2, while Fig. 2B and C show CV score 1 and CV score 2 as a function of daphnid aging and the direction of the associated changes in metabolite concentrations. The values are averages for all concentrations of each NP type. Error bars are standard errors.

magna individuals is quite similar to that of the 16-day old (Fig. 2). The metabolome of the *D. magna* exposed to PS NPs with different surface charges follows a similar pattern as the control group in that it changes in one direction from day 2 to 16 and then in another direction, until day 23, after which they change again, however the starting point and directions of the changes are slightly different (Fig. 2).

Effects on individual metabolites

Metabolite effects due to daphnid aging and exposure to surface charged PS NPs were identified using 2-way ANOVA. Metabolite variation between *D. magna* at different aging in the absence (control group) and in the presence of PS NPs (treatment) are shown in Fig. 3 and significant metabolites both overall and for the lowest metabolite concentration (3.2 μg L^{-1}) are listed in Table 1. In total, 15 significantly affected metabolites were identified from the ^{1}H NMR spectra (Fig. 3).

Table 1 *P*-values for metabolite responses to daphnid aging ('aging'), PS NP exposure to all concentrations ('PS NPs'), and the lowest concentration only ('3.2 μg L^{-1} of PS NPs') determined using 2-way ANOVA. The *p*-values are not corrected for multiple testing

Metabolite	Aging	PS NPs	3.2 μg L^{-1} of PS NPs
Asparagine	3.6×10^{-32}	3.1×10^{-8}	8.5×10^{-7}
Glutamate	4.2×10^{-26}	4.2×10^{-9}	1.4×10^{-7}
Glutamine	4.8×10^{-18}	0.014	0.13
Isoleucine	3.5×10^{-22}	2.9×10^{-7}	4.1×10^{-5}
Leucine	6.9×10^{-20}	3.2×10^{-6}	2.2×10^{-4}
Lysine	4.1×10^{-17}	3.1×10^{-6}	3.2×10^{-4}
Phenylalanine	5.0×10^{-19}	1.7×10^{-7}	3.5×10^{-5}
Tyrosine	1.5×10^{-9}	6.3×10^{-6}	2.1×10^{-4}
Valine	2.1×10^{-24}	6.2×10^{-8}	4.3×10^{-6}
Methionine sulfoxide	1.7×10^{-35}	1.8×10^{-9}	2.3×10^{-8}
Glucose	2.8×10^{-15}	0.25	0.15
Glycogen	7.9×10^{-5}	1.4×10^{-4}	9.2×10^{-6}
Unidentified sugar	1.2×10^{-6}	4.8×10^{-5}	1.7×10^{-6}
Nucleic acid(s)	1.1×10^{-31}	0.097	0.38
Isopropanol	1.4×10^{-9}	1.7×10^{-28}	8.6×10^{-17}

Discussion

In the present study, *D. magna* were exposed to low concentrations of differently surface charged PS-NPs for 37 days. Interestingly, positively and negatively charged particles induced similar metabolic changes. In general, positively surface charged PS NPs often exhibit greater effects compared to negatively surface charged NPs.[35] However, no difference in the toxicity, as similar to the results observed in the present study, have been seen in the toxicity towards *D. magna* after a life-time exposure to differently surface charged PS-NPs.[17] There are no clear answers regarding why positive functionalization shows higher toxicity compared to negative one. However, one of the explanations to the lack of differences in the toxicity can be that in the long-term experiment the particle's hydrophobic regions are more important than functional groups. Positively surface charged

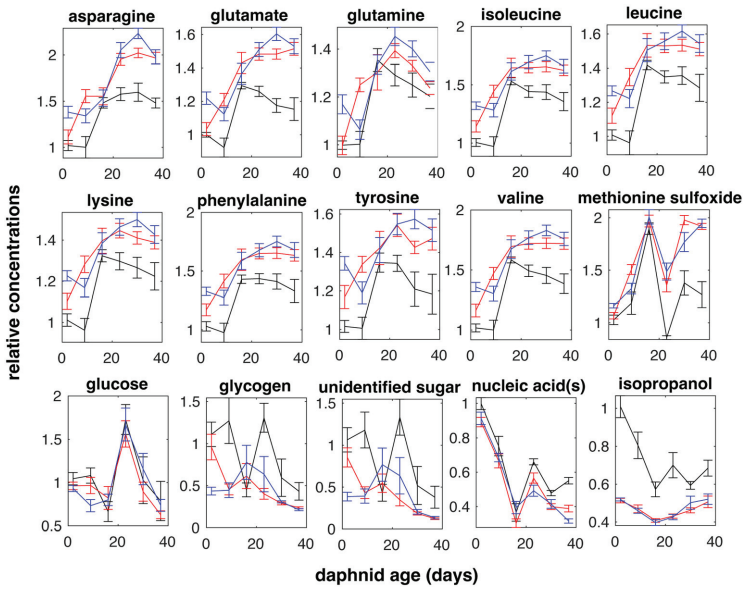

Fig. 3 Metabolite variations between *D. magna* at different daphnid aging in the control group (black line) and in the presence of either PS-NH_2 (blue line) or PS-COOH (red line) NPs. Error bars are standard errors.

particles are often seen as a model for cationic NPs, whereas negatively surface charged particles as anionic particles.[46] The role of hydrophobic regions for the toxicity can be enhanced by reducing the number of amino groups on the surface of the particle, by cationic groups binding with certain components to shield the positive charge, which consequently decreases the interaction between cell membrane and NPs.[46] Furthermore, it has been shown that the affinity of biomolecules binding to the surface of the particle with a carboxylic group is weaker at pH 7, which can further affect the presence of other molecules and ions and the toxicity.[47] The differences in biomolecules binding to PS NPs with amino and carboxylic groups have previously been shown for PS NPs after being filtrated by *D. magna*.[48]

Already at the lowest PS NP concentration (3.2 μg L^{-1}) there was a significant effect on the metabolome. This is far below the concentrations of nanoplastics found in different environments, such as Siberian Arctic tundra (50 μg L^{-1}), a forest landscape in southern Sweden (560 μg L^{-1}),[9] and snow in the remote high-altitude Alps, Austria (46 μg L^{-1}).[10] Furthermore, this concentration (3.2 μg L^{-1}) is within the concentration range of breakdown styrene oligomers in surface waters (between 0.17 μg L^{-1} and 4.26 μg L^{-1}) and in deep waters (0.31 μg L^{-1} and 4.31 μg L^{-1}) in the Pacific Ocean.[12] It is hundred times lower than previously measured toxic concentrations for life-time (103 days) exposure of *D. magna* to 62 nm PS-COOH and 53 nm PS-NH_2.[17] A low-dose stimulation and a high-dose inhibition is a common phenomenon, called hormesis, observed in biology:[49] at the lowest dose, organisms have a maximum stimulatory response in comparison with a higher concentration of toxicants. This can partly explain why we see effects already at the lowest concentrations used here.

The NP concentration of 3.2 μg L^{-1} is not only very low compared to concentrations used in other NP studies but is also low compared to a variety of pollutant concentrations used in ecotoxicity studies. For example, zebrafish *Danio rerio* has been exposed for 30 days to 44 nm PS NPs (1, 10, and 100 μg L^{-1})[50] and for 96 h to ~190 nm PE NPs (5×10^5 μg L^{-1}).[51] Additionally, *D. magna* has previously been exposed to MPs and NPs, for example, 24 h exposure to 20 μm and 30 μm PE MPs ($2–6 \times 10^4$ μg L^{-1}),[26] 5 days exposure to 52 nm PS NPs (5×10^3 μg L^{-1}),[34] and 21 days exposure to ~71 nm PS NPs ($500–2 \times 10^3$ μg L^{-1}).[52]

We observed that upon aging, the metabolome in both untreated control and PS NP exposed *D. magna* follow the same pattern (Fig. 1A). This suggests an unaffected timing of the daphnids' developmental stages (*e.g.*, juvenile, first and/or second egg development). Previously, Zhang and co-authors[53] showed that *D. similis* start to develop the first eggs in the brood chamber already after 5–7 days, whereas the second egg development might start after another 5–6 days.

A total of 15 significantly affected metabolites were identified (Table 1), 12 of which were affected in response to PS NPs. Many of these were amino acids that changed in the same way with daphnid aging and between control and treatment groups (Fig. 3). Amino acids have been shown to be intimately linked to most biochemical pathways related to stress.[30,54] For example, lysine is among amino acids that are stored by crustaceans as energy reserves during molting cycles.[55] Temporary periods of starvation are experienced during the molting process in crustaceans, such as prawns, crabs, or shrimps, during which individuals use reservoirs of amino acids.[55] An increased stress level could make the daphnid less resilient to other stress factors such as predators, lack of food, temperature, and ultraviolet (UV) radiation.

If we look at individual amino acids, an increase in lysine has been associated with alterations in molt frequency and disruption of normal hormone signaling.[56] The increase of frequency of molt has previously been shown in *D. magna* after exposure to 2 ± 1 μm PVC MPs.[57] Furthermore, the present data shows that glucose levels varied significantly due to daphnid aging but were not affected by PS NPs (Table 1). It is known that *Daphnia* species are able to maintain minimal levels of the energy molecule glucose for survival,[58] however the main change in glucose was observed at exactly day 23 (Fig. 3), which might be explained due to daphnid aging. Disturbed glucose metabolism has previously been observed in aged zebrafish.[59,60] Additionally, a short (24 h) exposure to 20 μm and 30 μm PE MPs have been shown to significantly interfere with energy metabolism in *D. magna*.[26]

Changes in aromatic amino acids such as phenylalanine and tyrosine have been associated with disruptions in catecholamine synthesis,[28] where elevated catecholamine levels as a response to environmental stressors.[61] Phenylalanine is the precursor to tyrosine, which is used to produce neurotransmitters such as octopamine and dopamine[62] and pigment compound melanin.[63] The increase in phenylalanine in response to PS NPs might lead to lower amount of pigmentation.[64,65] This is an important factor for daphnids as several *Daphnia* species have ability to maintain their pigmentation by coping and responding to UV radiation.[66]

The most significant effect of PS NP exposure was a decrease in isopropanol while similar changes with time are observed both control and treatment groups (Fig. 3). Microorganisms, for example *Lactobacillus brevis*, *Clostridium beijerinckii*, *C. aurantibutyricum*, *C. ragsdalei*, and *Acetobacterium woodii*, are known to produce isopropanol from acetone.[67–69] The decrease detected here might indicate that the bacterial conversion of acetone to isopropanol through isopropanol dehydrogenase is affected.[70]

Conclusions

In the present study, we aimed to answer how the *D. magna* metabolome is affected by PS NPs and their charge and concentration, as well as by daphnid aging, using ^{1}H NMR-based metabolomics. First, we wanted to see if there is an effect of PS NPs, and at which concentration such an effect occurs. Our results show that significant effects on amino

acids metabolism and the bacterial metabolite isopropanol were already observed at the lowest concentration (3.2 μg L^{-1}) used here. These effects appeared already after two days and remained throughout the experiment (37 days). Secondly, we wanted to see if PS NPs with different surface charges affect the metabolome differently. The results show that exposure to 53 nm PS-NH_2 and 62 nm PS-COOH NPs gave rise to very similar effects. This is an important observation, as PS-COOH NPs have previously been shown to be non-toxic after acute (24 h) exposure. Additionally, daphnids aging also had significant effects on amino acids metabolism and the bacterial metabolite isopropanol.

Metabolomics-based studies allow us to better understand the physiological state of an organism and its response to different types of stimuli, including pollutants. The obtained results highlight that daphnids' metabolism can be affected significantly regardless of the surface charge of PS NPs after a long-term exposure even at low concentrations. The present study shows the effect of PS NPs on the *D. magna* endometabolome, the metabolites kept by the *D. magna*, therefore future studies may also focus in the exometabolome, the metabolites that are excreted into the exposure medium. Here we used model PS particles with defined sizes and shapes. Future studies may evaluate the metabolic response after exposure to more environmentally realistic nanoplastics with greater diversity in shape and size.

Author contributions

Egle Kelpsiene: investigation, methodology, writing – original draft, review & editing. Tommy Cedervall: conceptualization, funding acquisition, methodology, supervision, writing – review & editing supervised the work. Anders Malmendal: NMR data analysis, methodology, writing – review & editing.

Conflicts of interest

The authors declare no competing interests.

Acknowledgements

Funding for the present study was provided by Mistra Environmental Nanosafety Program. We also would like to thank Dr. Anders Bay Nord at Swedish NMR Centre, University of Gothenburg, for his help with NMR samples analysis. We also would like to thank Dr. Martin Lundqvist for helping with zeta potential measurements.

References

1 Plastics the Facts 2021, **https://plasticseurope.org/wp-content/uploads/2021/12/Plastics-the-Facts-2021-web-final.pdf**, 2021, Accessed 9 Feb 2023.
2 R. C. Thompson, C. J. Moore, F. S. Vom Saal and S. H. Swan, Plastics, the environment and human health: current consensus and future trends, *Philos. Trans. R. Soc., B*, 2009, **364**, 2153–2166.
3 M. Rujnić-Sokele and A. Pilipović, Challenges and opportunities of biodegradable plastics: A mini review, *Waste Manage. Res.*, 2017, **35**, 132–140.
4 L. Lebreton and A. Andrady, Future scenarios of global plastic waste generation and disposal, *Palgrave Communications*, 2019, **5**, 6.
5 J. Soares, I. Miguel, C. Venâncio, I. Lopes and M. Oliveira, Perspectives on Micro (Nano) Plastics in the marine environment: biological and societal considerations, *Water*, 2020, **12**, 3208.
6 SAPEA, Science Advice for Policy by European Academies, A Scientific Perspective on Microplastics in Nature and Society, SAPEA, Berlin, 2019, DOI: **10.26356/microplastics**.
7 J. Gigault, A. Ter Halle, M. Baudrimont, P.-Y. Pascal, F. Gauffre, T.-L. Phi, H. El Hadri, B. Grassl and S. Reynaud, Current opinion: What is a nanoplastic?, *Environ. Pollut.*, 2018, **235**, 1030–1034.
8 A. Ter Halle, L. Jeanneau, M. Martignac, E. Jardé, B. Pedrono, L. Brach and J. Gigault, Nanoplastic in the North Atlantic Subtropical Gyre, *Environ. Sci. Technol.*, 2017, **51**, 13689–13697.
9 D. Materić, M. Peacock, J. Dean, M. Futter, T. Maximov, F. Moldan, T. Röckmann and R. Holzinger, Presence of nanoplastics in rural and remote surface waters, *Environ. Res. Lett.*, 2022, **17**, 054036.
10 D. Materić, E. Ludewig, D. Brunner, T. Röckmann and R. Holzinger, Nanoplastics transport to the remote, high-altitude Alps, *Environ. Pollut.*, 2021, **288**, 117697.
11 M. Sighicelli, L. Pietrelli, F. Lecce, V. Iannilli, M. Falconieri, L. Coscia, S. Di Vito, S. Nuglio and G. Zampetti, Microplastic pollution in the surface waters of Italian Subalpine Lakes, *Environ. Pollut.*, 2018, **236**, 645–651.
12 B. G. Kwon, K. Amamiya, H. Sato, S.-Y. Chung, Y. Kodera, S.-K. Kim, E. J. Lee and K. Saido, Monitoring of styrene oligomers as indicators of polystyrene plastic pollution in the North-West Pacific Ocean, *Chemosphere*, 2017, **180**, 500–505.
13 K. Amamiya, K. Saido, S.-Y. Chung, T. Hiaki, D. S. Lee and B. G. Kwon, Evidence of transport of styrene oligomers originated from polystyrene plastic to oceans by runoff, *Sci. Total Environ.*, 2019, **667**, 57–63.
14 K. Tallec, O. Blard, C. González-Fernández, G. Brotons, M. Berchel, P. Soudant, A. Huvet and I. Paul-Pont, Surface functionalization determines behavior of nanoplastic solutions in model aquatic environments, *Chemosphere*, 2019, **225**, 639–646.
15 A. Sukhanova, S. Bozrova, P. Sokolov, M. Berestovoy, A. Karaulov and I. Nabiev, Dependence of Nanoparticle Toxicity on Their Physical and Chemical Properties, *Nanoscale Res. Lett.*, 2018, **13**, 44–44.
16 K. Mattsson, E. V. Johnson, A. Malmendal, S. Linse, L.-A. Hansson and T. Cedervall, Brain damage and behavioural disorders in fish induced by plastic nanoparticles delivered through the food chain, *Sci. Rep.*, 2017, **7**, 11452.
17 E. Kelpsiene, O. Torstensson, M. T. Ekvall, L.-A. Hansson and T. Cedervall, Long-term exposure to nanoplastics reduces life-time in *Daphnia magna*, *Sci. Rep.*, 2020, **10**, 5979.

18 OECD, Test No. 202: Daphnia sp. Acute Immobilisation Test, 2004.
19 R. Lenz, K. Enders and T. G. Nielsen, Microplastic exposure studies should be environmentally realistic, *Proc. Natl. Acad. Sci. U. S. A.*, 2016, **113**, E4121–E4122.
20 H. C. Poynton, H. Wintz and C. D. Vulpe, Progress in ecotoxicogenomics for environmental monitoring, mode of action, and toxicant identification, *Adv. Exp. Biol.*, 2008, **2**, 21–323.
21 J. K. Nicholson, J. C. Lindon and E. Holmes, 'Metabonomics': understanding the metabolic responses of living systems to pathophysiological stimuli via multivariate statistical analysis of biological NMR spectroscopic data, *Xenobiotica*, 1999, **29**, 1181–1189.
22 C. J. Clarke and J. N. Haselden, Metabolic profiling as a tool for understanding mechanisms of toxicity, *Toxicol. Pathol.*, 2008, **36**, 140–147.
23 E. G. Nagato, B. P. Lankadurai, R. Soong, A. J. Simpson and M. J. Simpson, Development of an NMR microprobe procedure for high-throughput environmental metabolomics of *Daphnia magna*, *Magn. Reson. Chem.*, 2015, **53**, 745–753.
24 G. A. Nagana Gowda and D. Raftery, NMR-Based Metabolomics, *Adv. Exp. Med. Biol.*, 2021, **1280**, 19–37.
25 L. Li, H. Wu, C. Ji, C. A. van Gestel, H. E. Allen and W. J. Peijnenburg, A metabolomic study on the responses of *Daphnia magna* exposed to silver nitrate and coated silver nanoparticles, *Ecotoxicol. Environ. Saf.*, 2015, **119**, 66–73.
26 P. Wang, Q.-Q. Li, J. Hui, Q.-Q. Xiang, H. Yan and L.-Q. Chen, Metabolomics reveals the mechanism of polyethylene microplastic toxicity to *Daphnia magna*, *Chemosphere*, 2022, **307**, 135887.
27 T.-Y. Jeong and M. J. Simpson, *Daphnia magna* metabolic profiling as a promising water quality parameter for the biological early warning system, *Water Res.*, 2019, **166**, 115033.
28 H. C. Poynton, N. S. Taylor, J. Hicks, K. Colson, S. Chan, C. Clark, L. Scanlan, A. V. Loguinov, C. Vulpe and M. R. Viant, Metabolomics of microliter hemolymph samples enables an improved understanding of the combined metabolic and transcriptional responses of *Daphnia magna* to cadmium, *Environ. Sci. Technol.*, 2011, **45**, 3710–3717.
29 E. G. Nagato, C. Jessica, B. P. Lankadurai, D. G. Poirier, E. J. Reiner, A. J. Simpson and M. J. Simpson, 1H NMR-based metabolomics investigation of *Daphnia magna* responses to sub-lethal exposure to arsenic, copper and lithium, *Chemosphere*, 2013, **93**, 331–337.
30 E. G. Nagato, A. J. Simpson and M. J. Simpson, Metabolomics reveals energetic impairments in *Daphnia magna* exposed to diazinon, malathion and bisphenol-A, *Aquat. Toxicol.*, 2016, **170**, 175–186.
31 T. Vandenbrouck, O. A. H. Jones, N. Dom, J. L. Griffin and W. De Coen, Mixtures of similarly acting compounds in *Daphnia magna*: From gene to metabolite and beyond, *Environ. Int.*, 2010, **36**, 254–268.
32 D. Ebert, Introduction to *Daphnia* biology, *Ecology, Epidemiology and Evolution of Parasitism in Daphnia*, 2005, pp. 5–18.
33 R. Frankel, M. T. Ekvall, E. Kelpsiene, L.-A. Hansson and T. Cedervall, Controlled protein mediated aggregation of polystyrene nanoplastics does not reduce toxicity towards *Daphnia magna*, *Environ. Sci.: Nano*, 2020, **7**, 1518–1524.
34 R. Cui, S. W. Kim and Y.-J. An, Polystyrene nanoplastics inhibit reproduction and induce abnormal embryonic development in the freshwater crustacean *Daphnia galeata*, *Sci. Rep.*, 2017, **7**, 12095.
35 F. Nasser and I. Lynch, Secreted protein eco-corona mediates uptake and impacts of polystyrene nanoparticles on *Daphnia magna*, *J. Proteomics*, 2016, **137**, 45–51.
36 A. Pochelon, S. Stoll and V. I. Slaveykova, Polystyrene nanoplastic behavior and toxicity on crustacean *Daphnia magna*: media composition, size, and surface charge effects, *Environments*, 2021, **8**, 101.
37 V. P. Vaz, D. J. Nogueira, D. S. Vicentini and W. G. Matias, Can the sonication of polystyrene nanoparticles alter the acute toxicity and swimming behavior results for *Daphnia magna*?, *Environ. Sci. Pollut. Res.*, 2021, **28**, 14192–14198.
38 W. Lin, R. Jiang, S. Hu, X. Xiao, J. Wu, S. Wei, Y. Xiong and G. Ouyang, Investigating the toxicities of different functionalized polystyrene nanoplastics on *Daphnia magna*, *Ecotoxicol. Environ. Saf.*, 2019, **180**, 509–516.
39 F. Savorani, G. Tomasi and S. B. Engelsen, icoshift: A versatile tool for the rapid alignment of 1D NMR spectra, *J. Magn. Reson.*, 2010, **202**, 190–202.
40 F. Dieterle, A. Ross, G. Schlotterbeck and H. Senn, Probabilistic quotient normalization as robust method to account for dilution of complex biological mixtures. Application in 1H NMR metabonomics, *Anal. Chem.*, 2006, **78**, 4281–4290.
41 A. Craig, O. Cloarec, E. Holmes, J. K. Nicholson and J. C. Lindon, Scaling and normalization effects in NMR spectroscopic metabonomic data sets, *Anal. Chem.*, 2006, **78**, 2262–2267.
42 C. Spearman, "General Intelligence" Objectively Determined and Measured, *Am. J. Psychol.*, 1904, **15**, 201–293.
43 M. Bylesjö, A. Sjödin, D. Eriksson, H. Antti, T. Moritz, S. Jansson and J. Trygg, MASQOT-GUI: spot quality assessment for the two-channel microarray platform, *Bioinformatics*, 2006, **22**, 2554–2555.
44 Q. Cui, I. A. Lewis, A. D. Hegeman, M. E. Anderson, J. Li, C. F. Schulte, W. M. Westler, H. R. Eghbalnia, M. R. Sussman and J. L. Markley, Metabolite identification via the madison metabolomics consortium database, *Nat. Biotechnol.*, 2008, **26**, 162–164.
45 D. S. Wishart, D. Tzur, C. Knox, R. Eisner, A. C. Guo, N. Young, D. Cheng, K. Jewell, D. Arndt and S. Sawhney, HMDB: the human metabolome database, *Nucleic Acids Res.*, 2007, **35**, D521–D526.
46 A. E. Nel, L. Mädler, D. Velegol, T. Xia, E. M. Hoek, P. Somasundaran, F. Klaessig, V. Castranova and M. Thompson, Understanding biophysicochemical interactions at the nano–bio interface, *Nat. Mater.*, 2009, **8**, 543–557.

47 P. Rama, J. A. G. Urréa and Z. Abbas, Interfacial Interactions of Humic Acids with Polystyrene Nano-plastics in Aqueous/Ionic Environments: A Molecular dynamics exploration, *Environ. Sci.: Nano*, 2023, **10**, 1385–1393.
48 E. Kelpsiene, I. Brandts, K. Bernfur, M. T. Ekvall, M. Lundqvist, M. Teles and T. Cedervall, Protein binding on acutely toxic and non-toxic polystyrene nanoparticles during filtration by *Daphnia magna*, *Environ. Sci.: Nano*, 2022, **9**, 2500–2509.
49 E. J. Calabrese, Hormesis: why it is important to toxicology and toxicologists, *Environ. Toxicol. Chem.*, 2008, **27**, 1451–1474.
50 M. Teng, X. Zhao, C. Wang, C. Wang, J. C. White, W. Zhao, L. Zhou, M. Duan and F. Wu, Polystyrene nanoplastics toxicity to zebrafish: dysregulation of the brain–intestine–microbiota axis, *ACS Nano*, 2022, **16**, 8190–8204.
51 M. Sun, R. Ding, Y. Ma, Q. Sun, X. Ren, Z. Sun and J. Duan, Cardiovascular toxicity assessment of polyethylene nanoplastics on developing zebrafish embryos, *Chemosphere*, 2021, **282**, 131124.
52 Z. Liu, Y. Li, M. S. Sepúlveda, Q. Jiang, Y. Jiao, Q. Chen, Y. Huang, J. Tian and Y. Zhao, Development of an adverse outcome pathway for nanoplastic toxicity in *Daphnia pulex* using proteomics, *Sci. Total Environ.*, 2020, 144249.
53 B. Zhang, H. Zhang, C. Du, Q. X. Ng, C. Hu, Y. He and C. N. Ong, Metabolic responses of the growing *Daphnia similis* to chronic AgNPs exposure as revealed by GC-Q-TOF/MS and LC-Q-TOF/MS, *Water Res.*, 2017, **114**, 135–143.
54 D. Lane, R. Soong, W. Bermel, P. Ning, R. Dutta Majumdar, M. Tabatabaei-Anaraki, H. Heumann, M. Gundy, H. Bönisch, Y. Liaghati Mobarhan, M. J. Simpson and A. J. Simpson, Selective amino acid-only *in vivo* NMR: a powerful tool to follow stress processes, *ACS Omega*, 2019, **4**, 9017–9028.
55 S. Maity, A. Jannasch, J. Adamec, M. Gribskov, T. Nalepa, T. O. Höök and M. S. Sepúlveda, Metabolite profiles in starved *Diporeia* spp. using liquid chromatography-mass spectrometry (LC-MS) based metabolomics, *J. Crustacean Biol.*, 2012, **32**, 239–248.
56 G. A. LeBlanc, Crustacean endocrine toxicology: a review, *Ecotoxicology*, 2007, **16**, 61–81.
57 Y. Liu, J. Zhang, H. Zhao, J. Cai, Y. Sultan, H. Fang, B. Zhang and J. Ma, Effects of polyvinyl chloride microplastics on reproduction, oxidative stress and reproduction and detoxification-related genes in *Daphnia magna*, *Comp. Biochem. Physiol., Part C: Toxicol. Pharmacol.*, 2022, **254**, 109269.
58 N. N. Smirnov, *Physiology of the Cladocera*, Academic Press, 2017.
59 M. Liu, B. Sun, X. Zhou and L. Chen, Disturbed glucose metabolism by perfluorobutanesulfonate pollutant and benefit of young fecal transplantation in aged zebrafish, *Ecotoxicol. Environ. Saf.*, 2022, **241**, 113721.
60 A. M. Houbrechts, A. Beckers, P. Vancamp, J. Sergeys, C. Gysemans, C. Mathieu and V. M. Darras, Age-dependent changes in glucose homeostasis in male deiodinase type 2 knockout zebrafish, *Endocrinology*, 2019, **160**, 2759–2772.
61 S. G. Reid, N. J. Bernier and S. F. Perry, The adrenergic stress response in fish: control of catecholamine storage and release1Communicated by Dr P.W. Hochachka, Editor. 1, *Comp. Biochem. Physiol., Part C: Pharmacol., Toxicol. Endocrinol.*, 1998, **120**, 1–27.
62 M. D. McCoole, N. J. Atkinson, D. I. Graham, E. B. Grasser, A. L. Joselow, N. M. McCall, A. M. Welker, E. J. Wilsterman Jr, K. N. Baer and A. R. Tilden, Genomic analyses of aminergic signaling systems (dopamine, octopamine and serotonin) in *Daphnia pulex*, *Comp. Biochem. Physiol., Part D: Genomics Proteomics*, 2012, **7**, 35–58.
63 A. G. Scoville and M. E. Pfrender, Phenotypic plasticity facilitates recurrent rapid adaptation to introduced predators, *Proc. Natl. Acad. Sci. U. S. A.*, 2010, **107**, 4260–4263.
64 S. Fuchs, V. Behrends, J. G. Bundy, A. Crisanti and T. Nolan, Phenylalanine Metabolism Regulates Reproduction and Parasite Melanization in the Malaria Mosquito, *PLoS One*, 2014, **9**, e84865.
65 Y. Nagasaki, Y. Matsubara, H. Takano, K. Fujii, M. Senoo, J. Akanuma, K. Takahashi, S. Kure, M. Hara, Y. Kanegae, I. Saito and K. Narisawa, Reversal of Hypopigmentation in Phenylketonuria Mice by Adenovirus-Mediated Gene Transfer, *Pediatr. Res.*, 1999, **45**, 465–473.
66 L.-A. Hansson and S. Hylander, Effects of ultraviolet radiation on pigmentation, photoenzymatic repair, behavior, and community ecology of zooplankton, *Photochem. Photobiol. Sci.*, 2009, **8**, 1266–1275.
67 J.-S. Chen, Alcohol dehydrogenase: multiplicity and relatedness in the solvent-producing *clostridia*, *FEMS Microbiol. Rev.*, 1995, **17**, 263–273.
68 K. D. Ramachandriya, M. R. Wilkins, M. J. M. Delorme, X. Zhu, D. K. Kundiyana, H. K. Atiyeh and R. L. Huhnke, Reduction of acetone to isopropanol using producer gas fermenting microbes, *Biotechnol. Bioeng.*, 2011, **108**, 2330–2338.
69 K. Arslan, T. Schoch, F. Höfele, S. Herrschaft, C. Oberlies, F. Bengelsdorf, M. C. Veiga, P. Dürre and C. Kennes, Engineering *Acetobacterium woodii* for the production of isopropanol and acetone from carbon dioxide and hydrogen, *Biotechnol. J.*, 2022, **17**, 2100515.
70 D. T. Jones and D. Woods, Acetone-butanol fermentation revisited, *Microbiol. Rev.*, 1986, **50**, 484–524.

Supplementary Information

Metabolomics-based analysis in *Daphnia magna* after exposure to low environmental concentrations of polystyrene nanoparticles

Egle Kelpsiene[a,b], Tommy Cedervall[a,b*], and Anders Malmendal[c]

[a] Department of Biochemistry and Structural Biology, Lund University, P.O. Box 124, SE-221 00 Lund, Sweden

[b] NanoLund, Lund University, P.O. Box 118, SE-221 00, Lund, Sweden

[c] Department of Science and Environment, Roskilde University, P.O. Box 260 DK-4000 Roskilde, Denmark

*Corresponding author:
tommy.cedervall@biochemistry.lu.se

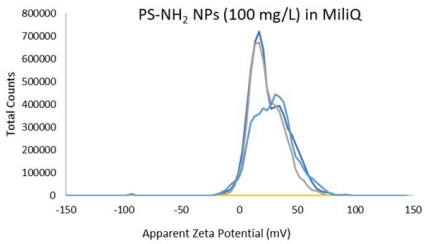

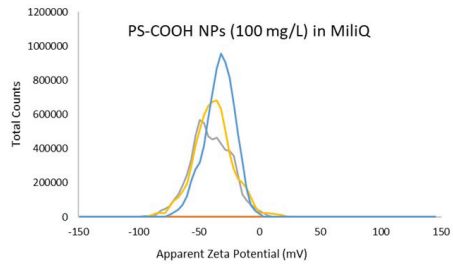

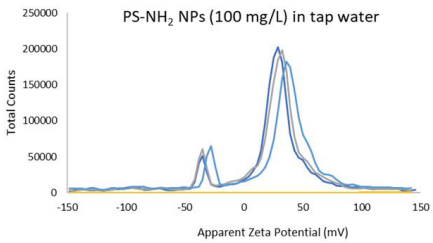

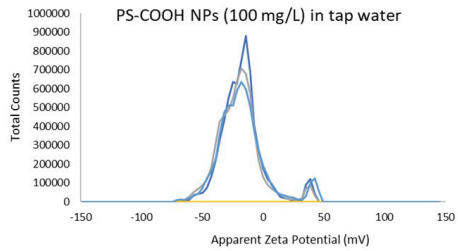

Supplementary Fig. 1. Zeta potential measurements for PS NPs used in the study. PS NPs were measured either in MiliQ water or in tap water at concentrations of 100 mg/L,

Table S1. MANOVA comparisons of effect of presence, concentration, and type of nanoparticles. P values for comparisons of scores from principal component analysis (PCA) to test effect of presence, concentration, and type of NPs at different daphnid ages using MANOVA. Conc = effect of concentration for all NPs, Conc NH_2 = effect of concentration for PS-NH_2 NPs, Conc COOH = effect of concentration for PS-COOH NPs, Nanotype = effect of nanoparticle type, Nano = effect of nanoparticles, Nano 3.2 µg/L = effect of nanoparticles at 3.2 µg/L, Nano 32 µg/L = effect of nanoparticles at 32 µg/L, Nano 320 µg/L = effect of nanoparticles at 320 µg/L.

Age (days)	2	9	16	23	30	37	median
Conc	3.2×10^{-2}	2.6×10^{-2}	8.2×10^{-1}	2.8×10^{-1}	6.6×10^{-1}	5.8×10^{-3}	1.6×10^{-1}
Conc NH_2	8.8×10^{-2}	1.5×10^{-2}	1.7×10^{-1}	2.0×10^{-4}	3.8×10^{-5}	2.5×10^{-1}	5.2×10^{-2}
Conc COOH	4.0×10^{-1}	2.1×10^{-3}	1.4×10^{-5}	3.1×10^{-2}	1.0×10^{-1}	6.0×10^{-7}	1.6×10^{-2}
Nanotype	1.4×10^{-3}	2.6×10^{-1}	4.4×10^{-1}	1.7×10^{-1}	4.9×10^{-4}	1.5×10^{-1}	1.6×10^{-1}
Nano	1.1×10^{-8}	2.1×10^{-4}	6.8×10^{-3}	3.6×10^{-6}	5.3×10^{-8}	1.3×10^{-7}	1.9×10^{-6}
Nano 3.2 µg/L	6.5×10^{-9}	1.3×10^{-2}	1.2×10^{-1}	7.3×10^{-4}	2.1×10^{-5}	1.1×10^{-7}	3.8×10^{-4}
Nano 32 µg/L	3.7×10^{-5}	2.3×10^{-5}	9.0×10^{-3}	3.8×10^{-6}	4.8×10^{-2}	7.2×10^{-3}	3.6×10^{-3}
Nano 320 µg/L	5.5×10^{-2}	1.6×10^{-9}	4.7×10^{-7}	1.1×10^{-5}	6.2×10^{-7}	6.4×10^{-9}	5.5×10^{-7}

Paper III

Environmental Science Nano

ROYAL SOCIETY OF CHEMISTRY

PAPER

View Article Online
View Journal | View Issue

Cite this: *Environ. Sci.: Nano*, 2022, **9**, 2500

Protein binding on acutely toxic and non-toxic polystyrene nanoparticles during filtration by *Daphnia magna*†

Egle Kelpsiene, [ab] Irene Brandts, [cd] Katja Bernfur,[a] Mikael T. Ekvall,[be] Martin Lundqvist, [ab] Mariana Teles[cd] and Tommy Cedervall *[ab]

Received 8th February 2022,
Accepted 27th May 2022

DOI: 10.1039/d2en00125j

rsc.li/es-nano

Nanomaterials can adsorb biomolecules to their surface and form a protein corona. Here we investigated the protein profile bound to different sizes of aminated and carboxylated polystyrene (PS) nanoparticles after passing through the digestive tract of the freshwater zooplankter *Daphnia magna*. We found that acutely toxic aminated 53 nm PS nanoparticles bind a different set of proteins compared to other non-toxic PS nanoparticles. The aminated PS nanoparticles bind a higher number of proteins, which are smaller and more acidic, compared to the proteins which bind to the PS nanoparticles that are non-toxic in acute toxicity tests. The proteins bound to toxic nanoparticles can be divided into two groups. One group of proteins which function is related to the digestive system, whereas the other group of proteins can be related to the epithelium, intracellular structures and processes. Finally, we observed that not only proteins bind to the surfaces of the nanoparticles. Triglycerides effectively bind to 200 nm carboxylated PS nanoparticles but not to the other tested nanoparticles. These results provide information about the composition of the corona formed on surfaces of nanoparticles after a short-term incubation with *D. magna* and give insights to what underlies the acute toxicity caused by nanoparticles.

Environmental significance

The increasing use of nanomaterial may lead to increasing exposure in the environment. Another source of nano-sized particles are breakdown particles from plastics and rubbers. Altogether nano-sized particles are a growing environmental concern. Although the toxicity of particles is known in many cases, surprisingly little is known about the mechanisms behind the toxicity. Detailed knowledge on how toxic and non-toxic nano-sized particles interact with filtrating organisms can not only explain the mechanisms behind the toxicity but also be used as an early guide to evaluate the expected toxicity of new material and products under development. This will facilitate the evaluation of the environmental impact of already present materials as well as future materials.

Introduction

Nanomaterials bring many revolutionary advantages to our modern way of living. Due to their small size (1–100 nm), shape and surface,[1] nanomaterials are widely used in biomedical applications, personal care items and engineering technologies.[2,3] However, as the use of nanomaterials increases, so does the need for careful investigations of the potential toxicity and interaction with biological matter,[4] especially when nanomaterials enter the natural environment.[5]

Once nanomaterials enter the environment or biological fluids, nanoparticles, including polystyrene (PS) nanoparticles, can adsorb biomolecules to their surfaces,[6,7] and form a layer, a so-called protein corona.[8–10] Protein corona formation and composition depends on several parameters, such as, nanoparticle size, surface characteristics,[11,12] medium conditions,[13] and time.[14,15] The characteristics of these protein corona are particularly relevant, as both the interaction with cell membranes and the cellular uptake are influenced by the adsorbed proteins.[16] Therefore, the corona becomes highly important when the cytotoxicity[17,18] or body distribution[19–21] of nanoparticles is

[a] *Department of Biochemistry and Structural Biology, Lund University, P.O. Box 124, SE-221 00 Lund, Sweden. E-mail: tommy.cedervall@biochemistry.lu.se*
[b] *NanoLund, Lund University, Box 118, SE-221 00 Lund, Sweden*
[c] *Department of Cell Biology, Physiology and Immunology, Universitat Autònoma de Barcelona, 08193 Barcelona, Spain*
[d] *Institute of Biotechnology and Biomedicine, Universitat Autònoma de Barcelona, 08193 Barcelona, Spain*
[e] *Department of Biology, Aquatic Ecology Unit, Lund University, Lund, Sweden*
† Electronic supplementary information (ESI) available. See DOI: **https://doi.org/10.1039/d2en00125j**

evaluated. Even though corona mainly contain proteins, the presence of other biomolecules such as sugars, nucleic acids and lipids is also expected,[20,22,23] and should be further investigated.

Daphnia magna, used in the present study, is a well-studied freshwater filter feeder. The genome of *D. magna* is fully sequenced, making it a suitable model organism to monitor biological responses to changes in the environment.[24] Moreover, *D. magna* is specifically appropriate to study nanoparticles, as they typically feed on particles ranging between 240 to 640 nm in size,[25] although they can also ingest particles up to 1000 nm.[26] During the last years, the toxicity of PS nanoparticles has been widely studied. In general, aminated PS (PS-NH_2) are more toxic than carboxylated PS (PS-COOH) due to the positive surface charge.[27] It has previously been shown that 50 nm PS-NH_2 are toxic to *D. magna* after 24 h exposure, whereas 200 nm PS-NH_2, and 60 nm and 200 nm PS-COOH are not acutely toxic.[28] More recently the importance of the surface charge on PS nanoparticles[29] and the size of PS-NH_2 (ref. 30) has been studied in detail. The weathering of PS nanoparticles and the eco-corona formation have been seen to influence nanoparticle, suggesting that biomolecules on the surface are important for the toxicity.[31,32] The importance of considering the eco-corona, including the protein corona, in testing nanomaterial has recently been reviewed,[7] but the current knowledge on the molecular events that initiate the toxic response is still limited.

A few previous studies have identified proteins bound to nanoparticles after being incubated with *D. magna*. For example, 25 nm gold nanoparticles filtrated by *D. magna* bound different proteins, compared to nanoparticles incubated in conditioned water, *i.e.* water that has been filtrated by *D. magna* without nanoparticles.[33] Interestingly, the protein corona formed on aminated PS particles in conditioned water was shown to depended on the presence of other organic molecules.[34] Another study showed that the protein corona formed after filtration by *D. magna* was different on freshly dispersed or medium-aged silver (Ag) and titanium dioxide (TiO_2) nanoparticles.[35] In the present study we show that toxic and non-toxic (as seen in acute toxicity tests) PS-NH_2 and PS-COOH nanoparticles binds different sets of proteins after passing through the digestive system of *D. magna*. This suggest that the most abundant proteins on the particles can be linked to their toxicity and encourage future studies to understand the links between particle toxicity and protein binding.

Material and methods

Nanoparticle preparation and characterization

Aminated PS nanoparticles, PS-NH_2 (53 and 200 nm), and carboxylated PS nanoparticles, PS-COOH (62 and 200 nm), were purchased from Bangs Laboratories Inc. (**https://www.bangslabs.com**). Before the experiments, nanoparticles were diluted to 10 mg mL^{-1} and dialyzed in a Standard RC Tubing, dialysis membrane (MWCO: 3.5 kD) for 72 h at 4 °C in 10 L of MilliQ water. The water was changed after 4 h the first day and once a day on the following days. To confirm the size of nanoparticles after dialysis, and ensure that there was no particle aggregation, nanoparticles were measured using both dynamic light scattering (DLS, DynaPro Plate Reader II, Wyatt instruments, USA) and differential centrifugal sedimentation (DCS, DC24000 UHR Disc Centrifuge, CPS Instruments Europe, Oosterhout, Netherlands).

The *z*-potential, performed at 25 °C using a Zetasizer Nano ZS instrument (Malvern Instruments, Worcestershire, UK), for the particles were determined both for a particle in MilliQ H_2O and four different buffers; 0.1 M glycine pH 2.2, 3.6, 8.6, and 10.6 (adjusted to the right pH with either HCL or NaOH). 2 μL of the 10% (w/v) stock solution was mixed with 98 μL MilliQ H_2O whereafter 1000 μL of the buffer was added and the sample was mixed. The final concentrations in the sample were ~0.9 M glycine and ~0.02% (w/v) particles.

The FTIR spectra were recorded using a Perkin Elmer Spectrum Two equipped with a UATR HR unit. Each sample was recorded with 64 scans between 450–4000 cm^{-1} and with 4 cm^{-1} nominal resolution. 2 μL of the stock solution (10% w/v) was added to the diamond surface and was left drying for 30 min before the spectrum was recorded.

Incubation with *D. magna*

Adult, at least one week old and that had not yet reproduced, *D. magna* individuals that came from the same population were used in the present study. The culture originates from Lake Bysjön, southern Sweden (55°40′31.3″N 13°32′41.9″E) and has been kept in a laboratory environment for several hundred generations. All cultures and experiments were maintained at 18 °C under an 8:16 h light/dark photoperiod. Before the incubation with nanoparticles, *D. magna* adults were kept in clean tap water for 24 h to allow evacuation of remaining algal cells from the gut (Fig. 1). During the exposure, *D. magna* (n = 15 individuals per tube) were placed into 15 mL tubes (in total there were four replicates for each group) containing a total volume of 5 mL tap water and the following exposure concentrations: 0 mg L^{-1} (control group), 16 mg L^{-1} (for 53 and 62 nm sized nanoparticles), and 224 mg L^{-1} (for 200 nm sized nanoparticles) of PS nanoparticles. Different concentrations were chosen due to the equivalent surface area for the different sizes of PS nanoparticles. Individuals were allowed to filter the water containing nanoparticles or water alone for 4 h. During the incubation, immobilized *D. magna* were removed. All *D. magna* individuals were removed from the tubes after the incubation period. The nanoparticle–protein complexes were recovered by centrifugation in Eppendorf tubes at 18 000*g* and 4 °C for 30 min with 1 mL total volume. After each centrifugation, 900 μL of supernatant was removed gently in order not to disturb the pellet. More exposure media, 900 μL was added to the same tube and centrifuged again. The procedure was

repeated until all the 5 mL of the sample had been centrifuged in the same tube.

Digestion of protein samples

Proteins were digested in solution as follow: the pH of the samples was adjusted to 7.8 by adding ammonium bicarbonate (ABC) to a final concentration of 50 mM. The proteins were reduced by the addition of DL-dithiothreitol (DTT, Sigma-Aldrich) in 50 mM ABC to a final concentration of 5 mM and incubated at 37 °C for 30 min, followed by alkylation using iodoacetamide (IAA, Sigma-Aldrich) with a final concentration of 12 mM and incubation in the dark for 20 min. Finally sequencing-grade modified trypsin (Promega, Madison, WI, USA) was added to a final concentration of 2 ng μL^{-1} and the samples were digested overnight at 37 °C. The next day formic acid (FA) was added to a final concentration of 0.5%. The samples were centrifuged at 15 kRCF for 10 min before the peptide solutions were extracted and transferred into new tubes. The peptides were cleaned up by C18 reversed-phase micro columns using a 2% ACN, 0.1% FA equilibration buffer and an 80% ACN, 0.1% FA elution buffer. The collected samples were dried in a fume hood and resuspended in 15 μL 2% ACN, 0.1% FA.

Proteins were also in gel digested as follow: from each experimental group (treatments and control), samples were prepared by adding 20 μl of SDS-PAGE loading buffer to the particle pellets or control tubes and 10 μL was loaded on a 4 to 12% premade SDS-PAGE (Bio-Rad). SDS has been shown to effectively desorb proteins from nanoparticle surfaces.[36] Protein bands were visualised, using Pierce™ Silver Stain Kit (Thermo Scientific) according to the manufacturer's protocol, then immediately cut into 1 × 1 mm gel pieces and destained. The gel pieces were washed twice with 50% acetonitrile (ACN, Sigma-Aldrich)/50 mM ABC and incubated for 30 min each time. After washing, the gel pieces were dehydrated using 100% ACN before the proteins were reduced with 25 μL 10 mM DTT in 50 mM ABC for 30 min at 37 °C. The DTT was removed, and the gel pieces were dehydrated using 100% ACN before the proteins were alkylated with 25 μL 55 mM iodacetamide in 50 mM ABC for 30 min in the dark at room temperature. The gel pieces were dehydrated one last time with 100% ACN before the proteins were digested by adding 25 μL 12 ng μL^{-1} trypsin (sequence grade modified trypsin porcine, Promega, Fitchburg, WI, USA) in 50 mM ABC and incubated on ice for 4 hours before 20 μL 50 mM ABC were added, and the protein was incubated overnight at 37 °C. The following day 10% (FA) was added to a final concentration of 0.5%, to get a pH of 2–3 to stop the digestion, before the peptide solutions were extracted and transferred into new tubes.

Peptide separation and mass spectrometry

Peptides were subjected to a reversed phase nano-LC source (Proxeon Biosystems, Odense, Denmark) coupled to an LTQ-Orbitrap Velos Pro mass spectrometer equipped with a nano Easy spray ion source (Thermo Fisher Scientific, Stockholm, Sweden). The chromatographic separation was performed on a 2 cm C18 Acclaim PepMap precolumn (75 mm i.d.) and a 15 cm C18 EASY-Spray LC capillary separation column (75 mm i.d., packed with 3 μm resin, column temperature 45 °C) from Thermo Fisher. The gradient was created by solvent A (1% ACN, 0.1% FA in water) and solvent B (100% ACN, 0.1% FA). A flow rate of 300 nL min^{-1} was used throughout the whole gradient, (0–30% B for 40 minutes, 30–50% 20 minutes, 50–95% for 10 minutes and 95% for 10 minutes). One full MS scan (resolution 60 000 at 400 m/z; mass range 400–1400 m/z) was followed by MS/MS scans of the 4 most abundant ion signals. Charge state screening was enabled where singly charged and unassigned ions were rejected. The precursor ions were isolated with 3 m/z isolation width and fragmented using collision induced dissociation (CID) at a normalized collision energy of 35. The dynamic exclusion window was limited to 500 and set to 30 s. The intensity threshold for precursor ions was set to 2500. The automatic gain control was set to 1×10^6 for both MS and MS/MS with ion accumulation times 100 ms.

Data analysis and protein identification

Raw files were converted to mgf-format by Mascot Distiller (version 2.6, Matrix Science) and identification of proteins were carried out with the Mascot Daemon software (version 2.4, Matrix Science). The following search settings were used: trypsin as protease, one allowed missed cleavage site, 5 ppm MS accuracy for peptides and 0.015 Da MS/MS accuracy, variable modifications: oxidation (M) and carbamidomethylation (C). The files were searched against an in-house created database containing all *Daphnia* protein sequences. To be considered a true protein identification all individual ion scores must have a higher score than the score given when using a significant threshold of $p < 0.005$. The mass spectrometry proteomics data have been deposited to the ProteomeXchange Consortium *via* the PRIDE[1] partner repository with the dataset identifier PXD033695. The isoelectric point was calculated using the site **https://web.expasy.org/compute_pi**.

Determination of total triglyceride concentration

In order to obtain a detectible level of total triglycerides, 3 replicates representing each treatment were pooled together and freeze dried. Analysis of total triglyceride concentration of each fraction was performed according to the manufacturer's instructions (Sigma-Aldrich, USA). Absorbance intensity was recorded at 540 nm using a ProbeDrum spectrophotometer (Probation Labs, Sweden).

Statistical analysis

Data were analysed using Student's t-test. All analysis was performed using the statistical computing software GraphPad Prism version 8.0.0 (224) for Windows (GraphPad Software, Inc., **https://www.graphpad.com**).

Results and discussion

The size of PS nanoparticles was determined by DLS before and after incubation with *D. magna*, Table S1.† There was a large increase of the size for the smaller particles after filtration by *D. magna* indicating that the particles aggregated.

In the present study, we incubated *D. magna* individuals with model PS nanoparticles for 4 h to identify which proteins were bound to the nanoparticles during filtration. The experimental outline is shown in Fig. 1. The nanoparticle concentrations were optimised to allow for proteins on the nanoparticles to be identified, maintaining similar surface areas among the different nanoparticle sizes. At these concentrations the 53 nm PS-NH_2 are acutely toxic to *D. magna*. Therefore, immobilized *D. magna* individuals were regularly observed and immediately removed. No death was, as expected, observed in the other nanoparticle treatments during the incubation time. After completed incubation, all zooplankters were removed in all experimental groups. DLS measurements showed that after 4 h of incubation with *D. magna*, the size of 53 nm PS-NH_2 nanoparticles increased 6.2 times, whereas 62 nm PS-COOH nanoparticles increased 1.5 times.

The first set of experiments compared which proteins bound to the acutely toxic 53 nm PS-NH_2 and the non-toxic 200 nm PS-NH_2. After the incubation with *D. magna* the protein–nanoparticles complexes were collected by centrifugation. The proteins were desorbed from the particles with SDS and separated using gel electrophoresis (Fig. 2). There is a considerable variation in the amount of proteins, but the pattern of proteins is the same. It appeared that a larger number of proteins were bound to 53 nm PS-NH_2 (Fig. 2A) compared to 200 nm PS-NH_2 (Fig. 2B). Interestingly,

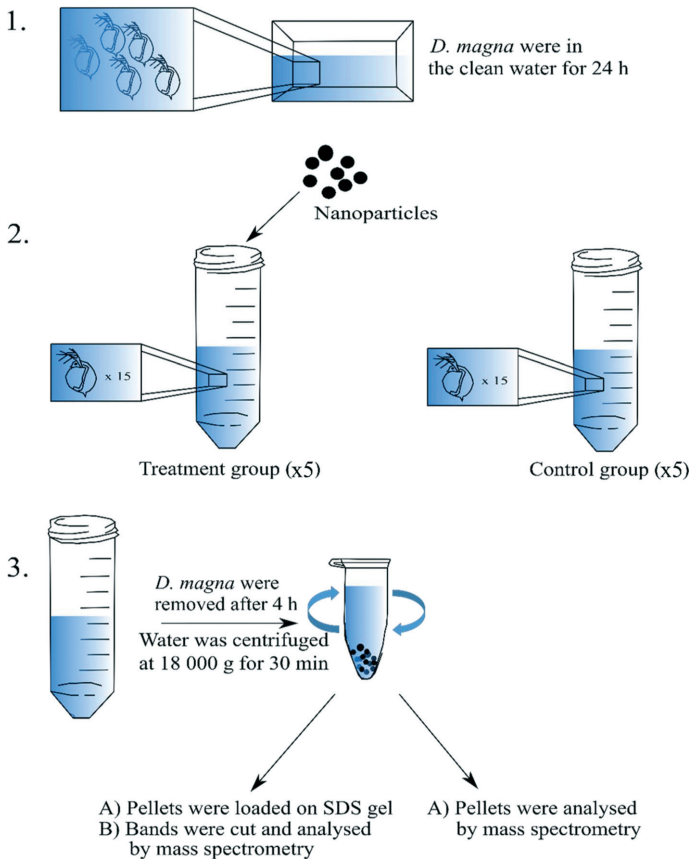

Fig. 1 Schematic illustration of the incubation experiment. Firstly (1), *D. magna* individuals were kept in the clean water for 24 h to remove the remaining algal cells from the gut. Then (2), 15 individuals were placed into 15 mL Falcon Tubes and left to filtrate the water for 4 h. Finally (3), the nanoparticle–protein complexes were recovered by centrifugation. In total there were five replicates (5 mL of total volume) for each treatment.

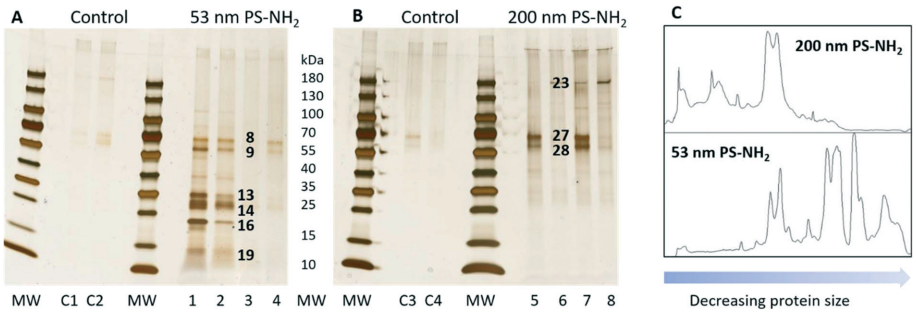

Fig. 2 Silver-stained SDS gels after 53 nm (A) and 200 nm (B) PS-NH_2 incubation with *D. magna* in comparison with a control group. Lane C1–C4, 1 to 4, and 5 to 8, represent four replicates for control, 53 nm PS-NH_2, and 200 nm PS-NH_2. The identity of proteins in bands marked with black numbers are listed in Table 1. The visualization of the size differences in proteins found in both gels (C).

the molecular sizes of the proteins appeared to be smaller for 53 nm PS-NH_2 compared to 200 nm PS-NH_2. A density scan of the gels further visualized these size differences, see Fig. 2C.

The visible protein bands were labelled with numbers (Fig. S1†), cut out from the gels and the proteins were identified using mass spectrometry. Only proteins that were identified based on at least two peptides with a significance threshold $p < 0.0005$ for the individual ion score were reported as true protein identifications. Under these conditions a total of 41 proteins were identified from 24 bands (Table S2†). The proteins were unequally distributed on the particles as 53 nm PS-NH_2 nanoparticles bound more proteins compared with 200 nm PS-NH_2 (27 *vs.* 6 proteins, respectively), confirming the conclusion from the visual observation. Only four proteins were bound to both types of nanoparticles (Fig. 3).

The silver staining of SDS-PAGE is a semi-quantitative method. Therefore, it is reasonable to assume that the most abundant proteins on the particles are represented in the most intensely stained protein bands in Fig. 2A and B. The identity of the proteins is presented in Table 1. The analysis of the most abundant proteins shows that the 53 nm and 200 nm PS-NH_2 bind distinctly different proteins. The 53 nm PS-NH_2 appears to bind two groups of proteins. One that can be related to the digestive system[37] as carboxypeptidase B, serine protease and chymotrypsin elastase family member 2A are among the most abundant proteins. The second group of proteins can be related to the epithelium, and intracellular structures and processes, for example, beta-klotho, actin, tubulin, elongation factors and histones. Klotho protein, which is a membrane-bound protein, plays an important role for a proper function of many organs.[38–40] It has previously been shown that disturbances of the *klotho* gene expression in mice might interfere with the lifespan or fertility.[38]

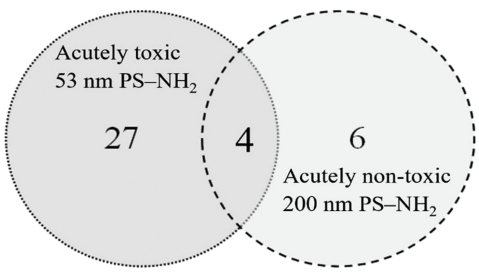

Fig. 3 Venn diagram compares the number proteins identified on 53 and 200 nm PS-NH_2 after identification using mass spectrometry after passing through the digestive system of *D. magna*.

Likewise, some proteins were uniquely bound to 200 nm PS-NH_2 nanoparticles. The most prominent are the following ones, vitellogenin-1, hemocyte protein-glutamine gamma-glutamyltransferase, and putative hemocyte protein-glutamine gamma-glutamyltransferase. Vitellogenin-1, is a precursor to egg yolk, plays a critical role in oogenesis,[41] and is especially highly expressed in female fish.[42] Interestingly, only 4 proteins, actin, chymotrypsin elastase family member 2A, elongation factor 1-alpha and histone H4 bound to both 53 nm and 200 nm PS-NH_2.

The protein corona has previously been determined on aminated PS particles in condition water, *i.e.*, water that has been filtered by *D. magna* excreting proteins and other biomolecules before the *D. magna* are removed and the particles added.[34] Some proteins found after filtration are also found on particles in conditioned water which is not surprising as the filtrated particles are exposed to both the environment in the intestine and the surrounding water.

To explain the striking difference in the number and identity of proteins bound to 53 nm and 200 nm PS-NH_2 we calculated the isoelectric point (pI) for each of the proteins (Tables 1 and S2†). The pI of proteins bound to 53 nm PS-NH_2 was, with a few exceptions, below 6, whereas, surprisingly, the pI of proteins bound to 200 nm PS-NH_2 was in general above 6 (Fig. S2†). This means that, in the media,

Table 1 Proteins were identified in the major bands based on the silver-stained gels. MW denotes molecular weight, pI denotes isoelectric point, and "NA" in pI denotes that pI was not available as the sequence contains several consecutive undefined amino acids

Treatment	Band	MW (kDa)	Protein name	Accession number	MW (kDa)	pI
53 nm PS-NH_2	8	70	Actin, alpha skeletal muscle (fragment)	A0A0N7ZDU7	35	5.4
			Tubulin beta chain	A0A0N7ZH16	52	4.75
			Tubulin alpha chain	A0A0P5ZYN7	50	4.94
			Fructose-bisphosphate aldolase	A0A0N8DTE5	39	8.30
			Heat shock 70 kDa protein cognate	A0A0P6DCT5	70	5.37
			ATP synthase subunit beta	A0A0P6CBB6	56	5.19
			Eukaryotic initiation factor 4A-II	A0A0P6CFN1	46	5.32
	9	60	Beta-klotho	A0A0N7ZV82	48	NA
	13	35	Carboxypeptidase B	A0A0N8AEM3		5.1
			Putative carboxypeptidase	A0A0N7ZFK6	31	6.2
				A0A0N7ZNY1	28	4.7
				A0A0N8A474	34	4.5
			Zinc carboxypeptidase	A0A0N8B2M1	45	6.5
			Poly(U)-specific endoribonuclease	A0A0N8AU82	41	4.5
			Serine protease	A0A0N7ZYN7	32	4.9
			Serine protease (fragment)	A0A0N7ZFA7	27	4.3
			Putative serine protease (fragment)	A0A0N8C2S1	17	4.5
			Trypsin serine protease	A0A0N8AZL9	32	4.8
	14	30	Serine protease	A0A0N7ZYN7	32	4.9
			Serine protease (fragment)	A0A0N7ZFA7	27	4.3
	16	22	Chymotrypsin elastase family member 2A	A0A0N7ZRR8	20	4.6
	19	15	Uncharcterized protein	A0A0N8AVI2	40	5.3
			C-type lectin domain family 6 member A	A0A0N7ZMI0	17	4.9
			Heat shock 70 kDa protein	A0A0N8AGX4	67	5.3
				A0A0P6A337	72	5.1
			Chymotrypsin elastase family member 2A	A0A0N7ZRR8	20	4.6
			Tubulin beta-4B chain	A0A0N8ERR7	34	4.8
			Tubulin beta chain	A0A0P6A486_9CRUS	57	NA
			Elongation factor 1-alpha	A0A0N7ZYV1	50	9.0
			ADP-ribosylation factor (fragment)	A0A0N8BN21	19	6.4
			Niemann-pick type C-2d	A0A0N7ZXW1	18	4.4
			Actin, alpha skeletal muscle (fragment)	A0A0N7ZDU7	35	5.7
			ATP synthase subunit beta	A0A0N7ZMA0	57	5.1
			Histone H4	A0A0N8AML8	11	11.3
200 nm PS-NH_2	23	190	Vitellogenin-1	A0A0N8ERH4	171	9.0
	27	70	Putative hemocyte protein-glutamine	A0A0N8AYD5	68	6.6
			gamma-glutamyltransferase	A0A0P5BFI8	58	5.9
	28	60	Hemocyte protein-glutamine	A0A0N7ZEH2	105	7.9
			gamma-glutamyltransferase	A0A0P4ZFG8	89	NA
			Lamin-A	A0A0P6IZ96	53	NA

the proteins bound to 53 nm PS-NH_2 generally had a negative net charge, whereas the proteins bound to 200 nm PS-NH_2 had a positive net charge. Although charge attractions can explain why proteins with a net negative charge bind to 53 nm PS-NH_2 it cannot explain why positively charged proteins, for example vitellogenin-1, with a pI of 9 and, therefore, a positive net charge in the media, bind to the 200 nm PS-NH_2. However, measuring the Z-potential of the two particles in tap water revealed that 53 nm PS-NH_2 had, as expected, a net positive charge (+30 mV), but the *z*-potential for 200 nm PS-NH_2, unexpectedly, was found to be negative (−28 mV). To further characterize the surface charge, the particle size and z-potential of four PS-NH_2 particles, including the 200 nm PS-NH_2, were measured at different pH 10.6, 8.7, 3.5, and 2.0 (Table 2). The rationale behind the choice of pH is that the PS-NH_2 amine groups, added as the functionalization and sulphone groups left from the original particle can be titrated and thereby change the stability and surface charge of the particles. As seen in Table 2 the *z*-potential decrease at high pH for the two small PS-NH_2 and the 180 nm PS-NH_2, whereas for the 200 nm PS-NH_2 the *z*-potential is close to neutral at low pH probably as a result of deprotonation and protonation, respectively. The changes in *z*-potential were reflected in the stability of the dispersion especially for the 200 nm PS-NH_2 that aggregated at low pH. A possible explanation of the different behaviour of the 200 nm PS-NH_2 is that there is a lower number of amine groups on the surface of the 200 nm PS-NH_2. Therefore, the surface chemistry was further characterized by FTIR spectrometry (Fig. S3–S5†). The areas with wavenumber ~1570 cm^{-1}, which have been assigned to the stretching vibrations of –NH_2,[43] and wavenumber ~1005 cm^{-1} which have been assigned to stretching vibrations of C–N bonds,[44] are present in all spectra for all PS-NH_2 particles indicating that there are amine groups present although in different amounts. Furthermore, in the spectra for 180 nm PS-NH_2 there is a

Table 2 The size and z-potential of PS-NH_2 at different pH

Nominal sizes (nm)	Diameter (nm)/polydispersity (%)				z-Potential (mV) with standard deviation			
	pH 10.6	pH 8.7	pH 3.5	pH 2.0	pH 10.6	pH 8.7	pH 3.5	pH 2.0
50	60/23 304/19[a]	51/23	48/20	50/21	26 ± 1	28 ± 0.7	30 ± 0.8	32 ± 2
53	67/24	58/25	56/12	58/31	21 ± 0.4	27 ± 1	35 ± 0.9	34 ± 2
180	165/13	167/17	168/13	176/19	−37 ± 0.8	−31 ± 0.6	33 ± 0.7	25 ± 4
200	232/20	222/17	444/24	413/32	−23 ± 0.7	−29 ± 0.6	−10 ± 0.3	−2 ± 0.5

[a] In this condition the particle dispersion has two peaks.

broad signal between 1000 and 1300 cm^{-1}, indicating sulphone groups. These signals are less prominent in the other particles. Overall, the characterization shows that there are amine groups on all particles but the number and the ratio between amine and sulfone groups vary among the different particles.

Next, we wanted to expand the number of particles in the analyses with the non-toxic 62 nm and 200 nm PS-COOH, as

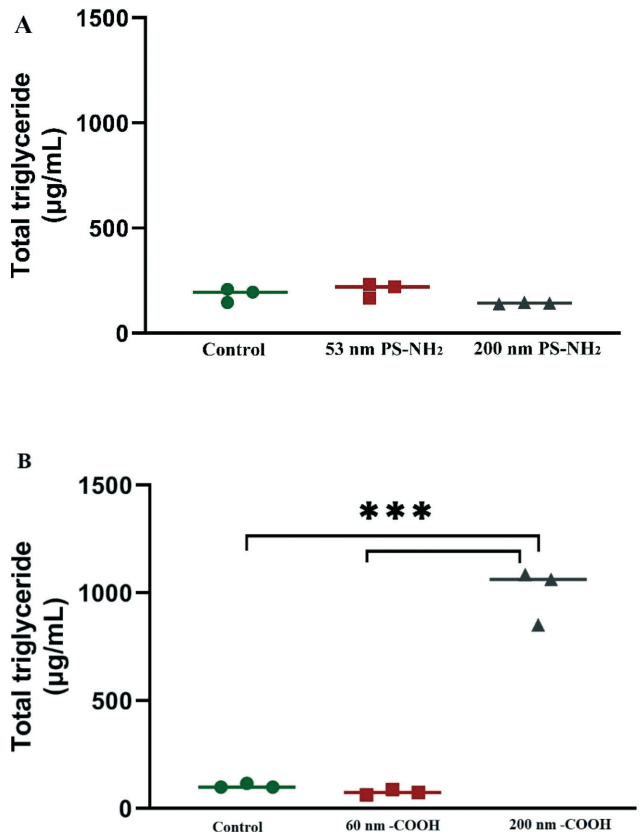

Fig. 4 Total triglyceride quantification on polystyrene (PS) nanoparticles after incubation with *D. magna* for 4 h. Comparison between PS-NH_2 (A) and PS-COOH (B) nanoparticles lipid corona. Samples were measured in triplicates and analysed by *t*-test. Horizontal lines show mean concentration calculated from the three data points. (***$p < 0.001$).

they have a different surface chemistry from aminated PS nanoparticles that could influence the protein binding. Despite several attempts we were not able to visualize any proteins using the above approach. This could be due to lower protein binding to the negatively charged particles or that less proteins could be desorbed from the particles. Therefore, we tried another approach in which the digestion of the proteins was made on the particles before identification with mass spectrometry. The identified proteins, using the same criteria for selection as above are reported in Table S3.† There were fewer proteins identified when the proteins were digested on the particles and only a few overlapping proteins between the different preparations of PS-NH_2 were observed (Tables S2 and S3†). This may be explained by that PS-NH_2 are able to strongly affect the structure of bound proteins[45] and thereby what parts of the proteins are accessible for the enzyme and what peptides will be released.

The main proteins found to be bound on the 200 nm PS-NH_2 are the same, *i.e.*, vitellogenin-1 and hemocyte protein-glutamine gamma-glutamyltransferase, regardless of the preparation method. Interestingly, these proteins are also among the main proteins identified on the 62 and 200 nm PS-COOH. Furthermore, vitellogenin and hemocyte protein-glutamine gamma-glutamyltransferase are also found on the pellets of 53 nm PS-NH_2. Vittelogenin-1 is one of the main proteins identified to bind to 25 nm gold particles filtered by *D. magna*,[33] indicating that this protein may in general bind to nanoparticles. Serine protease and actin were commonly bound to all nanoparticles when the proteins were digested in the pellet. Actin plays a major role in the structure and motility of cells in both muscle and non-muscle cells,[46] and changes in its expression can lead to toxicity.[47]

The bio-corona formed around PS nanoparticles can be composed of both proteins and lipids.[23] Therefore, we measured the total triglyceride concentration of each experimental fraction. Triglyceride concentration between 53 and 200 nm PS-NH_2 after incubation with *D. magna* was similar to the control group (Fig. 4A). However, triglyceride concentration in 200 nm PS-COOH nanoparticles after incubation with *D. magna* showed higher concentration compared to both control and 62 nm PS-COOH (Fig. 4B). Similarly, Lima *et al.*[23] showed that higher levels of total triglycerides were observed in lipid corona of 200 nm PS-COOH compared to smaller size particles (80 nm PS-COOH) after 1 h incubation in mouse serum.

Conclusions

There is a remarkable difference in proteins bound to PS nanoparticles that have shown to be toxic (53 nm PS-NH_2) and non-toxic (62 nm PS-COOH, 200 nm PS-COOH and 200 nm PS-NH_2) in acute toxicity tests. There is a size and charge difference as smaller acetic proteins bind to the toxic 53 nm PS-NH_2. The proteins which bind to acutely toxic 53 nm PS-NH_2 can be divided into two groups, the ones that are functionally related to the digestive system and the ones involved in various other functions. Furthermore, 53 nm PS-NH_2 bound the highest number of total and unique proteins compared to the other tested PS nanoparticles. There were several proteins, for example actin, carboxypeptidase B, chymotrypsin elastase family member 2A or beta-klotho, which were absent from the control group. It can be speculated that 53 nm PS-NH_2 toxicity could be due to the binding and depleting proteins that are important for the longevity of *D. magna* and/or damage the integrity of cells or tissues in the digestive system. On the other hand, non-toxic nanoparticles (200 nm PS-NH_2, 62 nm and 200 nm PS-COOH) appeared to bind to similar proteins. These proteins are mainly related to the epithelium and intracellular structures and processes. Even though the latter nanoparticles are shown to be non-toxic after acute exposure,[28] there were a couple of proteins (serine protease and vitellogenin-1), that bound to all nanoparticles, which partly could explain the toxicity of 62 nm PS-COOH after a long-term exposure.[47]

We found that neither 53 nm nor 200 nm PS-NH_2 bound to lipids, this could be due to the electrostatic repulsion between the positively charged parts of the lipid head and the positive group on the particle surface.[48] However, negatively charged 200 nm PS-COOH appeared to exhibit greater binding affinity compared to 62 nm PS-COOH. This suggests that the amount of lipids that binds to nanoparticles depends on the hydrophobicity of the nanoparticle surface, as well as nanoparticle size and/or curvature.[20]

The results presented in this study provide knowledge regarding what is happening after a short (4 h) incubation of PS nanoparticles together with *D. magna*. However, despite not being acutely toxic, 62 nm PS-COOH is shown to be toxic after long-term exposure.[47] We therefore conclude that including protein corona characterization at later time points in further studies can provide a better understanding regarding the toxicity of these, as well as other, nanoparticles.

In this study we have targeted the most abundant proteins on the PS particles after filtration as we believe these are the most relevant to explain the acute toxicity. Possible explanations for the toxicity are protein depletion and tissue rupture. Future experiments using the most abundant proteins, after cloning and expression, to cover the particle surface with a single protein could elucidate if the absorption of specific proteins affect the particle toxicity.

Author contributions

Egle Kelpsiene: investigation, methodology, writing – review & editing. Irene Brandts: investigation, methodology, writing – review & editing. Katja Bernfur: formal analysis, investigation, writing – review & editing. Mikael T. Ekvall: conceptualization, formal analysis, writing – review & editing. Martin Lundqvist: investigation, writing – review & editing. Mariana Teles: conceptualization, investigation,

methodology, writing – review & editing. Tommy Cedervall: conceptualization, funding acquisition, methodology, supervision, writing – original draft, writing – review & editing.

Conflicts of interest

There are no conflicts to declare.

Acknowledgements

Funding for the present study was provided by the Swedish Environmental Protection Agency and the MISTRA Environmental NanoSafety program.

References

1 P.-C. Lin, S. Lin, P. C. Wang and R. Sridhar, Techniques for physicochemical characterization of nanomaterials, *Biotechnol. Adv.*, 2014, **32**(4), 711–726.
2 K. McNamara and S. A. Tofail, Nanoparticles in biomedical applications, *Adv. Phys.: X*, 2017, **2**(1), 54–88.
3 R. Gupta and H. Xie, Nanoparticles in Daily Life: Applications, Toxicity and Regulations, *J. Environ. Pathol., Toxicol. Oncol.*, 2018, **37**(3), 209–230.
4 K. L. Aillon, Y. Xie, N. El-Gendy, C. J. Berkland and M. L. Forrest, Effects of nanomaterial physicochemical properties on in vivo toxicity, *Adv. Drug Delivery Rev.*, 2009, **61**(6), 457–466.
5 A. R. Petosa, D. P. Jaisi, I. R. Quevedo, M. Elimelech and N. Tufenkji, Aggregation and deposition of engineered nanomaterials in aquatic environments: role of physicochemical interactions, *Environ. Sci. Technol.*, 2010, **44**(17), 6532–6549.
6 M. Markiewicz, J. Kumirska, I. Lynch, M. Matzke, J. Koser and S. Bemowsky, *et al.*, Changing environments and biomolecule coronas: consequeences and challenges for the design of environmentally acceptable engineered nanoparticles, *Green Chem.*, 2018, **20**(18), 4133–4168.
7 F. Nasser, J. Constantinou and I. Lynch, Nanomaterials in the Environment Acquire an "Eco-Corona" Impacting their Toxicity to *Daphnia magna* - a Call for Updating Toxicity Testing Policies, *Proteomics*, 2020, **20**(9), e1800412.
8 M. P. Monopoli, C. Aberg, A. Salvati and K. A. Dawson, Biomolecular coronas provide the biological identity of nanosized materials, *Nat. Nanotechnol.*, 2012, **7**(12), 779–786.
9 A. E. Nel, L. Mädler, D. Velegol, T. Xia, E. M. Hoek and P. Somasundaran, *et al.*, Understanding biophysicochemical interactions at the nano-bio interface, *Nat. Mater.*, 2009, **8**(7), 543–557.
10 T. Cedervall, I. Lynch, S. Lindman, T. Berggård, E. Thulin and H. Nilsson, *et al.*, Understanding the nanoparticle–protein corona using methods to quantify exchange rates and affinities of proteins for nanoparticles, *Proc. Natl. Acad. Sci. U. S. A.*, 2007, **104**(7), 2050–2055.
11 I. Lynch and K. A. Dawson, Protein-nanoparticle interactions, *Nano Today*, 2008, **3**(1), 40–47.
12 M. Lundqvist, J. Stigler, G. Elia, I. Lynch, T. Cedervall and K. A. Dawson, Nanoparticle size and surface properties determine the protein corona with possible implications for biological impacts, *Proc. Natl. Acad. Sci. U. S. A.*, 2008, **105**(38), 14265–14270.
13 I. Lynch, K. A. Dawson, J. R. Lead and E. Valsami-Jones, Macromolecular coronas and their importance in nanotoxicology and nanoecotoxicology, *Frontiers of nanoscience*, Elsevier, 2014, vol. 7, pp. 127–156.
14 D. Dell'Orco, M. Lundqvist, C. Oslakovic, T. Cedervall and S. Linse, Modeling the time evolution of the nanoparticle-protein corona in a body fluid, *PLoS One*, 2010, **5**(6), e10949.
15 S. Tenzer, D. Docter, J. Kuharev, A. Musyanovych, V. Fetz and R. Hecht, *et al.*, Rapid formation of plasma protein corona critically affects nanoparticle pathophysiology, *Nat. Nanotechnol.*, 2013, **8**(10), 772–781.
16 S. Ritz, S. Schöttler, N. Kotman, G. Baier, A. Musyanovych, J. Kuharev, K. Landfester, H. Schild, O. Jahn, S. Tenzer and V. Mailänder, *et al.*, Protein corona of nanoparticles: distinct proteins regulate the cellular uptake, *Biomacromolecules*, 2015, **16**(4), 1311–1321.
17 J. A. Kim, A. Salvati, C. Åberg and K. A. Dawson, Suppression of nanoparticle cytotoxicity approaching in vivo serum concentrations: limitations of in vitro testing for nanosafety, *Nanoscale*, 2014, **6**(23), 14180–14184.
18 K. Saha, D. F. Moyano and V. M. Rotello, Protein coronas suppress the hemolytic activity of hydrophilic and hydrophobic nanoparticles, *Mater. Horiz.*, 2014, **1**(1), 102–105.
19 C. D. Walkey and W. C. Chan, Understanding and controlling the interaction of nanomaterials with proteins in a physiological environment, *Chem. Soc. Rev.*, 2012, **41**(7), 2780–2799.
20 E. Hellstrand, I. Lynch, A. Andersson, T. Drakenberg, B. Dahlbäck and K. A. Dawson, *et al.*, Complete high-density lipoproteins in nanoparticle corona, *FEBS J.*, 2009, **276**(12), 3372–3381.
21 C. C. Fleischer and C. K. Payne, Nanoparticle–cell interactions: molecular structure of the protein corona and cellular outcomes, *Acc. Chem. Res.*, 2014, **47**(8), 2651–2659.
22 S. Wan, P. M. Kelly, E. Mahon, H. Stockmann, P. M. Rudd and F. Caruso, *et al.*, The "sweet" side of the protein corona: effects of glycosylation on nanoparticle–cell interactions, *ACS Nano*, 2015, **9**(2), 2157–2166.
23 T. Lima, K. Bernfur, M. Vilanova and T. Cedervall, Understanding the lipid and protein corona formation on different sized polymeric nanoparticles, *Sci. Rep.*, 2020, **10**(1), 1–9.
24 T. Vandenbrouck, O. A. H. Jones, N. Dom, J. L. Griffin and W. De Coen, Mixtures of similarly acting compounds in *Daphnia magna*: From gene to metabolite and beyond, *Environ. Int.*, 2010, **36**(3), 254–268.
25 W. Geller and H. Müller, The filtration apparatus of Cladocera: filter mesh-sizes and their implications on food selectivity, *Oecologia*, 1981, **49**(3), 316–321.
26 P. Rosenkranz, Q. Chaudhry, V. Stone and T. F. Fernandes, A comparison of nanoparticle and fine particle uptake by *Daphnia magna*, *Environ. Toxicol. Chem.*, 2009, **28**(10), 2142–2149.

27 A. Sukhanova, S. Bozrova, P. Sokolov, M. Berestovoy, A. Karaulov and I. Nabiev, Dependence of Nanoparticle Toxicity on Their Physical and Chemical Properties, *Nanoscale Res. Lett.*, 2018, **13**(1), 44.
28 K. Mattsson, E. V. Johnson, A. Malmendal, S. Linse, L.-A. Hansson and T. Cedervall, Brain damage and behavioural disorders in fish induced by plastic nanoparticles delivered through the food chain, *Sci. Rep.*, 2017, **7**(1), 11452.
29 J. Saavedra, S. Stoll and V. I. Slaveykova, Influence of nanoplastic surface charge on eco-corona formation, aggregation and toxicity to freshwater zooplankton, *Environ. Pollut.*, 2019, **252**, 715–722.
30 A. Pochelon, S. Stoll and V. I. Slaveykova, Polystyrene Nanoplastic Behavior and Toxicity on Crustacean *Daphnia magna*: Media Composition, Size, and Surface Charge Effects, *Environments*, 2021, **8**(10), 101.
31 E. Besseling, B. Wang, M. Lurling and A. A. Koelmans, Nanoplastic Affects Growth of S. obliquus and Reproduction of *D. magna*, *Environ. Sci. Technol.*, 2014, **48**(20), 12336–12343.
32 F. Nasser and I. Lynch, Secreted protein eco-corona mediates uptake and impacts of polystyrene nanoparticles on *Daphnia magna*, *J. Proteomics*, 2016, **137**, 45–51.
33 K. Mattsson, R. Aguilar, O. Torstensson, D. Perry, K. Bernfur and S. Linse, *et al.*, Disaggregation of gold nanoparticles by *Daphnia magna*, *Nanotoxicology*, 2018, **12**(8), 885–900.
34 O. O. Fadare, B. Wan, K. Y. Liu, Y. Yang, L. X. Zhao and L. H. Guo, Eco-Corona vs Protein Corona: Effects of Humic Substances on Corona Formation and Nanoplastic Particle Toxicity in *Daphnia magna*, *Environ. Sci. Technol.*, 2020, **54**(13), 8001–8009.
35 L.-J. A. Ellis and I. Lynch, Mechanistic insights into toxicity pathways induced by nanomaterials in *Daphnia magna* from analysis of the composition of the acquired protein corona, *Environ. Sci.: Nano*, 2020, **7**(11), 3343–3359.
36 M. Lundqvist, T. Berggard, E. Hellstrand, I. Lynch, K. A. Dawson, S. Linse and T. Cedervall, Rapid and facile purification of apolipoprotein AI from human plasma using thermoresponsive nanoparticles, *J. Biomater. Nanobiotechnol.*, 2011, **2**(03), 258–266.
37 F. L. Carboxypeptidases, in *xPharm: The Comprehensive Pharmacology Reference*, ed. S. J. Enna and D. B. Bylund, Elsevier, New York, 2007, pp. 1–4.
38 M. Kuro-o, Y. Matsumura, H. Aizawa, H. Kawaguchi, T. Suga and T. Utsugi, *et al.*, Mutation of the mouse klotho gene leads to a syndrome resembling ageing, *Nature*, 1997, **390**(6655), 45–51.
39 S. A. Li, M. Watanabe, H. Yamada, A. Nagai, M. Kinuta and K. Takei, Immunohistochemical localization of Klotho protein in brain, kidney, and reproductive organs of mice, *Cell Struct. Funct.*, 2004, **29**(4), 91–99.
40 T. Shiraki-Iida, H. Aizawa, Y. Matsumura, S. Sekine, A. Iida and H. Anazawa, *et al.*, Structure of the mouse klotho gene and its two transcripts encoding membrane and secreted protein, *FEBS Lett.*, 1998, **424**(1–2), 6–10.
41 A. Hara, N. Hiramatsu and T. Fujita, Vitellogenesis and choriogenesis in fishes, *Fish. Sci.*, 2016, **82**(2), 187–202.
42 J. Gao, L. Lin, A. Wei and M. S. Sepúlveda, Protein corona analysis of silver nanoparticles exposed to fish plasma, *Environ. Sci. Technol. Lett.*, 2017, **4**(5), 174–179.
43 C. Ling, X. Y. Li, Z. Y. Zhang, F. Q. Liu, Y. Q. Deng and X. P. Zhang, *et al.*, High Adsorption of Sulfamethoxazole by an Amine-Modified Polystyrene-Divinylbenzene Resin and Its Mechanistic Insight, *Environ. Sci. Technol.*, 2016, **50**(18), 10015–10023.
44 A. Hernandez-Gordillo, S. Oros-Ruiz and R. Gomez, Preparation of efficient cadmium sulfide nanofibers for hydrogen production using ethylenediamine (NH2CH2CH2NH2) as template, *J. Colloid Interface Sci.*, 2015, **451**, 40–45.
45 R. Cukalevski, S. A. Ferreira, C. J. Dunning, T. Berggård and T. Cedervall, IgG and fibrinogen driven nanoparticle aggregation, *Nano Res.*, 2015, **8**(8), 2733–2743.
46 P. W. Gunning, U. Ghoshdastider, S. Whitaker, D. Popp and R. C. Robinson, The evolution of compositionally and functionally distinct actin filaments, *J. Cell Sci.*, 2015, **128**(11), 2009–2019.
47 E. Kelpsiene, O. Torstensson, M. T. Ekvall, L.-A. Hansson and T. Cedervall, Long-term exposure to nanoplastics reduces life-time in *Daphnia magna*, *Sci. Rep.*, 2020, **10**(1), 5979.
48 B. Munteanu, F. Harb, J. P. Rieu, Y. Berthier, B. Tinland and A. M. Trunfio-Sfarghiu, Charged particles interacting with a mixed supported lipid bilayer as a biomimetic pulmonary surfactant, *Eur. Phys. J. E: Soft Matter Biol. Phys.*, 2014, **37**(8), 72.

Supplementary Information

Protein binding on acutely toxic and non-toxic polystyrene nanoparticles during filtration by *Daphnia magna*

Egle Kelpsiene, [ab] Irene Brandts, [cd] Katja Bernfur, [a] Mikael T. Ekvall, [be] Martin Lundqvist,[ab] Mariana Teles, [cd] and Tommy Cedervall *[ab]

[a] Department of Biochemistry and Structural Biology, Lund University, Lund University, P.O. Box 124, SE-221 00 Lund, Sweden

[b] NanoLund, Lund University, Box 118, SE-221 00 Lund, Sweden

[c] Department of Cell Biology, Physiology and Immunology, Universitat Autònoma de Barcelona, 08193 Barcelona, Spain

[d] Institute of Biotechnology and Biomedicine, Universitat Autònoma de Barcelona, 08193 Barcelona, Spain

[e] Department of Aquatic Ecology Unit, Lund University, Lund, Sweden

*Corresponding author. e-mail: tommy.cedervall@biochemistry.lu.se

Supplementary Table 1. The size of PS particles before and after filtration by D. magna. All measurements are at least in triplicate.

Particle	**Before filtration**		**After filtration**	
	Diameter (nm)	Polydispersity (%)	Diameter (nm)	Polydispersity (%)

53 nm PS-NH_2	47 ± 1	10 ± 2	215 ± 12	multimodal
200 nm PS-NH_2	179 ±	1 ± 1	180 ± 2	6 ± 2
62 nm PS-COOH	61 ± 1	14 ± 2	95 ± 6	multimodal
200 nm PS-COOH	180 ± 4	8 ± 3	191 ± 6	7 ± 2

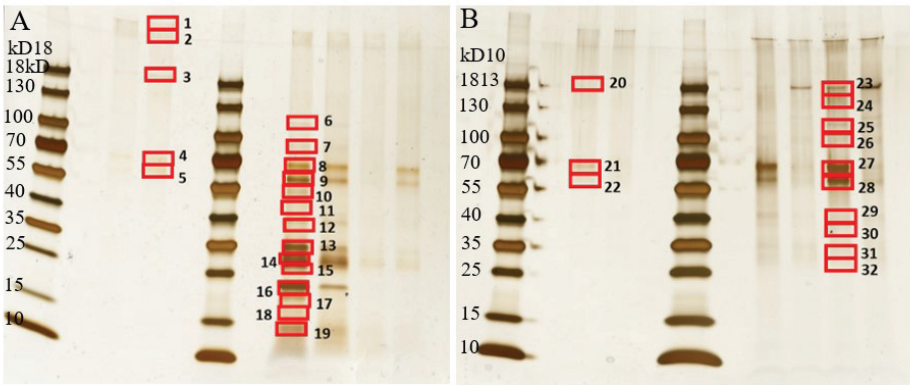

Supplementary Figure 1. SDS gels with silver staining. The numbers represent the bands used for mass spectrometry analyses for the different conditions. (A) Control group (1-5 bands) and 53 nm PS–NH_2 incubated with *D. magna* (6-19 bands). (B) Control group (20-22 bands) and 200 nm PS–NH_2 incubated with *D. magna* (23-32 bands).

Supplementary Table 2. All identified proteins with a score number of 50 or larger and at least two identified unique peptides. ("NA" – Pi was not available as the sequence contains several consecutive undefined amino acids).

Treatment	Band	MW	Protein name	Accession number	MW	pI
53 nm PS–NH_2	6	121	Protease m1 zinc metalloprotease	A0A0P5E8H8	109	4.59
				A0A0P6JK73	109	4.61
				A0A0N8AXC2	85	4.66
			Histone H4	A0A0N8AML8	11	11.33
	7	90	Neutral endopeptidase (Fragment)	A0A0N8A4R4	82	4.67
			Putative Neutral endopeptidase	A0A0P5QHD4	35	4.83
			Beta-galactosidase-1 protein 2	A0A0P4WLE9	63	4.53

			Protease m1 zinc metalloprotease	A0A0N8B8B4	89	4.58
			Lamin-A	A0A0P6IZ96	58	5.64
	8	70	Actin, alpha skeletal muscle	A0A0N8AKX4	41	5.49
				A0A0N7ZFH2	49	NA
			Tubulin beta chain	A0A0P6CCV0	49	4.78
				A0A0N7ZH16	52	4.75
			Tubulin alpha chain	A0A0P5ZYN7	50	4.94
			Fructose-bisphosphate aldolase	A0A0N8DTE5	39	8.30
			Heat shock 70 kDa protein cognate	A0A0P6DCT5	70	5.37
			Histone H2A (Fragment)	A0A0P6A1I4	14	11.23
			ATP synthase subunit beta	A0A0P6CBB6	56	5.19
			Eukaryotic initiation factor 4A-II	A0A0P6CFN1	46	5.32
			Histone H2B (Fragment)	A0A0P6A3S1	13	10.32
			Elongation factor 1-alpha	A0A0P5WWR3	50	9.10
			Armadillo segment polarity protein	A0A0P6IJT4	90	5.18
			ATP synthase subunit alpha (Fragment)	A0A0N8AAM5	51	NA
	9	55	Beta-klotho	A0A0N7ZV82	48	NA
			Glucosylceramidase	A0A0N8A576	61	4.66
			Adenosine deaminase CECR1-A	A0A0N7ZT57	53	4.75
			Alkaline phosphatase (Fragment)	A0A0N8B5J6	34	4.80
	10	55	Lamin-A	A0A0P6IZ96	58	5.64
	11	43	Actin, alpha skeletal muscle	A0A0N8AKX4	42	5.5
			Uncharacterized protein	A0A0N8E6U4	43	4.74
			Chymotrypsin elastase family member 2A	A0A0N7ZRR8	20	4.3
			Ubiquitin-40S ribosomal protein S27a	A0A0N7ZFP2	13	10.13
			Elongation factor 1-alpha	A0A0N7ZL24	49	8.81
			Calmodulin	A0A0P6C8L3	17	4.04
	12	38	Mannan endo-1	A0A0N8AWI2	49	5.7
			Putative Brain chitinase and chia	A0A0N8AJS7	31	4.4
	13	35	Carboxypeptidase B	A0A0P6GRN0	47	5.0
				A0A0N8A0G8	47	4.7
				A0A0N8DXD3	51	5.2
			Poly(U)-specific endoribonuclease	A0A0N8AU82	41	4.5
			Serine protease	A0A0N7ZYN7	32	4.9

			Zinc carboxypeptidase	A0A0N8ASM6	49	5.3
			Pancreatic triacylglycerol lipase	A0A0N8A9Z9	38	NA
			Uncharacterized protein	A0A0N7ZR74	50	4.56
	14	30	Serine protease	A0A0N7ZYN7	32	4.9
			Chymotrypsin elastase family member 2A	A0A0N7ZN74	33	5.4
			Neurexin IV	A0A0N8BJ04	32	4.2
	15	27	Chymotrypsin elastase family member 2A	A0A0N7ZN74	33	5.4
			Uncharacterized protein	A0A0N7ZEA0	20	4.53
			Metalloendopeptidase (Fragment)	A0A0N8BGG7	33	6.1
	16	22	Chymotrypsin elastase family member 2A	A0A0N7ZRR8	20	4.6
	17	19	Chymotrypsin elastase family member 2A	A0A0N7ZRR8	20	4.6
	19	15	Elongation factor 1-alpha	A0A0N7ZYV1	50	9.0
			Heat shock 70 kDa protein	A0A0N8AGX4	67	5.29
				A0A0N8CD53	71	5.14
			C-type lectin domain family 6 member A	A0A0N7ZMI0	17	4.9
			Actin, alpha skeletal muscle (Fragment)	A0A0P5ZI52	31	4.94
			Putative Chymotrypsin elastase family member 2A	A0A0N7ZSD8	28	NA
			Uncharacterized protein	A0A0N8AVI2	40	5.33
			ADP-ribosylation factor (Fragment)	A0A0N8BN21	19	6.4
			60S ribosomal protein L23 (Fragment)	A0A164I9D0	22	10.2
			Histone H4	A0A0N8AML8	11	11.3
			ATP synthase subunit beta	A0A0N7ZMA0	57	5.14
200 nm PS–NH_2	23	190	Vitellogenin-1	A0A0N8ERH4	171	9.0
	24	170	Vitellogenin-1	A0A0N8ERH4	171	9.0
			Actin, alpha skeletal muscle	A0A0N7ZDS7	37	5.7
	25	120	Hemocyte protein-glutamine gamma-glutamyltransferase	A0A0N8CBE8	105	7.9
				A0A0P5CTZ7	109	NA
				A0A0P5CW37	101	8.4
				A0A0N8AI27	105	8.2
			Putative Hemocyte protein-glutamine gamma-glutamyltransferase (Fragment)	A0A0P5MNQ2	45	5.90
			Histone H4	A0A0N8AML8	11	11.33
			Elongation factor 1-alpha	A0A0P5WWR3	50	9.10
			40S ribosomal protein S3	A0A0P6A3F6	27	9.68
			Actin, alpha skeletal muscle	A0A0N8AKX4	42	5.49

			40S ribosomal protein S1	A0A0P6CD52	18	10.99
			Putative Vitellogenin-1 (Fragment)	A0A0N8ABJ0	92	NA
			Eukaryotic initiation factor 4A-II	A0A0P6CFN1	46	5.32
			Elongation factor 1-gamma (Fragment)	A0A0P6CFP1	50	6.33
			60S ribosomal protein L8	A0A0P6CEH7	28	11.04
			40S ribosomal protein S14	A0A0N8B0M4	22	9.60
			Heat shock 70 kDa protein cognate	A0A0N7ZMQ1	71	5.25
				A0A0P6A337	72	5.10
			40S ribosomal protein S9	A0A0P6DE13	23	10.66
			40S ribosomal protein S25	A0A0P6CKS1	14	10.12
			40S ribosomal protein S26 (Fragment)	A0A0N8A385	18	10.80
	26	100	Hemocyte protein-glutamine gamma-glutamyltransferase	A0A0P5CTZ7	109	NA
				A0A0N8AI27	105	8.2
				A0A0P5C8I4	108	7.3
	27	70	Putative Hemocyte protein-glutamine gamma-glutamyltransferase	A0A0N8AYD5	68	6.6
			Double oxidase: two peroxidase domains	A0A0N8CQ82	131	NA
				A0A0N7ZFU0	54	9.2
	28	60	Hemocyte protein-glutamine gamma-glutamyltransferase	A0A0P5PVU7	93	NA
				A0A0N8AXK8	103	NA
				A0A0P5MNQ2	45	5.9
	29	45	Uncharacterized protein	A0A0N7ZTW3	59	5.98
	30	38	Uncharacterized protein	A0A0N7ZTW3	59	5.98
			Putative Hemocyte protein-glutamine gamma-glutamyltransferase	A0A0N8AYD5	68	6.6
	31	33	Hemocyte protein-glutamine gamma-glutamyltransferase	A0A0P5CTZ7	109	NA
				A0A0N8AI27	105	8.2
	32	30	Hemocyte protein-glutamine gamma-glutamyltransferase	A0A0P5CTZ7	109	NA
				A0A0N8AI27	105	8.2
			Chymotrypsin elastase family member 2A	A0A0N7ZRR8	20	4.6
Control	20	190	Vitellogenin-1	A0A0N8ERH4	171	9.0

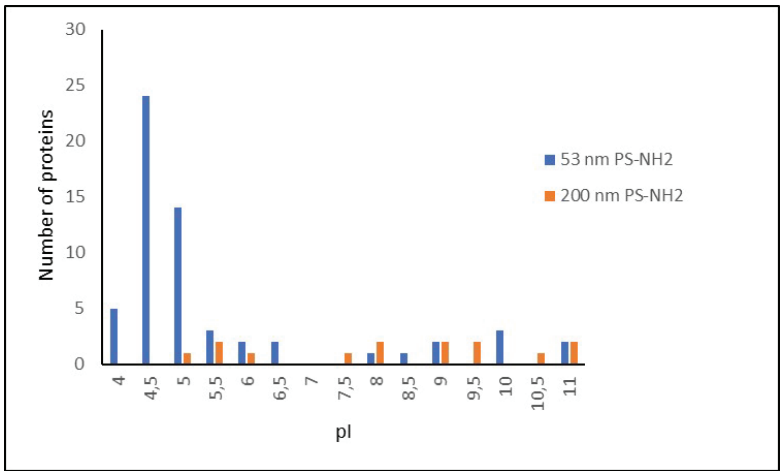

Supplementary Figure 2. The distribution pf proteins bound to 50 nm and 200 nm PS-NH_2. The proteins are grouped with pI between 4.0 to 4.5 and so on.

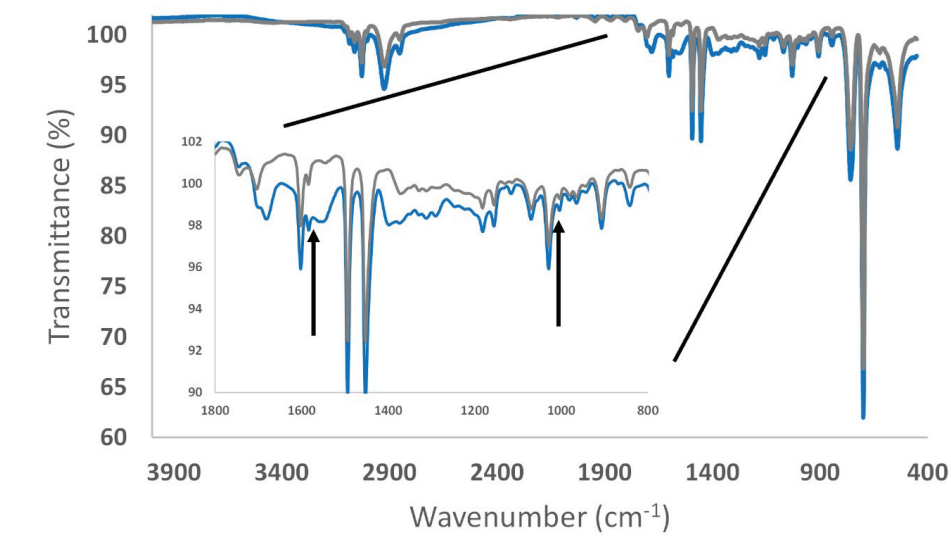

Supplementary Figure 3. Comparison between plain and amine polystyrene particles of the size ∽200 nm. ATR-FTIR spectrum for PS-NH2 200 nm in blue and PS 195 nm in gray. The inset is a zoom-in on the area of wavenumber 800 -1800 cm^{-1}. The two arrows point at signals at wavenumber ∽1570 cm^{-1} which have been assigned to the stretching vibrations of -NH_2 (Ref: 10.1021/acs.est.6b02846) and wavenumber ∽1005 cm^{-1} which have been assigned to stretching vibrations of C-N bonds (ref:10.1016/j.jcis.2015.03.052).

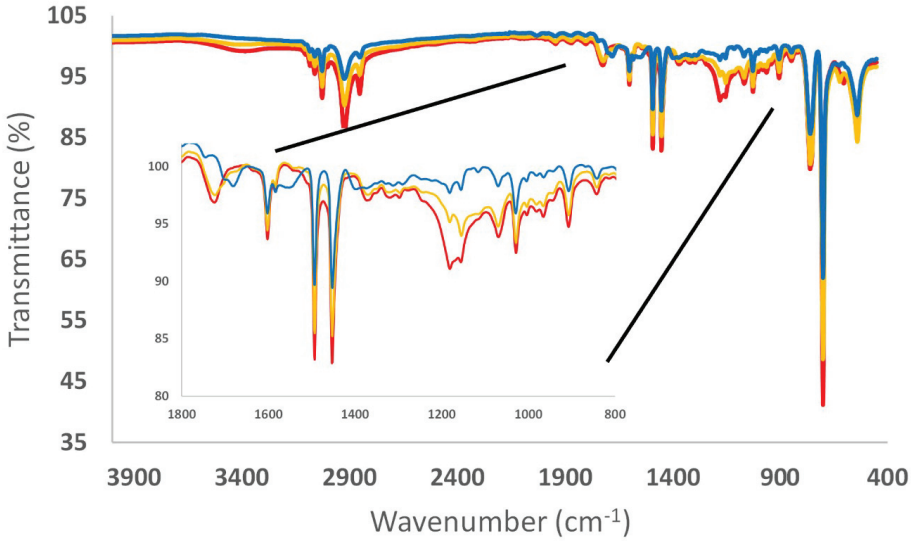

Supplementary Figure 4. Comparison between amine polystyrene particles of the size 50, 52, and 200 nm. ATR-FTIR spectrum for PS-NH2 200 nm in blue, PS-NH2 50 nm in red, and PS-NH2 52 nm in orange. The inset is a zoom-in on the area of wavenumber 800 - 1800 cm^{-1}.

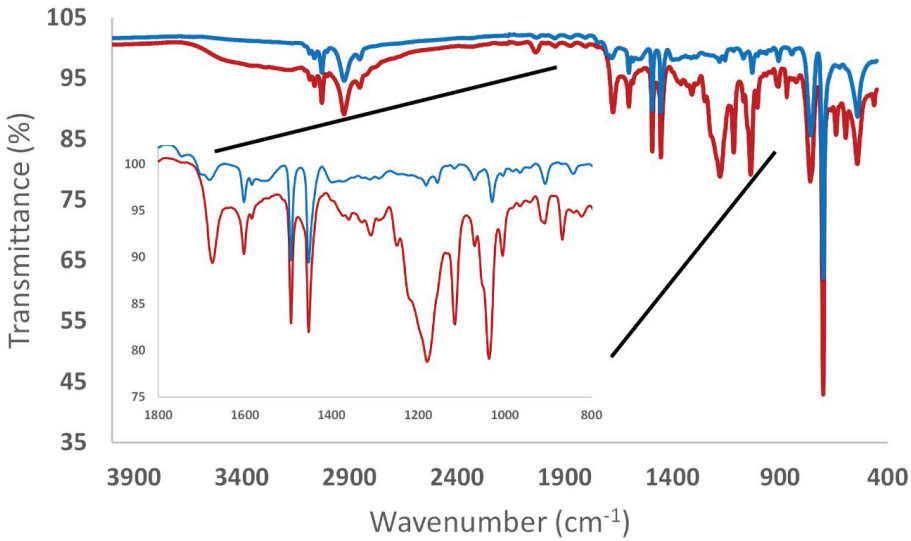

Supplementary Figure 5. Comparison between amine polystyrene particles of the size 180 and 200 nm. ATR-FTIR spectrum for PS-NH2 200 nm in blue and PS-NH2 180 nm in dark red. The inset is a zoom-in on the area of wavenumber 800 -1800 cm^{-1}.

Supplementary Table 3. Proteins were identified in the content of the pellets after nanoparticles were filtrated by the digestive system of *D. magna* for 4 h in comparison with a control group. All proteins with a score number of 50 or larger and at least two identified unique peptides were taken into consideration.

Treatment	Accession	Score	Num. of significant sequences	emPAI	Description
53 nm PS-NH_2	A0A0N8ERH4	1371	33	1.74	Vitellogenin-1
	A0A0P5XJT6	227	5	1.56	Uncharacterized protein (Fragment)
	A0A164FM53	148	3	10.53	Uncharacterized protein (Fragment)
	A0A0P5UGM5	115	3	0.99	Uncharacterized protein (Fragment)
	A0A0N8B1S8	1006	16	1.23	Hemocyte protein-glutamine gamma-glutamyltransferase
	A0A0N8AYD5	555	9	0.86	Putative Hemocyte protein-glutamine gamma-glutamyltransferase
	A0A0P5E182	416	9	0.74	Hemocyte protein-glutamine gamma-glutamyltransferase
	A0A0N7ZTW3	470	9	0.91	Uncharacterized protein (Fragment)
	A0A0N7ZU01	372	5	0.74	Di-domain hemoglobin
	A0A0P4XQ89	336	4	0.56	Di-domain hemoglobin
	A0A0P5F3Z1	190	4	0.68	Di-domain hemoglobin
	A0A0P5D088	247	4	0.83	Chymotrypsin elastase family member 2A (Fragment)
	A0A0N8BSM2	211	2	0.3	Uncharacterized protein

	A0A0N8AW39	194	2	0.3	Uncharacterized protein
	A0A0P5EK64	164	2	0.28	Uncharacterized protein (Fragment)
	A0A0N7ZE53	182	2	0.18	Uncharacterized protein
	A0A0N8BCY1	177	2	0.23	Chymotrypsin BI
	A0A0P5CJN7	159	2	1.25	Mucin peritrophin
	A0A0N7ZDU7	155	4	0.61	Actin, alpha skeletal muscle (Fragment)
	A0A0N7ZYN7	149	3	0.48	Serine protease
	J9R260	134	3	0.61	Trypsin 152 (Fragment)
	A0A0N7ZFA7	131	3	0.59	Serine protease (Fragment)
	A0A0N7ZMQ5	134	2	0.33	Putative Serine protease P76 (Fragment)
	A0A0P5HL93	123	5	0.23	Uncharacterized protein
	A0A0N7ZUL9	118	2	0.23	Uncharacterized protein (Fragment)
	A0A0P4Z5S1	117	2	0.5	Putative Secreted ferritin g subunit
200 nm PS-NH_2	A0A0N8ERH4	591	19	0.64	Vitellogenin-1
	A0A0P6B5M1	551	12	0.33	Vitellogenin-1
	A0A0P6CX53	537	13	0.44	Vitellogenin-1
	A0A0N8A166	294	3	0.27	Vitellogenin-1-like protein
	A0A0P5D5M6	269	4	0.4	Vitellogenin-1-like protein
	A0A0N8B626	169	4	0.1	Vitellogenin-1
	A0A0P6HJB7	290	6	0.88	Actin, alpha skeletal muscle
	A0A0N8A3C7	268	6	0.82	Actin, alpha skeletal muscle
	A0A0N7ZEH2	194	3	0.13	Hemocyte protein-glutamine gamma-glutamyltransferase
	A0A0N7ZYN7	188	4	0.68	Serine protease
	A0A0N7ZSD8	162	3	0.56	Putative Chymotrypsin elastase family member 2A

	A0A0N7ZES6	154	2	0.38	Obstructor-A
	A0A0A7CK57	149	4	0.52	Arginine kinase
	A0A0N7ZEE0	113	2	0.33	Gly d 3
	A0A0N7ZUW0	111	3	0.03	Mucin 5AC, oligomeric mucus/gel-forming
	A0A0N8AJS9	108	2	0.08	Uncharacterized protein (Fragment)
62 nm PS-COOH	A0A0N8ERH4	1160	29	1.29	Vitellogenin-1
	A0A0N8ACD3	328	5	0.3	Hemocyte protein-glutamine gamma-glutamyltransferase
	A0A0P5CTZ7	137	3	0.13	Hemocyte protein-glutamine gamma-glutamyltransferase
	A0A0P5PVU7	130	4	0.21	Hemocyte protein-glutamine gamma-glutamyltransferase
	A0A0N7ZEH2	86	4	0.18	Hemocyte protein-glutamine gamma-glutamyltransferase
	A0A0N7ZUW0	309	7	0.06	Mucin 5AC, oligomeric mucus/gel-forming
	A0A0N8A626	285	8	0.79	Uncharacterized protein
	A0A0N7ZYN7	210	3	0.5	Serine protease
	A0A0P5LBK9	204	3	0.13	Uncharacterized protein
	A0A0N8AGI9	201	3	0.12	Tissue factor pathway inhibitor
	A0A0N8AJD1	131	3	0.14	Tissue factor pathway inhibitor
	A0A0N8A945	197	4	0.52	Actin, alpha skeletal muscle
	A0A0N7ZTW3	136	3	0.25	Uncharacterized protein (Fragment)
200 nm PS-COOH	A0A0N8ERH4	875	22	0.9	Vitellogenin-1
	A0A0P5UGM5	200	3	0.99	Uncharacterized protein (Fragment)
	A0A0P5M5E3	175	4	0.67	Vitellogenin-1-like protein (Fragment)

	A0A0P5XJT6	160	4	1.12	Uncharacterized protein (Fragment)
	A0A164FM53	149	3	5.26	Uncharacterized protein (Fragment)
	A0A164G126	138	3	5.26	Uncharacterized protein (Fragment)
	A0A0N8A945	220	5	0.64	Actin, alpha skeletal muscle
	A0A0N8AUD4	212	3	0.11	Tissue factor pathway inhibitor
	A0A0N8AGI9	161	3	0.11	Tissue factor pathway inhibitor
	A0A0N7ZYN7	180	4	0.68	Serine protease
	A0A0N7ZSD8	154	3	0.56	Putative Chymotrypsin elastase family member 2A
	A0A0N7ZTW3	141	2	0.15	Uncharacterized protein (Fragment)
	A0A0N7ZUW0	112	4	0.03	Mucin 5AC, oligomeric mucus/gel-forming
Control	A0A0N7ZYN7	242	4	0.68	Serine protease
	A0A0N7ZSD8	200	3	0.56	Putative Chymotrypsin elastase family member 2A
	A0A0P6H0J1	148	3	0.44	Uncharacterized protein (Fragment)
	A0A0P5CAU9	125	2	0.59	Uncharacterized protein (Fragment)
	A0A0N7ZE19	117	2	0.52	Uncharacterized protein (Fragment)
	A0A0N8BCY1	148	2	0.23	Chymotrypsin BI
	A0A0N8AZL9	130	2	0.3	Trypsin serine protease
	A0A0N7ZUL9	129	2	4.69	Uncharacterized protein (Fragment)
	A0A0P4WVW2	102	2	7.58	Uncharacterized protein
	A0A0N7ZMQ5	101	2	5.92	Putative Serine protease P76 (Fragment)

Paper IV

PLOS ONE

RESEARCH ARTICLE

Prolonged survival time of *Daphnia magna* exposed to polylactic acid breakdown nanoplastics

Egle Kelpsiene[1,2], Melinda Rydberg[1], Mikael T. Ekvall[2,3], Martin Lundqvist[1,2], Tommy Cedervall[1,2]*

1 Department of Biochemistry and Structural Biology, Lund University, Lund University, Lund, Sweden, **2** NanoLund, Lund University, Lund, Sweden, **3** Department of Biology, Ecology Building, Aquatic Ecology Unit, Lund University, Lund, Sweden

* tommy.cedervall@biochemistry.lu.se

Citation: Kelpsiene E, Rydberg M, Ekvall MT, Lundqvist M, Cedervall T (2023) Prolonged survival time of *Daphnia magna* exposed to polylactic acid breakdown nanoplastics. PLoS ONE 18(9): e0290748. https://doi.org/10.1371/journal.pone.0290748

Editor: Arumugam Sundaramanickam, Annamalai University, INDIA

Received: March 9, 2023

Accepted: August 14, 2023

Published: September 5, 2023

Data Availability Statement: All relevant data are within the paper and its Supporting Information files.

Funding: TC Swedish Environmental Protection Agency. The funders had no role in study design, data collection and analysis, decision to publish, or preparation of the manuscript.

Competing interests: The authors have declared that no competing interests exist

Abstract

Polylactic acid nanoparticles (PLA NPs) according to food and drug administration are biodegradable and biocompatible polymers that have received a lot of attention due to their natural degradation mechanism. Although there is already available information concerning the effects of PLA microplastic to aquatic organisms, the knowledge about PLA NPs is still vague. In the present study, we analyzed the chemical composition of engineered PLA NPs, daily used PLA items and their breakdown products. We show that PLA breakdown products are oxidized and may contain aldehydes and/or ketones. The breakdown produces nano-sized particles, nanoplastics, and possibly other small molecules as lactide or cyclic oligomers. Further, we show that all PLA breakdown nanoplastics extended the survival rate in *Daphnia magna* in an acute toxicity assay, however, only PLA plastic cup breakdown nanoplastics showed a significant difference compared to a control group.

Introduction

Plastics are polymers with multiple applications and have an important role in our daily life. It has been estimated that between 1950 and 2020, global plastic production increased from 1.5 million metric tons to 367 million metric tons per year [1]. The increased production of plastics results in a growing amount of plastic material misplaced in the environment. Approximately between 60 to almost 100 million tons are mismanaged and ∼90% of it ends up in waterways and potentially reaches the oceans [2]. Therefore, the effects of plastic pollution on the aquatic environment have attracted both societal and scientific concerns [3–5].

Micro- (< 5 mm) and nano-sized(< 1 μm or <100 nm) particles can be either produced intentionally or degrade to smaller fragments under natural [6–9] or laboratory conditions [10–15]. Regardless of the particle preparation or size, their waste and breakdown products will eventually reach the natural environment and become a potential threat to both aquatic fauna and flora [16–19].

Main advantages of plastics are that they are light in weight, inert, long lasting and are cheap to produce. However, their high molecular weight, complex three-dimensional structure

and hydrophobic nature prevent their degradation which can lead to accumulation of enormous quantities in the natural environment [20]. Taking this into account, biodegradable or biocompatible plastics, such as polylactic acid (PLA)-based polymers, may be good candidates to replace non-biodegradable plastics [21].

PLA is classified as an aliphatic polyester because of the ester bonds that connect the monomer units [22]. PLA has received a lot of attention in the biomedicine field [23–25] due to its natural degradation *in situ* through hydrolysis mechanism, where water molecules break the ester bonds which create a polymer backbone [22]. Degradation products are composed of lactic acid and its short oligomers. These products are identified and metabolized by the body itself, which gives PLA an intrinsic biocompatibility that dampens the attainment of critical immune responses [22]. It is worth mentioning that PLA can be combined with biodegradable and non-biodegradable polymers, such as polyethylene (PE), polypropylene (PP), chitosan, polystyrene (PS), polyethylene terephthalate (PET) or polycarbonates [26]. Moreover, the addition of carbon nanotubes, ceramic nanoparticles, natural fibers, or cellulose while making composite materials [27–29]. This suggests that tracers of other polymers can be found in the PLA breakdown products.

Nanoparticles behavior and toxicity mainly depends on its size, shape and, surface charge [30,31]. Typical unwanted effects are related to oxidative stress, apoptosis, cytokine activation, loss of mitochondrial and lysosomal stability, genotoxic effects or DNA damage [32]. PLA nanoparticles (NPs) can provide additional adverse effects through their degradation products. It has been shown that engineered PLA NPs with sizes of 63 nm and 66 nm can be generally tolerated by human lung epithelial A549 cells (HLE A549), with no cytotoxicity and no secretion of pro-inflammatory mediators [33]. However, PLA NPs of the same sizes induced changes to the proteome of HLE A549 cells [33]. Additionally, *in vitro* study showed that ∼75 nm PLA NPs exhibited higher toxicity in RAW 264.7 macrophage cell line in comparison to larger ∼160 nm PLA NPs [34]. Additionally, smaller-sized PLA NPs (∼75 nm) induced a higher dose-dependent reactive oxygen species (ROS) production compared to larger-size (∼160 nm) PLA NPs [34].

Zimmermann and co-authors [35] showed that reproduction output was reduced significantly in the freshwater filter feeder *Daphnia magna* after exposure to 40 μm PLA microplastics (MPs) at 500 mg/L compared to a control group. Additionally, mortality of *D. magna* increased after exposure to 40 μm PLA MPs in a concentration-dependent manner (from 10 mg/L to 500 mg/L) to 60%. Authors also showed that *D. magna* has significantly lower mean body length at 500 mg/L of 40 μm PLA MPs [35]. Furthermore, it has been observed that ultraviolet radiation degraded products of PLA MPs (∼11 μm) at 25 mg/L elevated ROS levels, mitochondrial damage and apoptosis in zebrafish larvae [36].

Manufactured plastic NPs have been shown to be different compared to breakdown nanoplastics [11]. Therefore, in the present study, we characterized the chemical composition of pure engineered PLA NPs, bulk material of different PLA items that are available in supermarkets and used in daily life and their breakdown products. Additionally, we elucidated the toxicity of both engineered PLA NPs and PLA breakdown particles by using the well-studied model organism *D. magna*.

Materials and methods

Preparation of PLA nanoplastics

Manufactured PLA NPs (250 nm) were purchased from CD Bioparticles (www.cd-bioparticles.com). Before the experiments, PLA NPs were diluted to 10 mg/L and dialyzed in a

Standard RC Tubing, Dialysis Membrane (MWCO: 3.5 kD) for 72 h at 4 ˚C in 10 L of MiliQ water. The water was changed after 4 h the first day and once a day on the following days.

Different types of PLA items, such as soup cup lids, 3D printer filaments, and plastic cups, were bought in supermarkets in Lund, Sweden. The PLA breakdown nanoplastics were prepared in the similar manner as published previously for PS and high-density polyethylene (HDPE) [10,11]. Briefly, 2 g of PLA product was cut into small pieces (ca. 1x1 cm) into a glass beaker. The beaker was then filled with 200 mL tap water and the blender was turned on at maximum speed for 2 minutes. A 50 mL syringe was used to remove 100 mL of the water, which was filtered through a 0.8 μm cellulose acetate syringe-filter (Whatman, GE) into a glass bottle storage container. If more particle solution was needed, the larger beaker was filled with another 100 mL tap water, and the blending process and filtering was repeated. The same exact breakdown procedure was repeated using MiliQ water, as it was used for nanoplastics characterization.

Characterization of PLA nanoplastics

The number concentration and size of both dialyzed and non-dialyzed PLA NPs, and PLA breakdown nanoplastics were analyzed by nanoparticle tracking analysis (NTA) NanoSight LM10 (Amesbury, UK) on the same day as particles were prepared (i.e., day 0) and 6 days after breakdown procedure to evaluate if any aggregation of particles occurred. Additionally, the size of PLA breakdown nanoplastics were measured in Mili-Q water on day 0 of the breakdown procedure by using dynamic light scattering (DLS) on a Zetasizer Nano S (Malvern instruments, Worcestershire, UK). The zeta potential using Zetasizer Ultra or Zetasizer Nano ZS (Malvern Instruments, Worcestershire, UK) was used to measure the stability of nanoplastics. Before the zeta potential measurements, PLA nanoplastics were concentrated using a VivaFlow (VIVAFLOW 50, Sartorius) to improve the data collection. Measurements were repeated three times and data is presented as an average value.

Fourier transformed infrared spectrometry (FTIR) was performed on a Spectrum Two (PerkinElmer) using the software PerkinElmer Spectrum IR version 10.7.2 in the spectra range of 4000–450 nm. The samples for the PLA bulk material were added directly on the crystal, whereas liquid samples (5 μL) added on the crystal were left to evaporate before measurements. The acquired spectra were compared to the spectra in the software library.

PLA NPs and PLA soup lid nanoplastics were additionally analyzed by transmission electron microscopy (TEM). Briefly, 2 μL of the sample was added to a pioloform-coated single slot grid (Ted Pella, Cu, Pelco Slot Grids, USA), and left to air dry overnight. The samples were then inserted into a JEOL JEM-1400 PLUS TEM operated at 100 kV (JEOL Ltd., Japan), where micrographs were obtained using TEM Centre for JEM1400 Plus software.

Study organism

The freshwater filter feeder *D. magna* was used in the present study as a model organism. The original culture originates from lake Bysjön (55˚ 40′ 31.3″ N, 13˚ 32′ 41.9″E) and has been kept under controlled laboratory conditions for several generations. The *D. magna* cultures were fed *ad libitum* 2–3 times a week with a culture of the green algae *Scenedesmus* sp. All cultures were maintained at 18˚C at 8:16 h light/dark photoperiod.

Acute toxicity tests

Before the toxicity test, PLA products were broken in the tap water which was first filtered through 0.2 μm syringe filter to remove any bacteria that might come with the tap water. First, we evaluated the effects of PLA broken down nanoplastics on *D. magna*. There were four

experimental groups: control group, soup lid nanoplastics, 3D printer filament nanoplastics, and plastic cup nanoplastics. The particle solution was aliquoted to 50 mL Falcon tubes with a total volume of 25 mL. One *D. magna* (2–3 days old) that came from the same culture was randomly distributed into each tube (in total 15 replicates per each treatment).

Secondly, we investigated the effects of engineered PLA NPs on *D. magna* individuals. One *D. magna* (2–3 days old) were randomly assigned to 50 mL Falcon tubes (in total 10 replicates for each treatment) with a total volume of 25 mL. *D. magna* were exposed to dialyzed PLA NPs (with different dilution factors, 1:1, 1:10, or 1:100), non-dialyzed PLA NPs (with different dilution factors, 1:1, 1:10, or 1:100) or water only (control). The highest concentration (1:1) for dialyzed or non-dialyzed PLA NPs was 10 mg/L. During all toxicity tests, individuals were checked once a day until all of them were immobilized, and during the exposure period *D. magna* were not fed.

Statistical analysis

Kaplan Meier survival curves analysis were performed using the statistical computing software GraphPad Prism version 9.3.1 (471) for Windows (GraphPad Software, Inc., ww.graphpad.com). The analysis performed were the Log Rank (Mantel-Cox) test and the Gehan-Breslow-Wilcoxon test.

Results and discussion

Characterization of PLA nanoplastics

NTA measurements showed that the mean size was ∼170 nm for all PLA breakdown nanoplastics, and ∼270 nm for PLA NPs (Fig 1A). To ensure that nanoplastics did not aggregate, NTA measurements were repeated 6 days after the breakdown procedure, showing that PLA nanoplastics´ dispersions were stable (Fig 1B). DLS measurements showed that sizes of PLA nanoplastics were between ∼130 and 170 nm (Fig 1C), with a low polydispersity for PLA nanoplastics and higher polydispersity for PLA NPs (Fig 1D). Zeta potential measurements showed that all PLA NPs and PLA breakdown nanoplastics had negative surface charge (-22.13, -9.59 and -14.94 for PLA soup lid breakdown nanoplastics, PLA plastic cup breakdown nanoplastics and PLA NPs, respectively). Interestingly, PLA 3D printer filament nanoplastics had both negative and positive surface charges (-44.41 and 42.67). Sizes of PLA NPs were additionally measured by NTA after dialysis to ensure that dialysis did not induce particle aggregation (S1 Fig in S1 File). PLA NPs and PLA soup lid nanoplastics were further analyzed by TEM, showing that PLA NPs were round-shaped single particles as well as mainly dendritic-shaped aggregates (Fig 2A and 2B), whereas PLA soup lid nanoplastics were irregular in both shapes and size (Fig 2C and 2D).

The chemical signature of the pure engineered 250 nm PLA NPs was determined by FTIR. Obtained spectra had peaks at ∼2930 cm^{-1} between ∼1750 cm^{-1} and 1090 cm^{-1}region (S2 Fig in S1 File). Similarly, peaks of PLA particles were observed at the same wavelengths in other studies [37–39], suggesting that our PLA NPs were pure and with no additives. The spectrum of PLA NPs was used as a reference spectrum to compare the spectra of different PLA products and chemical changes during the breakdown procedure.

The spectrum of bulk material of PLA plastic cup, PLA soup lid and PLA 3D printer filament showed a similarity of 92%, 90% and 86%, respectively, to spectrum obtained for pure engineered 250 nm PLA NPs (Fig 3). In addition, PLA products had peaks at ∼2930 cm^{-1} and between ∼1750 cm^{-1} and 1090 cm^{-1}region, and some less pronounced peaks around ∼750 cm^{-1} region compared to a spectrum obtained for PLA NPs (Fig 3).

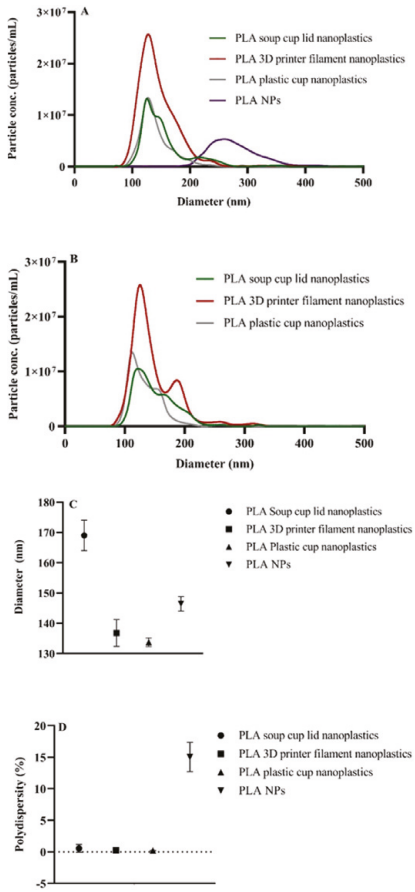

Fig 1. The distribution of PLA NPs and breakdown fractions determined by NTA (A-B) and DLS (C-D). Each sample is an average from five recordings. Measurements for NTA were performed the same day (day 0) of the breakdown procedure (A) and 6 days after the breakdown procedure (B). PLA NPs and breakdown products sizes (C) and polydispersity (D) were measured in triplicates by DLS on day 0.

https://doi.org/10.1371/journal.pone.0290748.g001

The spectrum obtained for PLA bulk materials have sharp peaks between ~1000 cm^{-1} and ~2000 cm^{-1} due to triple bonds (e.g., C≡C or C≡N), which within the breakdown procedure start to be less pronounced (Fig 4). Broad peaks between ~3500 and ~3000 cm^{-1} region and smaller peaks at ~1700 cm^{-1} for PLA breakdown nanoplastics might be due to of O–H or C = O stretching vibrations, of ethers or carbonates [10,40]. This implies that oxidation, as well as aldehydes and/or ketones were formed during the degradation of PLA products [41], additionally breakdown products include lactide or cyclic oligomer both by ester interchange and by chain homolysis route of PLA [41,42].

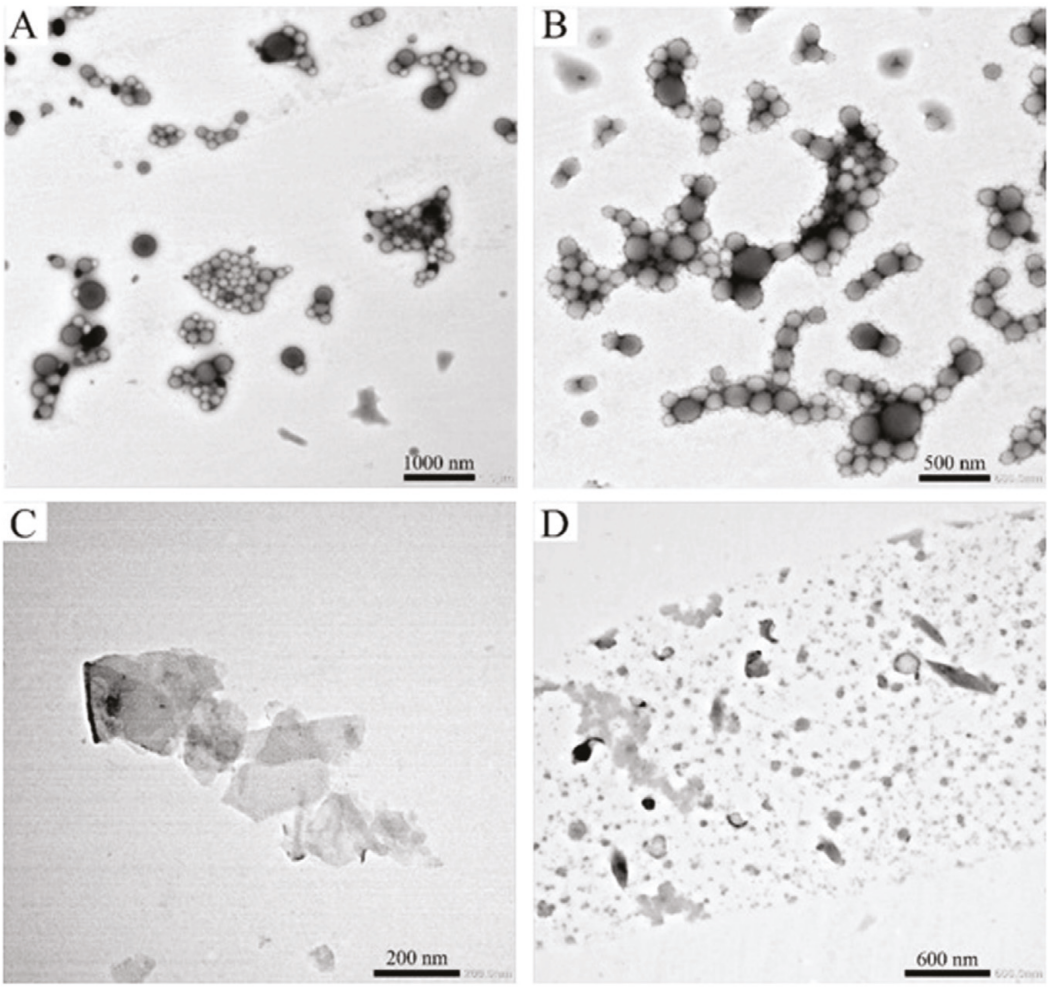

Fig 2. TEM images of PLA NPs (A-B) and PLA soup lid breakdown nanoplastics (C-D). TEM images showed that majority of the particles were around 100–150 nm.

https://doi.org/10.1371/journal.pone.0290748.g002

Acute toxicity tests

First, we investigated the effects of PLA breakdown nanoplastics on *D*. *magna*. The data the survival of *D*. *magna* was significantly extended after exposure to PLA plastic cup nanoplastics ($\chi^2_{(1)} = 4.93$, $p < 0.01$, Fig 5) in comparison with a control group, whereas other PLA breakdown nanoplastics did not have any significant effects towards *D*. *magna* survival.

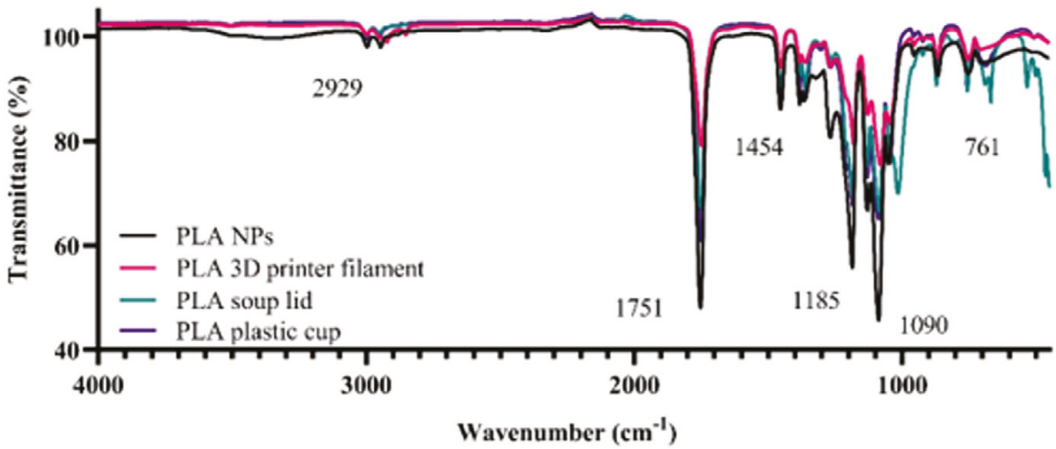

Fig 3. FTIR spectra of the different PLA bulk materials in comparison with engineered PLA NPs.

https://doi.org/10.1371/journal.pone.0290748.g003

Secondly, we wanted to investigate if engineered PLA NPs would have the same or similar effect as PLA breakdown products. Additionally, as previously, it has been highlighted by several authors the importance of washing nanoparticles to remove additives before performing toxicity studies [43,44], therefore here, we compared dialyzed versus non-dialyzed PLA NPs with different dilution factors (S3 Fig in S1 File). The data shows that PLA NPs did not extend or affect the survival for *D. magna* after exposure to 10 mg/L either dialyzed or non-dialyzed PLA NPs in comparison with control group ($\chi^2_{(1)} = 0.03$, $p > 0.99$, overall analysis for all treatments, Fig 6).

In the present study, we have observed that *D. magna* survival was significantly extended after exposure to PLA plastic cup breakdown nanoplastics. Even though other PLA breakdown nanoplastics used in the study did not have significant effects on *D. magna* survival, however there was a trend for prolonged survival after exposure to PLA soup lid nanoplastics and PLA 3D printer filament nanoplastics. Ekvall and co-authors [10] showed a similar tendency, as exposure of HDPE to *D. magna* prolonged the survival in a life-time (~ 100 days) experiment, after removal of small molecules, smaller than ~ 10 kDa. The extended survival for exposed individuals can be potentially explained by the growth of bacterial communities and interaction with breakdown nanoplastics. The fact that *Daphnia* individuals were not fed with algae during the exposure, suggest that bacteria might come from *Daphnia* itself. Cooper and Cressler [45] analyzed *D. magna* microbiota and found out that *Pedobacter*, *Flavobacterium*, *Polaromonas*, *Limnohabitans* and unclassified Burkholderiaceae were most abundant bacteria genera among other 18 genera present in *D. magna* samples. Similar results were obtained by other authors showing that *D. magna* microbiome was dominated by Proteobacteria and Bacteroidetes phylum [46–49]. A possible advantage from bacteria, for example *Pedobacter*, *Limnohabitans* or *Polaromons*, that they are able to provide amino acids and/or biosynthesize vitamins [45], which can serve fitness benefits to the host [50–52].

Bacterial communities can interact with NPs, including nanoplastics, and form a slimy and slippery layer called biofilm [53,54]. Biofilm is an aggregate of microorganisms living in a self-

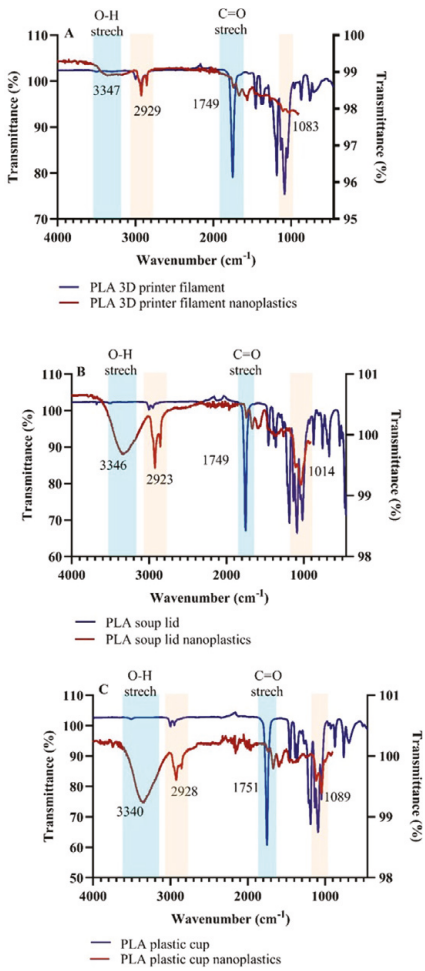

Fig 4. FTIR spectra of different PLA bulk material (blue line, left Y axis) and their breakdown products (red line, right Y axis). Light orange color indicates peaks that are indicated similarities between bulk material and its breakdown products, whereas light blue color indicates oxidation that occurred during the breakdown process in PLA nanoplastics.

https://doi.org/10.1371/journal.pone.0290748.g004

produced matrix of extracellular polymeric substances (EPS) which can adhere to both biotic or abiotic surfaces [54–56]. Additionally, plastics leach dissolved organic matter during plastic degradation [57,58]. This leachate coming from the plastic can provide energy for bacterial growth [59,60]. It has been shown that bacterial growth was 1.72 times higher with plastic leachate from plastic bags made of low-density PE due to the added carbon, which was more accessible than

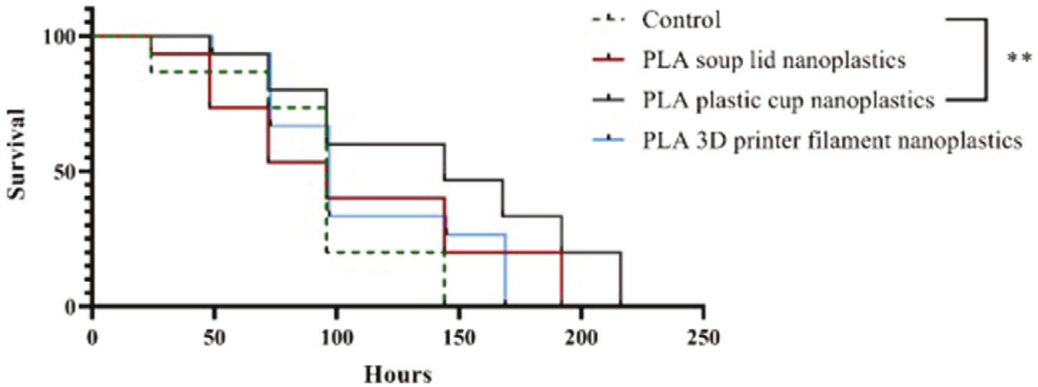

Fig 5. Survival of *Daphnia magna* exposed to different PLA breakdown nanoplastics. The curve of PLA 3D printer filament nanoplastics was nudged on Y axis by 1.00 data units for clearer vision. In total there were 15 replicates for each treatment. Asterisk indicates significant difference among the treatments estimated over the study period, $^{**}p<0.01$.

https://doi.org/10.1371/journal.pone.0290748.g005

natural organic matter [61]. The bacteria then can be fed by *D. magna* and used as nutrients [62], which can explain the prolonged survival observed in the present study. Biofilms on the aggregates can improve animal nutrition, especially when there is low food availability [63]. Amariei and co-authors [64] showed that *D. magna* decreased mortality after 14-day exposure to bio-fouled PE MPs with irregular shape and size ranging from 10 to 50 μm in contrast to pristine PE MPs. Biofilm consumption has been shown to increase the survival and growth rates for several cultivated organisms, such as tilapias *Orechromis niloticus*, whiteleg shrimp *Litopenaeus vannamei*, and fringe-lipped carp *Labeo fimbriatus* [65–67]. Microorganisms that are present in

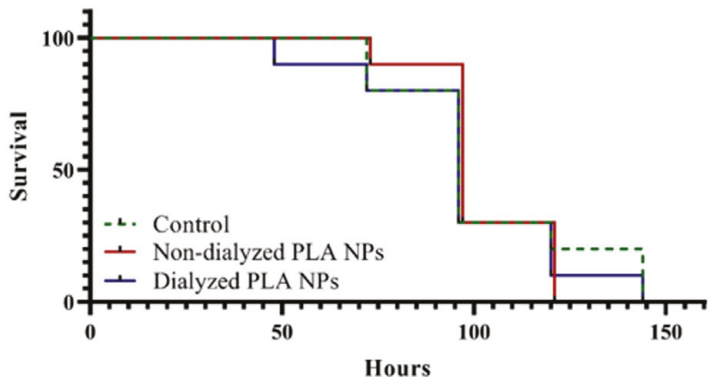

Fig 6. Survival of *Daphnia magna* exposed to dialyzed and non-dialyzed 250 nm PLA NPs. The curve of non-dialyzed PLA NPs was nudged on Y axis by 1.00 data units for clearer vision. There were 10 replicates for each treatment.

https://doi.org/10.1371/journal.pone.0290748.g006

the biofilm provide with essential nutrients such as polyunsaturated fatty acid, sterols, amino acids, vitamins and pigment that help to improve development of organisms [68]. Additionally, biofilms have been observed on surfaces of different type of plastics, such as PLA, PP, PE, polyvinyl chloride, HDPE, and low-density PE [69–71].

So far, micro- and nano-sized particles have been mainly studied in terms on their adverse effects to organisms due to the particle size and/or surface charge. However, the phenomenon observed in the present study, where daphnids extended the survival after exposure to different PLA breakdown nanoplastics, highlights the need to take a closer look at the microbial composition and nutrient quality of the biofilm and its interaction with nanomaterials by using different type of plastics. Further, considering that various plastic types might contain different additives, which can to some extent influence the bacterial composition, future studies should focus on analyzing biofilm bacterial composition and its interaction with both pure nanomaterials and their additives. Finally, studies should include longer incubation time and/or seasonal factors.

Supporting information

S1 File. S1 Fig. Sizes of PLA NPs were measured before and after dialysis by using NTA to ensure that particle aggregation did not occur during dialysis; S2 Fig. Spectra of engineered 250 nm PLA NPs obtained by FTIR; S3 Fig. Survival of *Daphnia magna* exposed to non-dialyzed (Fig A) dialyzed (Fig B) 250 nm PLA NPs with different dilution factors. The highest concentration (1:1) for both dialyzed and non-dialyzed PLA NPs was 10 mg/L. The experiment was performed at once, however for clearer vision survival curves for non-dialyzed and dialyzed in comparison with a control are shown separately. No statistically significances were observed among the treatments. In total there were 10 replicates for each treatment. Experiment was repeated 3 times.
(DOCX)

Acknowledgments

We would like to thank Dr. Ola Gustafsson at the Department of Biology, Lund University, for his help with TEM.

Author Contributions

Conceptualization: Tommy Cedervall.

Funding acquisition: Tommy Cedervall.

Investigation: Egle Kelpsiene, Melinda Rydberg, Mikael T. Ekvall, Martin Lundqvist.

Methodology: Egle Kelpsiene, Melinda Rydberg, Mikael T. Ekvall, Martin Lundqvist, Tommy Cedervall.

Supervision: Tommy Cedervall.

Writing – original draft: Egle Kelpsiene, Melinda Rydberg.

Writing – review & editing: Egle Kelpsiene, Melinda Rydberg, Mikael T. Ekvall, Martin Lundqvist, Tommy Cedervall.

References

1. Plastics the Facts 2021 https://plasticseurope.org/wp-content/uploads/2021/12/Plastics-the-Facts-2021-web-final.pdf. 2021:Accessed 9 Feb 2023.

2. Lebreton L, Andrady A. Future scenarios of global plastic waste generation and disposal. Palgrave Communications. 2019; 5(1):6.
3. Soares J, Miguel I, Venâncio C, Lopes I, Oliveira M. Perspectives on Micro (Nano) Plastics in the marine environment: biological and societal considerations. Water. 2020; 12(11):3208.
4. De Sá LC, Oliveira M, Ribeiro F, Rocha TL, Futter MN. Studies of the effects of microplastics on aquatic organisms: what do we know and where should we focus our efforts in the future? Science of the total environment. 2018; 645:1029–39. https://doi.org/10.1016/j.scitotenv.2018.07.207 PMID: 30248828
5. Davison SMC, White MP, Pahl S, Taylor T, Fielding K, Roberts BR, et al. Public concern about, and desire for research into, the human health effects of marine plastic pollution: Results from a 15-country survey across Europe and Australia. Global Environmental Change. 2021; 69:102309.
6. Zhang K, Hamidian AH, Tubić A, Zhang Y, Fang JKH, Wu C, et al. Understanding plastic degradation and microplastic formation in the environment: A review. Environmental pollution (Barking, Essex: 1987). 2021; 274:116554. https://doi.org/10.1016/j.envpol.2021.116554 PMID: 33529891
7. Wagner M, Scherer C, Alvarez-Muñoz D, Brennholt N, Bourrain X, Buchinger S, et al. Microplastics in freshwater ecosystems: what we know and what we need to know. Environmental Sciences Europe. 2014; 26(1):1–9. https://doi.org/10.1186/s12302-014-0012-7 PMID: 28936382
8. Andrady AL. Microplastics in the marine environment. Marine Pollution Bulletin. 2011; 62(8):1596–605. https://doi.org/10.1016/j.marpolbul.2011.05.030 PMID: 21742351
9. Barnes DKA, Galgani F, Thompson RC, Barlaz M. Accumulation and fragmentation of plastic debris in global environments. Philos Trans R Soc Lond B Biol Sci. 2009; 364(1526):1985–98. https://doi.org/10.1098/rstb.2008.0205 PMID: 19528051
10. Ekvall MT, Gimskog I, Hua J, Kelpsiene E, Lundqvist M, Cedervall T. Size fractionation of high-density polyethylene breakdown nanoplastics reveals different toxic response in *Daphnia magna*. Scientific Reports. 2022; 12(1):3109.
11. Ekvall MT, Lundqvist M, Kelpsiene E, Šileikis E, Gunnarsson SB, Cedervall T. Nanoplastics formed during the mechanical breakdown of daily-use polystyrene products. Nanoscale Advances. 2019; 1(3):1055–61. https://doi.org/10.1039/c8na00210j PMID: 36133186
12. Magrì D, Sanchez-Moreno P, Caputo G, Gatto F, Veronesi M, Bardi G, et al. Laser ablation as a versatile tool to mimic polyethylene terephthalate nanoplastic pollutants: characterization and toxicology assessment. ACS nano. 2018; 12(8):7690–700. https://doi.org/10.1021/acsnano.8b01331 PMID: 29944342
13. Lambert S, Wagner M. Formation of microscopic particles during the degradation of different polymers. Chemosphere. 2016; 161:510–7. https://doi.org/10.1016/j.chemosphere.2016.07.042 PMID: 27470943
14. Mattsson K, Björkroth F, Karlsson T, Hassellöv M. Nanofragmentation of Expanded Polystyrene Under Simulated Environmental Weathering (Thermooxidative Degradation and Hydrodynamic Turbulence). Frontiers in Marine Science. 2021;7.
15. Ji Y, Wang C, Wang Y, Fu L, Man M, Chen L. Realistic polyethylene terephthalate nanoplastics and the size-and surface coating-dependent toxicological impacts on zebrafish embryos. Environmental Science: Nano. 2020; 7(8):2313–24.
16. Reichelt S, Gorokhova E. Micro-and nanoplastic exposure effects in microalgae: a meta-analysis of standard growth inhibition tests. Frontiers in Environmental Science. 2020; 8:131.
17. Kelpsiene E, Torstensson O, Ekvall MT, Hansson L-A, Cedervall T. Long-term exposure to nanoplastics reduces life-time in *Daphnia magna*. Scientific Reports. 2020; 10(1):5979.
18. Mattsson K, Johnson EV, Malmendal A, Linse S, Hansson L-A, Cedervall T. Brain damage and behavioural disorders in fish induced by plastic nanoparticles delivered through the food chain. Scientific Reports. 2017; 7(1):11452. https://doi.org/10.1038/s41598-017-10813-0 PMID: 28904346
19. Setälä O, Fleming-Lehtinen V, Lehtiniemi M. Ingestion and transfer of microplastics in the planktonic food web. Environmental Pollution. 2014; 185:77–83. https://doi.org/10.1016/j.envpol.2013.10.013 PMID: 24220023
20. Kale SK, Deshmukh AG, Dudhare MS, Patil VB. Microbial degradation of plastic: a review. Journal of Biochemical Technology. 2015; 6(2):952–61.
21. Haider TP, Völker C, Kramm J, Landfester K, Wurm FR. Plastics of the future? The impact of biodegradable polymers on the environment and on society. Angewandte Chemie International Edition. 2019; 58(1):50–62. https://doi.org/10.1002/anie.201805766 PMID: 29972726
22. Casalini T, Rossi F, Castrovinci A, Perale G. A perspective on polylactic acid-based polymers use for nanoparticles synthesis and applications. Frontiers in bioengineering and biotechnology. 2019:259. https://doi.org/10.3389/fbioe.2019.00259 PMID: 31681741

23. Tyler B, Gullotti D, Mangraviti A, Utsuki T, Brem H. Polylactic acid (PLA) controlled delivery carriers for biomedical applications. Advanced drug delivery reviews. 2016; 107:163–75. https://doi.org/10.1016/j.addr.2016.06.018 PMID: 27426411

24. P Pawar R, U Tekale S, U Shisodia S, T Totre J, J Domb A. Biomedical applications of poly (lactic acid). Recent patents on regenerative medicine. 2014; 4(1):40–51.

25. Alam F, Shukla VR, Varadarajan K, Kumar S. Microarchitected 3D printed polylactic acid (PLA) nanocomposite scaffolds for biomedical applications. Journal of the Mechanical Behavior of Biomedical Materials. 2020; 103:103576. https://doi.org/10.1016/j.jmbbm.2019.103576 PMID: 32090905

26. Saini P, Arora M, Kumar M. Poly(lactic acid) blends in biomedical applications. Adv Drug Deliv Rev. 2016; 107:47–59. https://doi.org/10.1016/j.addr.2016.06.014 PMID: 27374458

27. Hamad K, Kaseem M, Ayyoob M, Joo J, Deri F. Polylactic acid blends: The future of green, light and tough. Progress in Polymer Science. 2018; 85:83–127.

28. Zhou Y, Lei L, Yang B, Li J, Ren J. Preparation and characterization of polylactic acid (PLA) carbon nanotube nanocomposites. Polymer Testing. 2018; 68:34–8.

29. Murariu M, Dubois P. PLA composites: From production to properties. Advanced Drug Delivery Reviews. 2016; 107:17–46. https://doi.org/10.1016/j.addr.2016.04.003 PMID: 27085468

30. Sukhanova A, Bozrova S, Sokolov P, Berestovoy M, Karaulov A, Nabiev I. Dependence of Nanoparticle Toxicity on Their Physical and Chemical Properties. Nanoscale Res Lett. 2018; 13(1):44-. https://doi.org/10.1186/s11671-018-2457-x PMID: 29417375

31. Luyts K, Napierska D, Nemery B, Hoet PH. How physico-chemical characteristics of nanoparticles cause their toxicity: complex and unresolved interrelations. Environmental science: processes & impacts. 2013; 15(1):23–38. https://doi.org/10.1039/c2em30237c PMID: 24592425

32. Ganguly P, Breen A, Pillai SC. Toxicity of Nanomaterials: Exposure, Pathways, Assessment, and Recent Advances. ACS Biomaterials Science & Engineering. 2018; 4(7):2237–75. https://doi.org/10.1021/acsbiomaterials.8b00068 PMID: 33435097

33. da Luz CM, Boyles MSP, Falagan-Lotsch P, Pereira MR, Tutumi HR, de Oliveira Santos E, et al. Polylactic acid nanoparticles (PLA-NP) promote physiological modifications in lung epithelial cells and are internalized by clathrin-coated pits and lipid rafts. Journal of nanobiotechnology. 2017; 15(1):1–18.

34. Da Silva J, Jesus S, Bernardi N, Colaço M, Borges O. Poly (D, L-Lactic Acid) nanoparticle size reduction increases its immunotoxicity. Frontiers in Bioengineering and Biotechnology. 2019; 7:137. https://doi.org/10.3389/fbioe.2019.00137 PMID: 31245366

35. Zimmermann L, Göttlich S, Oehlmann J, Wagner M, Völker C. What are the drivers of microplastic toxicity? Comparing the toxicity of plastic chemicals and particles to *Daphnia magna*. Environmental Pollution. 2020; 267:115392.

36. Zhang X, Xia M, Su X, Yuan P, Li X, Zhou C, et al. Photolytic degradation elevated the toxicity of polylactic acid microplastics to developing zebrafish by triggering mitochondrial dysfunction and apoptosis. Journal of Hazardous Materials. 2021; 413:125321. https://doi.org/10.1016/j.jhazmat.2021.125321 PMID: 33582471

37. Chieng BW, Azowa IN, Yunus W, Wan MZ, Hussein MZ, editors. Effects of graphene nanopletelets on poly (lactic acid)/poly (ethylene glycol) polymer nanocomposites. Advanced Materials Research; 2014: Trans Tech Publ.

38. Rocca-Smith J, Lagorce-Tachon A, Iaconelli C, Bellat J, Marcuzzo E, Sensidoni A, et al. How high pressure CO 2 impacts PLA film properties. Express Polymer Letters. 2017; 11(4).

39. Mofokeng JP, Luyt A, Tábi T, Kovács J. Comparison of injection moulded, natural fibre-reinforced composites with PP and PLA as matrices. Journal of Thermoplastic Composite Materials. 2012; 25(8):927–48.

40. Jang BN, Wilkie CA. The thermal degradation of bisphenol A polycarbonate in air. Thermochimica acta. 2005; 426(1–2):73–84.

41. Zou H, Yi C, Wang L, Liu H, Xu W. Thermal degradation of poly (lactic acid) measured by thermogravimetry coupled to Fourier transform infrared spectroscopy. Journal of thermal analysis and calorimetry. 2009; 97(3):929–35.

42. McNeill I, Leiper H. Degradation studies of some polyesters and polycarbonates—2. Polylactide: degradation under isothermal conditions, thermal degradation mechanism and photolysis of the polymer. Polymer degradation and stability. 1985; 11(4):309–26.

43. Pikuda O, Xu EG, Berk D, Tufenkji N. Toxicity Assessments of Micro- and Nanoplastics Can Be Confounded by Preservatives in Commercial Formulations. Environmental Science & Technology Letters. 2019; 6(1):21–5.

44. Heinlaan M, Kasemets K, Aruoja V, Blinova I, Bondarenko O, Lukjanova A, et al. Hazard evaluation of polystyrene nanoplastic with nine bioassays did not show particle-specific acute toxicity. Science of The

Total Environment. 2020; 707:136073. https://doi.org/10.1016/j.scitotenv.2019.136073 PMID: 31869615

45. Cooper RO, Cressler CE. Characterization of key bacterial species in the *Daphnia magna* microbiota using shotgun metagenomics. Scientific Reports. 2020; 10(1):652.
46. Gorokhova E, Motiei A, El-Shehawy R. Understanding biofilm formation in ecotoxicological assays with natural and anthropogenic particulates. Frontiers in microbiology. 2021:1663. https://doi.org/10.3389/fmicb.2021.632947 PMID: 34276580
47. Qi W, Nong G, Preston JF, Ben-Ami F, Ebert D. Comparative metagenomics of *Daphnia* symbionts. BMC genomics. 2009; 10(1):1–21.
48. Motiei A, Brindefalk B, Ogonowski M, El-Shehawy R, Pastuszek P, Ek K, et al. Disparate effects of antibiotic-induced microbiome change and enhanced fitness in *Daphnia magna*. PloS one. 2020; 15(1): e0214833.
49. Mushegian AA, Walser JC, Sullam KE, Ebert D. The microbiota of diapause: how host–microbe associations are formed after dormancy in an aquatic crustacean. Journal of Animal Ecology. 2018; 87 (2):400–13. https://doi.org/10.1111/1365-2656.12709 PMID: 28556095
50. Reveillaud J, Anderson R, Reves-Sohn S, Cavanaugh C, Huber JA. Metagenomic investigation of vestimentiferan tubeworm endosymbionts from Mid-Cayman Rise reveals new insights into metabolism and diversity. Microbiome. 2018; 6(1):1–15.
51. Hansen AK, Moran NA. Aphid genome expression reveals host–symbiont cooperation in the production of amino acids. Proceedings of the National Academy of Sciences. 2011; 108(7):2849–54. https://doi.org/10.1073/pnas.1013465108 PMID: 21282658
52. Douglas AE. The microbial dimension in insect nutritional ecology. Functional Ecology. 2009; 23(1):38–47.
53. Deschênes L, Ells T. Bacteria-nanoparticle interactions in the context of nanofouling. Advances in Colloid and Interface Science. 2020; 277:102106. https://doi.org/10.1016/j.cis.2020.102106 PMID: 31981890
54. Costerton JW, Stewart PS, Greenberg EP. Bacterial biofilms: a common cause of persistent infections. Science. 1999; 284(5418):1318–22. https://doi.org/10.1126/science.284.5418.1318 PMID: 10334980
55. Gupta P, Sarkar S, Das B, Bhattacharjee S, Tribedi P. Biofilm, pathogenesis and prevention—a journey to break the wall: a review. Archives of microbiology. 2016; 198(1):1–15. https://doi.org/10.1007/s00203-015-1148-6 PMID: 26377585
56. Huang H, Peng C, Peng P, Lin Y, Zhang X, Ren H. Towards the biofilm characterization and regulation in biological wastewater treatment. Applied microbiology and biotechnology. 2019; 103(3):1115–29. https://doi.org/10.1007/s00253-018-9511-6 PMID: 30483847
57. Galgani L, Engel A, Rossi C, Donati A, Loiselle SA. Polystyrene microplastics increase microbial release of marine chromophoric dissolved organic matter in microcosm experiments. Scientific reports. 2018; 8(1):14635. https://doi.org/10.1038/s41598-018-32805-4 PMID: 30279474
58. Gewert B, Plassmann M, Sandblom O, MacLeod M. Identification of chain scission products released to water by plastic exposed to ultraviolet light. Environmental Science & Technology Letters. 2018; 5 (5):272–6.
59. Romera-Castillo C, Pinto M, Langer TM, Álvarez-Salgado XA, Herndl GJ. Dissolved organic carbon leaching from plastics stimulates microbial activity in the ocean. Nature communications. 2018; 9 (1):1430. https://doi.org/10.1038/s41467-018-03798-5 PMID: 29651045
60. Zhu L, Zhao S, Bittar TB, Stubbins A, Li D. Photochemical dissolution of buoyant microplastics to dissolved organic carbon: rates and microbial impacts. Journal of hazardous materials. 2020; 383:121065. https://doi.org/10.1016/j.jhazmat.2019.121065 PMID: 31518809
61. Sheridan EA, Fonvielle JA, Cottingham S, Zhang Y, Dittmar T, Aldridge DC, et al. Plastic pollution fosters more microbial growth in lakes than natural organic matter. Nature Communications. 2022; 13 (1):4175. https://doi.org/10.1038/s41467-022-31691-9 PMID: 35882837
62. Porter KG, Feig YS, Vetter EF. Morphology, flow regimes, and filtering rates of *Daphnia*, *Ceriodaphnia*, and *Bosmina* fed natural bacteria. Oecologia. 1983; 58(2):156–63.
63. Kirk KL. Effects of suspended clay on *Daphnia* body growth and fitness. Freshwater Biology. 1992; 28 (1):103–9.
64. Amariei G, Rosal R, Fernández-Piñas F, Koelmans AA. Negative food dilution and positive biofilm carrier effects of microplastic ingestion by *D. magna* cause tipping points at the population level. Environmental Pollution. 2022; 294:118622.
65. Huchette SM, Beveridge MC, Baird DJ, Ireland M. The impacts of grazing by tilapias (*Oreochromis niloticus* L.) on periphyton communities growing on artificial substrate in cages. Aquaculture. 2000; 186(1–2):45–60.

66. Bratvold D, Browdy CL. Effects of sand sediment and vertical surfaces (AquaMatsTM) on production, water quality, and microbial ecology in an intensive *Litopenaeus vannamei* culture system. Aquaculture. 2001; 195(1–2):81–94.

67. Mridula R, Manissery J, Keshavanath P, Shankar K, Nandeesha M, Rajesh K. Water quality, biofilm production and growth of fringe-lipped carp (*Labeo fimbriatus*) in tanks provided with two solid substrates. Bioresource technology. 2003; 87(3):263–7.

68. Thompson FL, Abreu PC, Wasielesky W. Importance of biofilm for water quality and nourishment in intensive shrimp culture. Aquaculture. 2002; 203(3–4):263–78.

69. Bhagwat G, O'Connor W, Grainge I, Palanisami T. Understanding the fundamental basis for biofilm formation on plastic surfaces: role of conditioning films. Frontiers in Microbiology. 2021; 12:687118. https://doi.org/10.3389/fmicb.2021.687118 PMID: 34248907

70. Ganesan S, Ruendee T, Kimura SY, Chawengkijwanich C, Janjaroen D. Effect of biofilm formation on different types of plastic shopping bags: Structural and physicochemical properties. Environmental Research. 2022; 206:112542. https://doi.org/10.1016/j.envres.2021.112542 PMID: 34929185

71. Pinto M, Langer TM, Hüffer T, Hofmann T, Herndl GJ. The composition of bacterial communities associated with plastic biofilms differs between different polymers and stages of biofilm succession. PloS one. 2019; 14(6):e0217165. https://doi.org/10.1371/journal.pone.0217165 PMID: 31166981

Supplementary Information

Prolonged survival time of *Daphnia magna* exposed to polylactic acid breakdown nanoplastics

Egle Kelpsiene [a,b], Melinda Rydberg [a], Mikael T. Ekvall [c,b], Martin Lundqvist [a,b], and Tommy Cedervall [a,b*]

[a] Department of Biochemistry and Structural Biology, Lund University, Lund University, P.O. Box 124, SE-221 00 Lund, Sweden

[b] NanoLund, Lund University, Box 118, SE-221 00 Lund, Sweden

[c] Aquatic Ecology Unit, Department of Biology, Ecology Building, Lund University, 223 62 Lund,

Sweden

*Corresponding author: tommy.cedervall@biochemistry.lu.se

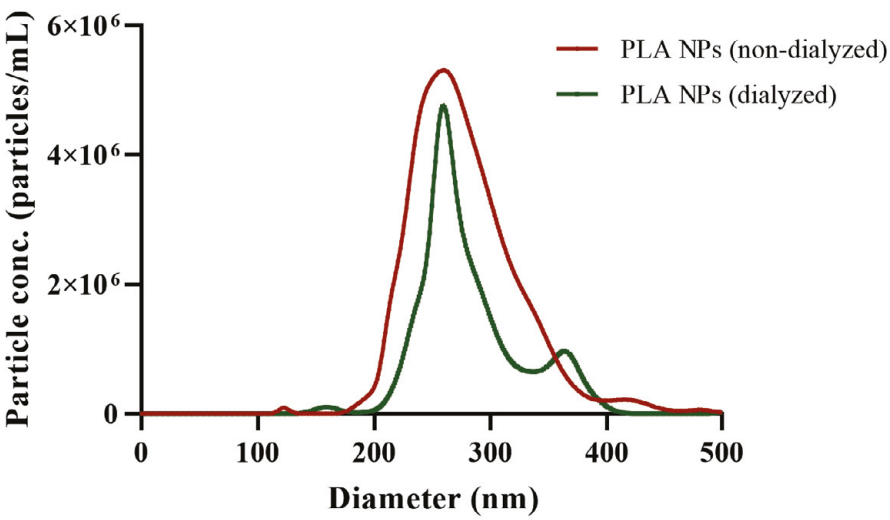

Supplementary Figure 1. Sizes of PLA NPs were measured before and after dialysis by using NTA to ensure that particle aggregation did not occur during dialysis.

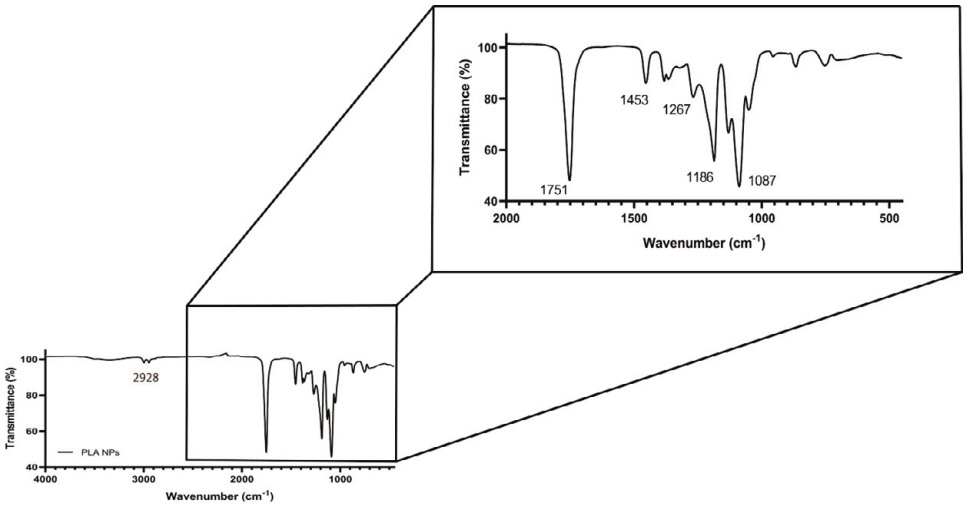

Supplementary Figure 2. Spectra of engineered 250 nm PLA NPs obtained by FTIR.

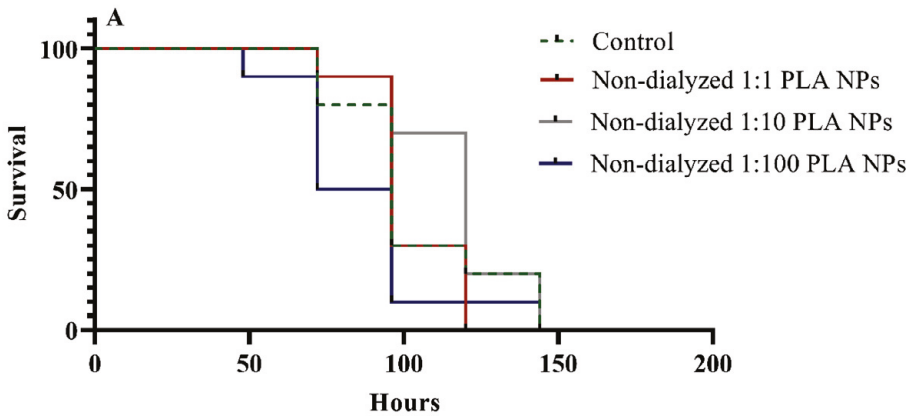

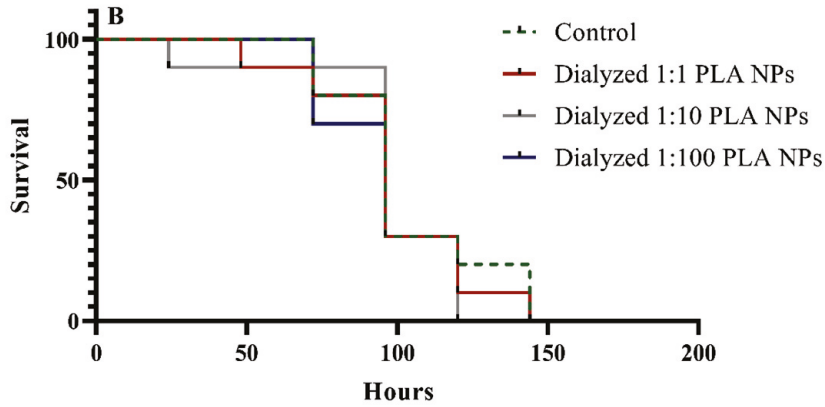

Supplementary Figure 3. Survival of *Daphnia magna* exposed to non-dialyzed (Figure A) dialyzed (Figure B) 250 nm PLA NPs with different dilution factors. The highest concentration (1:1) for both dialyzed and non-dialyzed PLA NPs was 10 mg/L. The experiment was performed at once, however for clearer vision survival curves for non-dialyzed and dialyzed in comparison with a control are shown separately. No statistically significances were observed among the treatments. In total there were 10 replicates for each treatment. Experiment was repeated 3 times.